AWARD NUMBER: W81XWH-14-1-0479

TITLE: ING4 Loss in Prostate Cancer Progression

PRINCIPAL INVESTIGATOR: Cynthia Miranti, PhD

CONTRACTING ORGANIZATION: Van Andel Research Institute
                               Grand Rapids, MI 49503

REPORT DATE: October 2016

TYPE OF REPORT: Annual

PREPARED FOR: U.S. Army Medical Research and Materiel Command
               Fort Detrick, Maryland 21702-5012

REPORT DOCUMENTATION PAGE

1. REPORT DATE	2. REPORT TYPE	3. DATES COVERED
October 2016	Annual	23 Sep 2015 – 22 Sep 2016

4. TITLE AND SUBTITLE

ING4 Loss in Prostate Cancer Progression

5a. CONTRACT NUMBER

5b. GRANT NUMBER
W81XWH-14-1-0479

5c. PROGRAM ELEMENT NUMBER

6. AUTHOR(S)

Cynthia Miranti, PhD.

E-Mail: cindy.miranti@vai.org

5d. PROJECT NUMBER

5e. TASK NUMBER

5f. WORK UNIT NUMBER

7. PERFORMING ORGANIZATION NAME(S) AND ADDRESS(ES)

Van Andel Research Institute
333 Bostwick Ave NE
Grand Rapids, MI 49503-2518

8. PERFORMING ORGANIZATION REPORT NUMBER

9. SPONSORING / MONITORING AGENCY NAME(S) AND ADDRESS(ES)

U.S. Army Medical Research and Materiel Command
Fort Detrick, Maryland 21702-5012

10. SPONSOR/MONITOR'S ACRONYM(S)

11. SPONSOR/MONITOR'S REPORT NUMBER(S)

12. DISTRIBUTION / AVAILABILITY STATEMENT

Approved for Public Release; Distribution Unlimited

13. SUPPLEMENTARY NOTES

14. ABSTRACT

The goal of this project is to identify specific differentiation events whose disruption by Myc and Pten leads to aggressive PCa. Our Aims are to 1) determine how ING4 controls prostate epithelial differentiation; 2) determine how loss of ING4 impacts tumorigenesis; and 3) determine how loss of ING4 in patients relates to tumor progression. We found the following: 1) Notch3 is a target of p38MAPK and Myc signaling required for differentiation. 2) CREB1 and ATF1 differentially control ING4 expression during differentiation, and aberrant CREB/ATF1 activation in tumor cells prevents ING4 expression and differentiation. 3) Miz1 is an ING4 target that enhances differentiation that is absent in tumor cells. 4) JFK is an ING4 target that suppresses ING4 expression through ubquitination. 5) Erg negatively impacts differentiation, but only when expressed in the AR-positive cells. We have identified targets of Myc, ING4, and CREB that can be used to screen human tissues proposed in Aim 3 to identify aggressive tumors.

15. SUBJECT TERMS

Prostate epithelial differentiation, Myc, ING4, chromatin, integrins, Erg, Pten, Miz1, CREB, Notch, p38, prostate cancer oncogenesis,TMA, mouse model, human model.

16. SECURITY CLASSIFICATION OF:			17. LIMITATION OF ABSTRACT	18. NUMBER OF PAGES	19a. NAME OF RESPONSIBLE PERSON USAMRMC
a. REPORT	b. ABSTRACT	c. THIS PAGE			19b. TELEPHONE NUMBER *(include area code)*
Unclassified	Unclassified	Unclassified	Unclassified	113	

Table of Contents

1. Introduction

Being able to determine which PCa patients have indolent disease and require minimal treatment, versus those who will die unless aggressively treated, remains a major challenge. The goal of this project is to test the **hypothesis** that Myc normally promotes prostate epithelial differentiation through chromatin remodeling mediated by ING4, such that loss of ING4 is required for Myc oncogenesis, which leads to aggressive disease through suppression of differentiation. Our **specific aims** are: <u>Aim 1: Determine how ING4 controls prostate epithelial differentiation</u>. We hypothesize that Myc normally promotes prostate epithelial differentiation through chromatin remodeling mediated by ING4. <u>Aim 2: Determine how loss of ING4 impacts tumorigenesis</u>. We hypothesize that loss of ING4 cooperates with specific oncogenes to disrupt terminal differentiation, which is required for aggressive tumorigenesis. <u>Aim 3: Determine how loss of ING4 in patients relates to tumor progression.</u> Our objectives are to 1) establish if there is a correlation between ING4 loss and over expression of Myc, Erg fusions, or Pten loss, and the relationship to disease recurrence in patients; and 2) determine how ING4 expression correlates with the expression of known differentiation markers in the tumors.

2. Keywords

Prostate epithelial differentiation, Myc, ING4, chromatin, integrins, Erg, Pten, Miz1, CREB, Notch, p38, prostate cancer oncogenesis, TMA, mouse model, human model

3. Accomplishments

The major goals of the project:
<u>Underlined</u> dates indicate completed tasks. Those that are partially completed are marked by *.

Specific Aim 1: Determine how ING4 controls prostate epithelial differentiation

Major Task 1: ING4 and Myc Targets
        Subtask 1a: Determine how ING4 impacts expression of three Myc target genes
                <u>Months 1-2</u>
        Subtask 1b: Carry out Myc ChIP analysis of three Myc target genes
                <u>Months 3-6</u>

Major Task 2: ING4 and EZH1/2
        Subtask 2a: Determine how ING4 impacts EZH1/2 expression
                <u>Months 7-8</u>
        Subtask 2b: Identify EZH1/2 targets controlled by ING4
                <u>Months 9-11</u>
        Milestone #1: Prepare manuscript for publication
                <u>Months 11-12</u>

Major Task 3: Global targets
        Subtask 3a: Initiate ChIP studies by optimizing and validating techniques
                <u>Months 1-6</u>

Subtask 3b: Isolate mRNA for RNA-Seq studies
        Months 5-6
Subtask 3c: Set up ChIP studies for sequencing
        Months 6-20
Subtask 3d: Run RNA-Seq studies
        Months 6-20
Subtask 3e: Analysis of ChIP-Seq and RNA-Seq data
        Months 21-28*
Subtask 3f: Validation of hits in model
        Months 28-34*
Milestone #2: Prepare manuscript for publication
        Months 35-36

Specific Aim 2: Determine how loss of ING4 impacts tumorigenesis

Major Task 4: Oncogenic Suppression of ING4 and Tumorigenesis
        Subtask 4a: IACUC animal protocol approval (80 mice).
                Months 1-3
        Subtask 4b: Generation of oncogenic iPrEC cell line combinations
                Months 1-3
        Subtask 4c: Testing of cell line combinations in vitro and in vivo
                Months 4-8
        Subtask 4d: Analysis of tumor tissues
                Months 9-12*
        Subtask 4e: Analysis of tumor cell lines in 3D models
                Months 13-15

Major Task 5: Oncogenic Control of ING4 Expression
        Subtask 5a: Measure ING4 mRNA and protein in oncogenic lines
                Months 9
        Subtask 5b: Measure ING4 mRNA and protein stability in oncogenic lines
                Months 10-11
        Subtask 5c: Assess oncogenic effects on ING4 promotor
                Months 10-15
        Milestone #3: Prepare manuscript for publication
                Months 16-17*

Major Task 6: ING4 Loss and Myc Cooperation in Tumorigenesis
        Subtask 6a: IACUC animal protocol approval (720 mice)
                Months 1-3
        Subtask 6b: Initiate in vitro fertilization to generate Pb-Myc and ING4 KO breeders
                Months 4-6
        Subtask 6c: Breeding to generate double mutant mice
                Months 6-12
        Subtask 6d: Monitoring and analysis of tumor development
                Months 13-24*

Subtask 6e: Assessment of tumor pathology and IHC
            Months 25-30
Milestone #4: Prepare manuscript for publication
            Months 31-32

Specific Aim 3: Determine how loss of ING4 in patients relates to tumor progression

Major Task 7: Regulatory processes
            Subtask 7a: Apply for TMA samples from PCBN
                        <u>Months 1-3</u>
            Subtask 7b: IRB paperwork and approval
                        <u>Months 1-3</u>

Major Task 8: Correlation of ING4 Loss with Outcome and Oncogenic Events
            Subtask 8a: Optimization of IHC staining on VARI tester TMA
                        <u>Months 1-6</u>
            Subtask 8b: IHC staining of PCBN arrays
                        Months 7-16*
            Subtask 8c: Statistical analysis of data
                        Months 17-18

Major Task 9: ING4 Loss and Tumor Differentiation
            Subtask 9a: Optimization of IHC staining on VARI tester TMA
                        <u>Months 19-24</u>
            Subtask 9b: IHC staining of PCBN and VARI arrays
                        Months 25-32*
            Subtask 9c: Statistical analysis of data
                        Months 32-34
            Milestone #5: Prepare manuscript for publication
                        Months 35-36

**What we accomplished under these goals:**

Aim 1: Determine how ING4 controls prostate epithelial differentiation. We hypothesized that Myc normally promotes prostate epithelial differentiation through chromatin remodeling mediated by ING4. Thus, to figure out how Myc and ING4 cooperate to promote differentiation, we need to identify relevant targets of Myc and ING4. We took 2 approaches, interrogation of 'best guess' targets (**Tasks 1 and 2**), and a global approach using RNA-Seq and ChIP-Seq (**Task 3**).

        In **Task 1** we looked at genes known to be regulated by Myc, specifically ODC, cyclin D1, and integrin α6. We found that ING4 suppresses ODC and cyclin D1 expression, and Myc does not ChIP on those targets in differentiating PrECs. We are currently working on integrin α6 as detailed further under Task 3 (**Fig. 4**).

        In **Task 2** we interrogated 2 known chromatin modifying enzymes, EZH1/2 as possible targets of ING4. ING4 did not ChIP on these promoters, EZH1 expression was unchanged, and EZH2 expression went down upon ING4 induction. Thus, although EZH2 loss is likely

important for differentiation, it is not an ING4 target. Thus, our initial milestone of preparing a manuscript on these proposed Myc and ING4 targets was not achieved. However, we were much more successful at identifying both Myc and ING4 targets in Task 3 using RNA-Seq, which will allow us to reach a slightly delayed publication milestone.

For **Task 3**, we set up 3 major RNA-seq studies. The first was a time course of normal PrEC differentiation compared to tumorigenic PrECs (EMPs – Erg+Myc overexpression+Pten shRNA (See Aim 2)) taken at days 0, 4, 8, 11, 14, and 17 of differentiation. In the second experiment, to identify ING4-specific targets we compared normal PrECs differentiated for 10 days (time of peak ING4 expression), PrECs constitutively overexpressing ING4 differentiated for 3 days (these cells accelerate differentiation), PrECs expressing shING4 differentiated for 10 days, and undifferentiated PrECs. The third experiment was designed to identify both p38-MAPK and Myc targets. We previously determined that p38-MAPK is essential for initiating differentiation (Lamb *et al.*, 2010), and Myc is a target of p38. Therefore, we generated a Tet-inducible PrEC line to express constitutively active MMK6, the p38 upstream activator. A short pulse of doxycycline is sufficient to induce p38 phosphorylation and Myc induction 2-fold (equivalent to what we see in normal differentiating cells), peaking at 7 hours (**Fig. 1a**). Using an RNA-Seq technique which measures newly synthesized RNA, called Bru-Seq (Paulsen *et al.*, 2014), we compared untreated to 7 hour doxycycline-treated MKK6 cells.
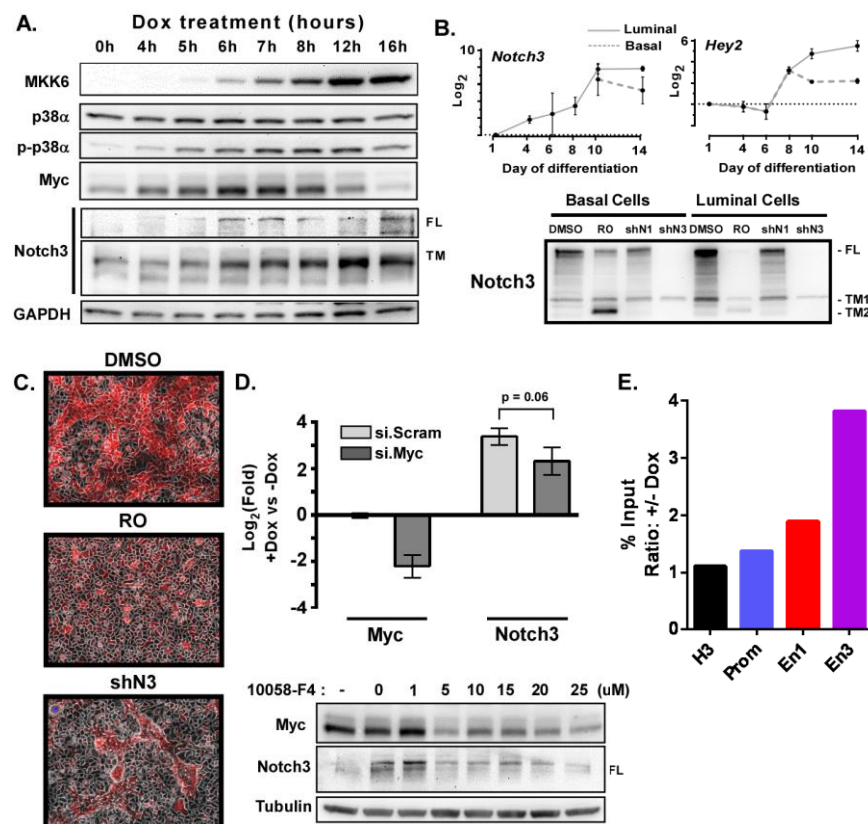
**Figure 1: Notch3 induction requires Myc. A.** MKK6 was induced in PrECs with a 4 hour doxycycline (Dox) pulse. Levels of MKK6, p38α, active p38α (p-p38α), Myc, Notch3 (full length (FL) or cleaved (TM), and GAPDH over time (hours (h)) measured by immunoblotting. **B.** Notch3 and Hey2 mRNA (graphs) measured by qRT-PCR at different times during differentiation. Top (secretory cells) and Bot (basal cells) were separated at days 8 and 10. Notch3 protein (full length (FL) or cleaved (TM1/TM2)) measured by immunoblotting in basal and luminal cells differentiated 16 days in the presence of vehicle (DMSO), γ-secretase inhibitor RO4929097 (RO) or Notch1 or Notch3 shRNA (shN1, shN3). **C.** PrECs treated as above and immunostained for E-cadherin (marks the luminal cells). **D.** MKK6 induced in PrECs for 7 hours after treatment with Myc (si.Myc) or scrambled (si.Scram) siRNA (graph) or Myc inhibitor (10068-F4) (blot). Levels of Myc or Notch3 mRNA (graph) or protein (blot) were measured in MKK6 cells induced with doxycycline (Dox). **E.** Myc ChIP on Notch3 promoter (Prom), enhancer 1 (En1) and enhancer 3 (En3) in MKK6 cells induced with doxycycline (+Dox) compared to uninduced cells (-).

Several sets of analyses were run on the RNA-Seq data sets. For the p38/Myc data we used GSEA to first subtract out stress-response genes known to be activated by p38-MAPK and to focus on those genes associated with differentiation, cytoskeleton, and cell adhesion (since differentiation is associated with the latter two events). The most highly induced gene in this list was Notch3. Correspondingly we observed induction of Notch3 full length and activated TM form 7-8 hours after MMK6 induction (**Fig. 1a**). Notch3 was also identified in the ING4 and time course RNA-Seq data. We then determined the relationship between Myc and Notch3 during differentiation. Some of our findings include 1) Notch3 mRNA and its target Hey2 is induced over 20-fold over the course of differentiation, and the majority of Notch3 protein ends up in the differentiated luminal cells (**Fig 1b**); 2) Blocking Notch3 with shRNA blocks differentiation (**Fig 1c**); 3) Inhibiting Myc reduces Notch3 induction (**Fig. 1d**), but Myc alone is not sufficient to induce Notch3; and 4) Myc ChIPs on two enhancers of the Notch3 gene (**Fig. 1e**). Thus, we identified at least one new Myc target. We finished these studies and a manuscript is ready to be submitted.

In the second analysis, we took all the significant hits (those which changed by 2x or more in the time course and the ING4-manipulated cells) and passed them through Gene-Go to determine which transcription factors could be responsible for driving the expression of those genes. In addition to finding Myc and AR targets as expected, the factor with the most hits was CREB. What was even more striking, is that the set of CREB targets induced in normal PrECs during differentiation were completely different from the CREB targets induced in the tumorigenic EMP cells (**Fig. 2a**). To validate these findings, we monitored CREB and ATF1 (CREB binding partner) activation during differentiation and in the tumorigenic EMP cells. CREB activity is transiently induced during normal differentiation and peaks when ING4 is highest. ATF1 activation is also transient, but peaks a few days earlier when ING4 is induced (**Fig 2b**). In EMP cells, CREB and ATF1 were constitutively activated. We validated some of the CREB targets, demonstrating that BLIMP1 and C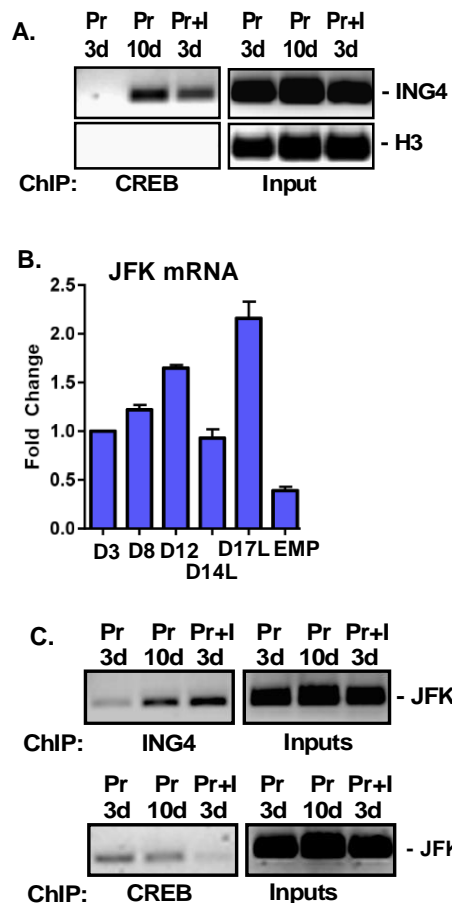LDN1 are dramatically induced at the same time CREB is activated in normal PrECs, and are poorly induced in EMP cells (**Fig 2c**).
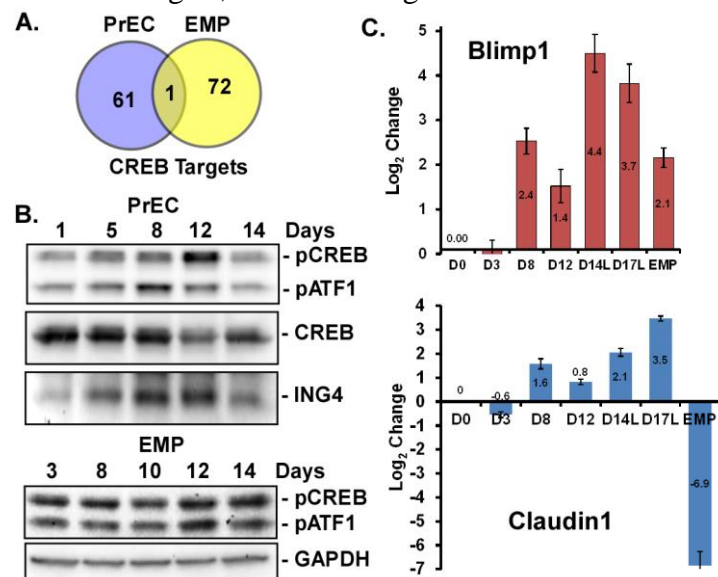
Figure 2: CREB Dynamics Differ Between Normal and Tumor Cells. A. The intersection of genes whose expression is increased in normal PrECs vs tumorigenic EMP cells that are transcriptional targets of CREB. **B.** CREB and ATF1 activation (pCREB, pATF1) as measured by phospho-immunoblotting various times (days) during PrEC and EMP cell differentiation compared to ING4 expression. **C.** CREB targets, Blimp1 and Claudin1 mRNA levels measured by qRT-PCR during PrEC differentiation and in EMP cells. D=days, L=luminal cells.

We used CREB/ATF1 and ING4 ChIP to begin teasing out the relationship between ING4 and CREB/ATF1 and to identify ING4 targets. We found CREB/ATF1 (antibody used for the ChIP does not distinguish CREB from ATF1) bound at the ING4 promoter (**Fig. 3a**) and ING4 overexpression enhanced this binding, suggesting ING4 influences CREB/ATF1 binding

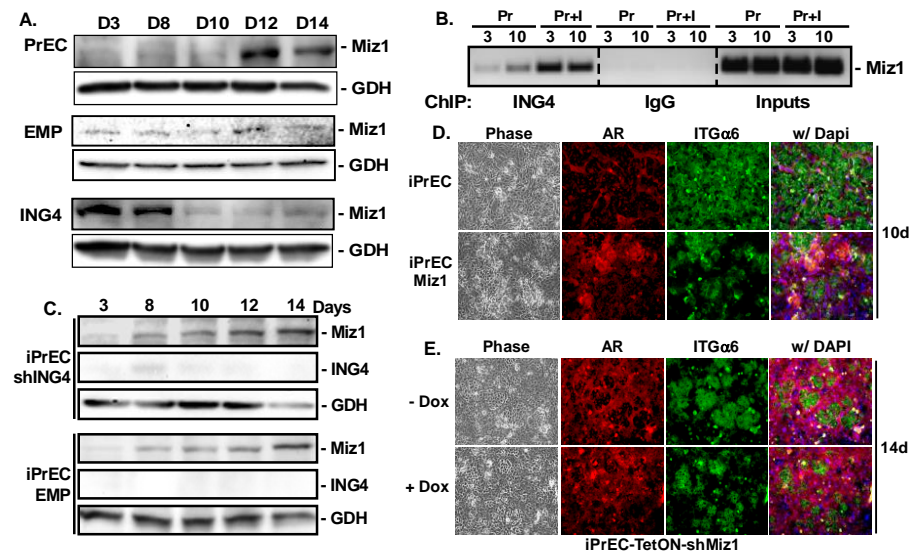to its own promoter. We saw a 2-fold increase in expression of the ING4 E3 ligase (**Fig 3b**), JFK (Yan *et al.*, 2015). We found both ING4 and CREB/ATF1 bound to the promoter of JFK (**Fig. 3c**). However, in this case overexpression of ING4 resulted in increased ING4 binding as would be expected for a direct target, but ING4 over expression actually suppressed CREB/ATF1 binding at the JFK promoter. This suggests ING4 might limit the ability of CREB/ATF1 to induce JFK or change how JFK is induced. From these data we propose a working hypothesis whereby ING4 is initially induced by ATF1 (based on time course in Fig. 2b) and ING4 enhances CREB binding at the ING4 promoter (where CREB might limit ING4 expression), but at the same time induces JFK in a CREB/AFT1-independent manner to activate its own destruction later in differentiation, by activating its E3 ligase. We are currently preparing a manuscript for publication on the JFK data.

Figure 3: CREB binds ING4 promoter, and ING4 binds the promoter of its own E3 ligase, JFK. A. ChIP of CREB bound to ING4 promoter in normal PrECs (Pr) and PrECs overexpressing ING4 (Pr+I) at days 3 and 10 (3d, 10d) of differentiation. **B**. JKF mRNA levels in differentiating PrECs over time (D=days) and in tumorigenic EMP cells. L=luminal cells. **C.** ChIP of ING4 and CREB bound to JFK promoter in normal PrECs (Pr) and PrECs overexpressing ING4 (Pr+I) at days 3 and 10 (3d, 10d) of differentiation.

From the RNA-Seq data we also identified Miz1 as another ING4 target. Miz1 is a transcriptional repressor that suppresses Myc activity. In keratinocytes, the Miz1/Myc repressor binds integrin α6 and β1 promoters and is required to suppress their expression in suprabasal cells (Gebhardt *et al.*, 2006). We measured integrin mRNA during differentiation and found that integrin α3 and β4 were turned off 3 days before integrin α6 or β1. This supported our previous data based on immunostaining (Lamb *et al.*, 2010). Loss of integrin α3 and β4 coincided with Myc and Notch3 induction, while loss of integrin α6 and β1 coincided with ING4 expression. We found Miz1 expression is induced around the same time as ING4 during differentiation (**Fig. 4a**), and over expression of ING4 directly induces Miz1. Using ChIP we found increased ING4 binding to the Miz1 promoter 10 days after differentiation compared to 3 days. Overexpression of ING4 resulted in ING4 binding constitutively (at day 3) to the Miz1 promoter (**Fig 4b**). Conversely, when we knock-down ING4, or look at EMP cells which do not express ING4, there is no induction of Miz1 (**Fig 4c**). We then overexpressed Miz1, and found that like ING4, Miz1 over expression is sufficient to accelerate differentiation (**Fig. 4d**). Thus, there is tight correlation between ING4 and Miz1. We expected that when we knocked down Miz1 we would prevent integrin a6/b1 loss and prevent differentiation. But in fact loss of Miz1 had no impact on differentiation (**Fig 4e**). We even made use of a dominant mutant of Miz1 that is unable to bind Myc, and expression of this mutant also did not block differentiation. Thus, although Miz1 is a clear target of ING4, Miz1 is not absolutely necessary for luminal cell differentiation. We have now published this study (Berger *et al.*, 2016).

9

Figure 4: Miz1 is an ING4 target. A. Miz1 expression measured by immunoblotting in normal PrECs, tumorigenic EMP, and PrECs overexpressing ING4 at different days during differentiation. **B.** ChIP of ING4 on the Miz1 promoter in normal PrECs (Pr) and PrECs overexpressing ING4 (Pr+I) at days 3 and 10 (3d, 10d) of differentiation. **C.** Miz1 expression measured by immunoblotting in tumorigenic EMP and PrECs overexpressing ING4 at different days during differentiation. **D.** Miz1 overexpression resulted in more differentiation at day 10. Red = AR (luminal), Green = integrin a6 (basal). **E.** Loss of Miz1 had no impact on differentiation.

Thus, we made substantial progress, more than expected, successfully identifying both Myc and ING4 targets required for normal PrEC differentiation, and gained a better understanding of how ING4 controls differentiation. In addition, we identified other important markers of PrEC differentiation, Notch3, BLIMP1, Cldn1, CREB, ATF1, and JFK, and shown that some of these targets are disrupted in the tumorigenic EMP cells. We are well poised to begin to interrogate these markers in human tissues and relate them to patient outcomes as proposed in Aim 3. We also have additional potential Myc and ING4 targets within our RNA-Seq data to validate and study.

We have completed the sequencing on the ING4 ChIP experiments and will be analyzing this soon. We expect to identify additional ING4 targets which will be validated in our differentiation model and interrogated in the human tissues.

Aim 2: Determine how loss of ING4 impacts tumorigenesis. We hypothesize that loss of ING4 cooperates with specific oncogenes to disrupt terminal differentiation, which is required for aggressive tumorigenesis. Our published data indicate that ING4 is lost in 60% of primary prostate cancers. However, we do not know how ING4 is lost. We know that overexpression of Myc + Erg + Pten loss (EMP) generates tumorigenic cells that lose ING4 expression and fail to differentiate in vitro (Berger *et al.*, 2014). The goals of this aim are to determine which oncogenes are most important for ING4 loss in PCa development and progression using oncogenic manipulation of iPrECs in xenografts (**Task 4**), in vitro (**Task 5**) and development of an engineered mouse model (**Task 6**).

For **Task 4 and 5**, we want to identify which combination of oncogenes, i.e. Myc, Erg, or loss of Pten, is required to induce ING4 loss, prevent differentiation, and induce tumorigenesis. Thus far, we determined that overexpression of Myc, Erg, Myc+Erg, or loss of Pten alone, is not sufficient to induce tumors in orthotopic xenograft injections in vivo, is not sufficient to prevent differentiation in vitro, and do not suppress ING4 expression. We still need to test Pten in combination with either Erg or Myc alone.

During these studies we became concerned that we were not detecting any impact of Erg overexpression on differentiation or tumorigenesis, and yet this should be an oncogene. Our original strategy was to overexpress the N-terminal truncated version of Erg found in tumors off a constitutive promoter such that it is expressed in both basal and luminal cells during differentiation. However, in human PCa this oncogene is only expressed in luminal-like cells in which AR is expressed. Thus, we re-engineered this gene to be expressed under the control of the PSA ARE enhancer and stably introduced it into PrECs. When we induce the differentiation of these cells, we saw luminal-specific induction of Erg (**Fig. 5a**). In these cells, it appeared that luminal cells would initially appear, but were not stable and appeared to be dying and would disappear (**Fig. 5b**). Cell death was confirmed by now see major alterations in their differentiation (**Fig 5c**). Thus, we propose there is something about Erg expression in luminal cells, and its absence in basal cells that is critical for its oncogenic properties. In the RNA-Seq data from the MMK6/p38/Myc induced differentiation model, one of the striking findings is the decrease in expression of Erg and almost all the ETV family members (all those found in PCa gene fusions), but not Ets genes. This suggests there is a fundamental relationship between Erg/ETV loss in normal cells and its retention specifically in luminal cells that may drive PCa development.

This finding is fundamentally important because it changes our thinking about how Erg functions as an oncogene. Unfortunately, many studies trying to identify Erg targets have used constitutive expression of Erg, and we would argue this will give erroneous results. The ARE is required to provide the right timing and context in which to express Erg.
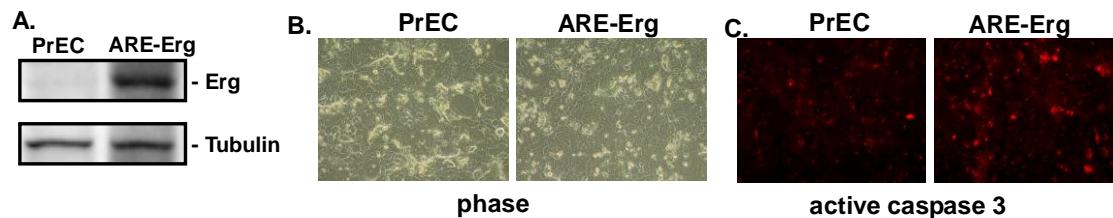
Figure 5: Erg under Control of Androgen Negatively Impacts Differentiation. A. Level of Erg and tubulin expression measured by immunoblotting in normal PrECs and PrECs expressing ARE-Erg after 21 days of differentiation. **B.** PrECs and PrECs with ARE-Erg differentiated for 16 days and viewed by phase contrast. Piles of luminal cells are appearing in the PrEC culture, but only single cells are appearing in ARE-Erg cells. **C.** PrECs and PrECs with ARE-Erg differentiated for 21 days and immunostained for cleaved/active caspase 3. More dead cells appear in the ARE-Erg cultures.

We tested the tumorigenicity of the ARE-Erg cell lines in various combinations with Myc and/or shPten overexpression. As previously noted, shPten alone was not efficient at generating tumors, and we saw a few prostate nodules with just ARE-Erg expression (**Table 1**). We still need to verify tumor vs PIN for these prostates. All the different combinations gave much more robust tumor phenotypes then we saw previously with constitutive Erg; and most striking the triple combination produced visible metastases in 1 mouse. Tissues were collected to look more closely for additional metastases. Thus, ARE-Erg in the context of the Myc and/or Pten was much more aggressive and tumorigenic than constitutive Erg.

TABLE 1: Tumors production

Cell Line Injected	# Tumors
iPEC37.ARE-Erg cl.3	4/10
iPEC37.ARE-Erg+Myc	9/10
iPEC37.ARE-Erg+shPten(B)	7/10
iPEC37.ARE-Erg+Myc+shPten(B)	7/10 1/10 mets
iPEC37+Myc+shPten(B)	7/10
iPEC37+shPten(B)	1/10

We know ING4 is lost in the EMP (Erg+Myc+shPten) cells, and not in the EM (Erg+Myc) cells (Berger *et al.*, 2014). Therefore, Pten contributes in some way to ING4 loss in tumors. During differentiation, Pten is elevated early (**Fig. 6a**), but decreases after ING4 is induced and CREB becomes active (after day 10). In EMP cells, CREB/ATF1 is constitutively activated (see Fig. 2b); therefore, we propose that Pten acts to suppress CREB/ATF1 activation in normal differentiation until the right time, and its loss leads to constitutive CREB/ATF1 activation. Loss of Pten results in elevated Akt activity due to loss of lipid phosphatase activity, and Akt is a potent activator of CREB (Caravatta *et al.*, 2008). However, it has also been reported that Pten itself can dephosphorylate and inactivate CREB, particularly when associated with differentiation (Gu *et al.*, 2011; Lyu *et al.*, 2015). We obtained 2 Pten dominant acting mutants, one which inactivates lipid phosphatase activity (G129E) and one that inactivates both the lipid and protein phosphatase (C124S) activity. We overexpressed these in PrECs (**Fig 6b**), and find that blocking only protein phosphatase activity (C124S), but not lipid phosphatase (G129E) results in constitutive CREB/ATF1 activation (**Fig. 6c**) as early as 4 days after differentiation, before it is detected in normal PrECs. We observed a corresponding increase in ING4 expression (Fig. 6c) and these cells still differentiate. In fact they differentiate more rapidly and do so in 4x less concentration of differentiation factors (**Fig. 6d**). This is consistent with our finding that loss of Pten alone doesn't suppress ING4 or differentiation and that CREB/ATF1 may induce ING4 (see Fig. 3a). Thus, there is a second event triggered by Myc or Erg, in addition to Pten loss that is required to suppress ING4.

Figure 6: Pten Protein Phosphatase Activity Sets the Timing of Differentiation, CREB Activation and Induction of ING4. A. Pten expression was measured by immunoblotting of PrECs differentiated for 3, 8, 10, 12 or 14 days (d). **B.** Pten expression was measured by immunoblotting of normal PrECs, EMPs, or PrECs overexpressing Pten mutants G129E or C124S. **C.** Activated CREB/ATF1 (P-CREB) and ING4 levels were measured by immunostaining PrECs and Pten mutant cell lines differentiated for 4 days. This early in differentiation, normal PrECs and the lipid phosphatase mutant (G129E) have low levels of P-CREB, but no ING4, while the lipid/protein phosphatase mutant (C124S) has dramatically increased P-CREB and ING4 expression. **D.** Differentiation is accelerated in the lipid/protein phosphatase mutant (C124S) under suboptimal levels of differentiation factors. Differentiation was measured by immunostaining for AR in the luminal layer (red) and integrin α6 (green) in the basal layer. Many more luminal cells with more robust AR staining was observed in the C124S mutant cells.
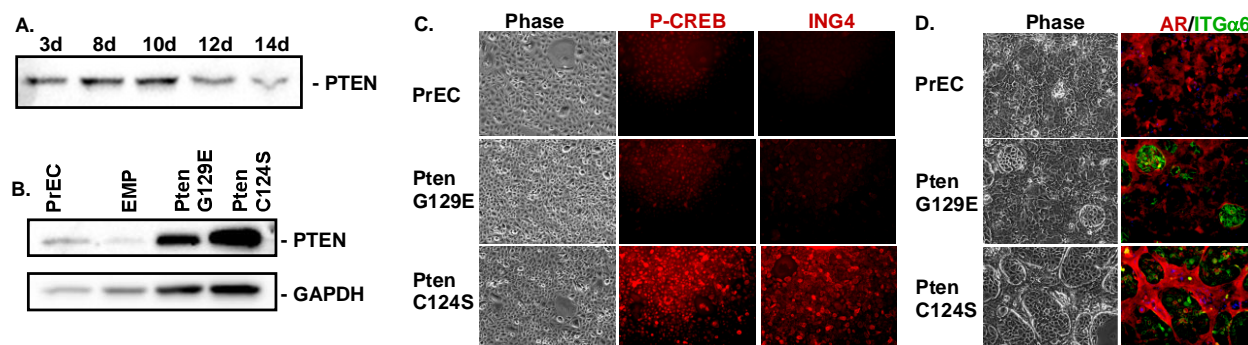
In **Task 6**, we proposed to cross ING4 KO mice to Pb-Myc mice to determine if loss of ING4 will accelerate the slow development of PCa seen in the Pb-Myc mice. We obtained and successfully re-derived the ING4 mice into FVB/n mice. We crossed the hets and attempted to identify the homozygotes. We had lots of problems with the PCR screening of these mice, but after contacting the lab which generated these mice and following their protocol, we seemed to be on track and it appeared as if we had identified some homozygotes. However, upon rescreening and isolating tissues with known high ING4 expression, we could not detect any loss in ING4 expression. These mice were generated by gene-trap insertion. Unfortunately, the only data validating that ING4 was the target of the insertion was a PCR screen – no southern or gene walking strategy was employed. The original paper only screened for mRNA in one tissue and never looked at protein. Our antibody, which we know is specific for ING4 (the target is lost in shING4 cells and elevated in ING4 overexpressing cells) detected abundant ING4 in several tissues of "KO" mice. Thus, we do not believe that this gene insertion disrupted the ING4 gene. It should be noted that no DOD monies were used to generate the CRISPR mice, since this was not an original objective of the SOW.

To overcome this obstacle, we initiated a CRISPR approach to delete ING4 in mice. The Animal Modeling Core at Van Andel Institute has developed an efficient and robust CRISPR program. Injections have been performed and we are awaiting mice. We have worked out the PCR assay to screen the mice. Once we have these mice, they will be crossed to the Pb-Hi-Myc mice. We do not believe ING4 KO will be embryonic lethal, as loss of other members in this family are not lethal.

In the meantime, we began breeding the Pb-Myc mice, which are on a FVB background, into mixed BL6 background to be compatible with the double cross. Tumors/prostates have all been isolated from these control mice.

Aim 3: Determine how loss of ING4 in patients relates to tumor progression. Our objectives for this aim are to 1) establish if there is a correlation between ING4 loss and over expression of Myc, Erg fusions, or Pten loss, and the relationship to disease recurrence in patients (**Task 8**); and 2) determine how ING4 expression correlates with the expression of known differentiation markers in the tumors (**Task 9**). We first had to get IRB and TMA paper work initiated (**Task 7**).

Task 7: We successfully applied for and obtained IRB approval and TMAs from VARI for our test samples and final arrays. We submitted an application to PCBN to obtain TMAs for these studies. They requested better validation of our antibodies. We demonstrated its specificity by lack of staining in shING4 cells, and elevated staining when ING4 was over

expressed. The staining is nuclear as anticipated. PCBN sent a tester array to make sure the antibody works in their array system. It worked well. We are now ready to move on.

Task 8: In the meantime, I directly contacted Dr. De Marzo at Johns Hopkins about potentially collaborating on this study since he is the expert on Pten and Myc IHC in prostate cancer. It turns out he has already conducted studies looking at Pten, Myc, and Erg expression in the PCBN samples we requested. Thus, he is willing to share that data with us for comparison and analysis of our ING4 staining when we receive the PCBN samples. He was extremely helpful in defining exactly what is needed to validate our antibody and to receive the PCBN samples. He requested that we first complete an 80 sample TMA which has clinical parameters. If that is successful, he will send the outcomes TMA. We have requested the 80 sample TMA.

Task 9: Now that we have identified Myc and ING4 targets that are important for PrEC differentiation (Aim 1), we are identifying and testing antibodies to P-CREB, Pten, and Notch3 for their specificity and IHC staining on the VARI TMAs. To date we have interrogated ING4, P-CREB, and Pten on the same TMA at VARI. Statistical analysis of these data indicate 1) ~60% of the tumors have elevated nuclear P-CREB (Fig 7a), 2) 65% of the samples with low ING4, have high P-CREB (Fig 7b), 3) strikingly 85% of those samples with low ING4 also have low Pten (Fig 7c), and although it didn't quite reach significance 4) 65% of the samples with low ING4 also had low Pten and high P-CREB (Fig. 7d). Further validation of these findings will be required on the PCBN TMAs, but the predicted relationship between loss of Pten, leading to increased P-CREB and suppression of ING4 seems to hold true in prostate cancer samples.
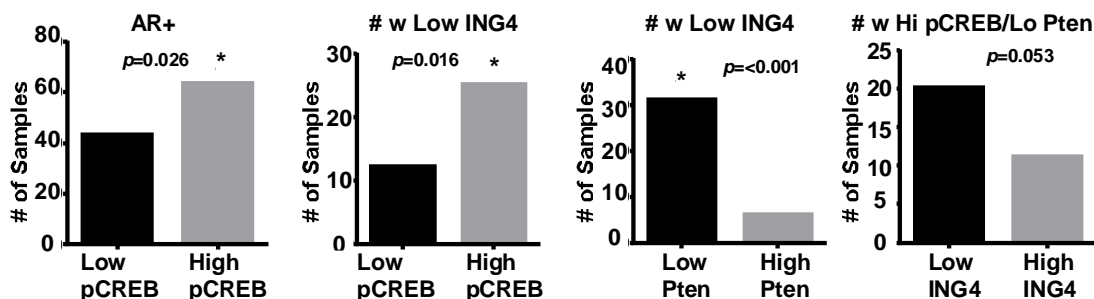
Figure 7: IHC staining of patient samples indicates a strong relationship between loss of Pten, increased P-CREB, and suppression of ING4. Consecutive slices from a TMA of 50 primary prostate cancer samples and 12 normal samples were immune-stained with antibodies to ING4, P-CREB, and Pten. Intensity of staining was graded from 0 to 3, with 0-1 being no staining or low staining and 2-3 being moderate to strong staining. Chi square z test was used to compare correlations between the different proteins.

What opportunities for training and professional development has the project provided?
Nothing to Report

How were the results disseminated to communities of interest?
Nothing to Report."

Plans to accomplish the goals during the next reporting period:

Aim 1: Determine how ING4 controls prostate epithelial differentiation.
We have essentially completed all the studies in Aim1 except for the final analysis and validation of the ChIP-Seq data. We anticipate identifying some ING4 targets that will be important for

controlling prostate epithelial differentiation and will generate a publication from these data. We will validate some of those targets in the human TMAs in Aim3. We will finish publishing the Notch3 and JFK data. We initially proposed there would be a dependency relationship between Notch3 and ING4. However, knocking down Notch3 did not change ING4 expression and conversely knocking down ING4 did not impact Notch3 induction. Thus, these appear to be independent events, both of which are required for differentiation. Thus, we will need to look for other signaling pathways that control ING4 expression.

Aim 2: Determine how loss of ING4 impacts tumorigenesis.
We have completed the majority of the studies in Aim 2 except for the last animal study: crossing ING4-/- mice to the PB-Myc mice. Because of the unanticipated finding that the ING4 mouse was not null, we set about to take a different approach. We are generating ING4 KO mice using CRISPR. The injections have been completed, and we have offspring which we are currently screening. Once we have identified a KO mouse, we will begin crossing to the PB-Myc mice. We have already collected the tumors from the control mice.

Aim 3: Determine how loss of ING4 in patients relates to tumor progression.
Now that we have optimized and validated the ING4 antibody, shown it works on a tester TMA from PCBN, and have successfully stained the staging TMA, we are now ready to work on the outcomes array. In addition, we will be screening these arrays for our ING4 targets.

4. Impact

What was the impact on the development of the principal discipline(s) of the project?
The principal disciplines of our project are cancer biology, prostate cancer, oncogenesis, and differentiation. 1) We are the only lab working with this prostate differentiation model and the first to show the involvement of ING4 in prostate epithelial differentiation – and indeed the first to show ING4 has anything to do with differentiation in any model. We were also the first to demonstrate ING4 is lost in PCa, and to define its relationship to Myc, a well-established oncogene in PCa. 2) We've gone on to identify a potential link between Pten (a well-established tumor suppressor in PCa) and ING4 through CREB. Only a few in vitro studies have interrogated CREB in PCa cell lines; none have looked in human tissues or defined its targets. Previous studies suggest there is a relationship between elevated cAMP/CREB signaling and aggressive disease and therapy resistance. Thus, defining how CREB normally functions in PrECs and how its dysregulation promotes aggressive PCa will be critical to defining indolent from lethal disease. 3) We are the first to identify Notch3 as a crucial Myc target and driver of PrEC differentiation. Notch dysregulation is known to be associated with advanced PCa. It will be important to determine if Notch3 specifically is altered in tumors. 4) We are the first to begin to decipher the exact mechanisms by which several known PCa onocgenes i.e. Myc, Erg, and loss of Pten, contribute to PCa development through dysregulation of differentiation. 5) Our finding that AR-specific expression of the Erg fusion gene is crucial for its ability to disrupt differentiation is a fundamental advancement. How Erg functions as an oncogene is poorly understood. Our studies indicate that its specific expression within a luminal-like population (and its absence from basal cells), is important. Thus, analysis of potential oncogenic Erg targets has to take this into consideration and calls into question some of the target data and models using constitutive overexpression of Erg. 5) This work will contribute to defining the cell of

15

origin in PCa. Moreover, because these studies use human cells, the mechanisms that are specifically important in human disease, as opposed to mice, will be better defined.

What was the impact on other disciplines?
Nothing to Report

What was the impact on technology transfer?
Nothing to Report

What was the impact on society beyond science and technology?
Nothing to Report.

5. Changes/Problems
We encountered problems with being able to validate the ING4 KO mice as actually being KO mice. The mouse supposedly was generated with a gene trap; however, we were unable to 1) validate the site of insertion, 2) demonstrate any loss in ING4 protein expression in several tissues even after 3 generation crosses, and 3) did not detect any changes in ING4 mRNA. Upon consultation with another PI who also tried to work with the mice, we both concluded they are not ING4 KO mice. Since the Vivarium Core at VARI has developed efficient and effective techniques for using CRISPR in mice, we decided to generate ING4 KO mice using CRISPR. Once we have those, we will cross them to Pb-Myc mice as originally planned.

6. Products

Publications
The following publications relevant to this project were published. Copies are in the appendix.

> Berger PL, Frank SB, Schulz VV, Nollet EA, Edick MJ, Holly B, Chang TA, Hostetter G, Kim S and **Miranti CK**. 2014. Transient induction of ING4 by MYC drives prostate epithelial cell differentiation and its disruption drives prostate tumorigenesis. **Cancer Res** 74:3357-68.

> Berger PL, Winn ME, and **Miranti CK**. 2016. Miz1, a Novel Target of ING4, Can Drive Prostate Luminal Epithelial Cell Differentiation. **The Prostate**, accepted.

> Frank SB, Schultz VV, and Miranti CK. 2016. A Streamlined Method for the Design and Cloning of shRNAs into an Optimized Dox-inducible Lentiviral Vector. **BMC Biotechnology**, submitted.

> Frank SB, Berger PL, Ljungman M and **Miranti CK**. 2016. Prostate Luminal Cell Differentiation requires Notch3 Induction via p38α-MAPK and Myc. **Development**, ready for submission.

Books or other non-periodical, one-time publications.
None

Conferences and presentations
Posters:

      <u>Frank SB</u> and Miranti CK. 2014. p38-MAPK Regulation of Notch via Myc is Required for Prostate Epithelial Cell Differentiation. Society for Basic Urologic Research. Dallas, TX, November 13-16.

      Frank SB, Berger PL and <u>Miranti CK</u>. 2015. Myc governs a prostate epithelial differentiation program involving chromatin remodeling protein ING4 and Notch3: Disruption of which is necessary for human prostate cancer development. AACR: MYC: From Biology to Therapy. San Diego, CA, Jan 7-10.

      Berger PL, Watson M, Winn ME and <u>Miranti CK</u>. 2015. Elucidating ING4 Targets Important in Prostate Epithelial Cell Differentiation and Examining CREB as a Key Regulator of ING4 Expression. Society for Basic Urologic Research. Fort Lauderdale, FL, Nov 12-15.

      Berger PL, Watson M, Winn ME and <u>Miranti CK</u>. 2015. Key Intermediate Progenitor in Luminal Prostate Epithelial Differentiation Dictates Susceptibility to Myc Overexpression and Pten Loss in Prostate Cancer Cell of Origin. AACR: Developmental Biology and Cancer. Boston, MA, Nov 30-Dec 3.

Presentations:

      <u>Miranti, CK</u>. 2015. Elucidating ING4 Targets Important in Prostate Epithelial Cell Differentiation and Examining CREB as a Key Regulator of ING4 Expression. SUBR Annual Meeting: Environment-Gene Interface in Urologic Disease, Fort Lauderdale, FL, Nov 12-15.

      <u>Miranti, CK</u>. 2015. SwitchING4 Prostate Cancer: A Differentiation Control Switch that Defines the Cell of Origin for Prostate Cancer, University of AZ, Tucson, AZ, Dec 7.

Other Products

<u>HUMAN In Vitro Differentiation Model:</u> This model utilizes primary or immortalized basal epithelial cells isolated from patients. Cells are grown to confluency in defined medium and then treated with DHT and KGF. Over a period of 14-20 days, a subset of basal cells differentiate into functional secretory luminal cells (Lamb *et al.*, 2010). This model was initially developed using primary cells by a graduate student, Dr. Laura Lamb, who received a DOD Predoctoral Award for this work. We have since generated 2 immortalized cell lines and obtained one from Dr. John Isaacs. All three lines behave similar to the primary cells. These lines have now been stably modified to express a host of different genes or shRNA, either constitutively or under control of Tet-R or ARE. These cell lines and model greatly expand the HUMAN repertoire of tools available for PCa research.

Mouse Model: We are crossing Pb-Myc-Hi mice to ING4 KO mice. If successful, we anticipate this will generate a more aggressive Myc model for PCa. We will have also generated an ING4 KO mouse using CRISPR. Both will be made available to anyone wanting them.

RNA-Seq Data: We generated 3 sets of RNA-Seq data. This data defines the mRNA transcriptional program of normal HUMAN prostate epithelial differentiation from basal cells into luminal cells, from luminal cells to tumor cells, and defines those genes targeted by ING4, Myc, and p38-MAPK during differentiation. Two of the three datasets are now publically available at GEO.

ChIP-Seq Data: We generated one set of ChIP-Seq data to identify the genes that ING4 binds during prostate epithelial differentiation. This data set will be submitted to GEO at the time of publication.

7. Participants & Other Collaborating Organizations

What individuals have worked on the project?

Van Andel Research Institute
Name: Cindy Miranti
Project Role: Principal Investigator
Research Identifier:
Nearest Person Month Worked: 2 (Year 1) + 2 (Year 2) = 4
Contribution to the project: Supervised and directed the project. Obtained necessary IACUC and IRB approvals. Managed, analyzed, and interpreted data. Submitted and presented abstracts at meetings. Wrote this report.

Name: Penny Berger
Project Role: Research Technician
Research Identifier:
Nearest Person Month Worked: 10 (Year 1) + 8 (Year 2) = 18
Contribution to the project: Designed, executed, interpreted, and prepared data on ING4, Miz1, and JFK. Managed and initiated the ING4 and Pb-Myc mouse breeding and crosses. Did the Xenograft studies. Worked on validating the ING4, Miz1, and P-CREB antibody for future IHC/TMA tissue studies.

Name: Sander Frank
Project Role: Graduate Student (MSU)
Research Identifier:
Nearest Person Month Worked: 6 (Year 1) + 6 (Year 2) = 12
Contribution to the project: Designed, executed, interpreted, and prepared data on p38-MAPK, Myc, and Notch3. Assisted with molecular biology and development of reagents on many aspects of the project.

Name: McLane Watson
Project Role: Assistant Research Technician

Researcher Identifier:
Nearest Person Month Worked: 4 (Year 1) + 2 (Year 2) = 6
Contribution to the project: Worked with Bioinformatics Core to analyze RNA-seq data. Validated and conducted CREB and Pten experiments.
Funding Support: Internal funds from VARI were used for salary support.

Translational Genomics Research Institute
Name: Suwon Kim
Project Role: Sub-contract PI
Research Identifier (e.g. ORCID ID):
Nearest Person Month Worked: 1 (Year 1) + 1 (Year 2) = 2
Contribution to the project: Ensured the progress and completion of RNA sequencing by working with the Collaborative Sequencing Center at TGen and communicated the data to the PI
Funding Support: The salary support was from the University of Arizona funds allocated for faculty salary.

Name: Madeline Keenen
Project Role: Technician
Research Identifier (e.g. ORCID ID):
Nearest Person Month Worked: 1
Contribution to the project: Performed QC of the RNA samples and initial steps of library preparation for the sequencing.

Has there been a change in the active other support of the PD/PI(s) or senior/key personnel since the last reporting period?
Nothing to Report.

What other organizations were involved as partners?
Nothing to Report

8. Special Reporting Requirements
None

9. Appendices

1. Berger PL, Frank SB, Schulz VV, Nollet EA, Edick MJ, Holly B, Chang TA, Hostetter G, Kim S and **Miranti CK**. 2014. Transient induction of ING4 by MYC drives prostate epithelial cell differentiation and its disruption drives prostate tumorigenesis. **Cancer Res** 74:3357-68.
2. Berger PL, Winn ME, and **Miranti CK**. 2016. Miz1, a Novel Target of ING4, Can Drive Prostate Luminal Epithelial Cell Differentiation. **The Prostate**, accepted.
3. Frank SB, Schultz VV, and Miranti CK. 2016. A Streamlined Method for the Design and Cloning of shRNAs into an Optimized Dox-inducible Lentiviral Vector. **BMC Biotechnology**, submitted.

4. Frank SB, Berger PL, Ljungman M and **Miranti CK**. 2016. Prostate Luminal Cell Differentiation requires Notch3 Induction via p38α-MAPK and Myc. **Development**, ready for submission.

Citations

Berger, P.L., Frank, S.B., Schulz, V.V., Nollet, E.A., Edick, M.J., Holly, B., Chang, T.T., Hostetter, G., Kim, S., and Miranti, C.K. (2014). Transient induction of ING4 by Myc drives prostate epithelial cell differentiation and its disruption drives prostate tumorigenesis. Cancer Res *74*, 3357-3368.

Berger, P.L., Winn, M.E., and Miranti, C.K. (2016). Miz1, a Novel Target of ING4, Can Drive Prostate Luminal Epithelial Cell Differentiation. *The Prostate*, accepted.

Caravatta, L., Sancilio, S., di Giacomo, V., Rana, R., Cataldi, A., and Di Pietro, R. (2008). PI3-K/Akt-dependent activation of cAMP-response element-binding (CREB) protein in Jurkat T leukemia cells treated with TRAIL. J Cell Physiol *214*, 192-200.

Gebhardt, A., Frye, M., Herold, S., Benitah, S.A., Braun, K., Samans, B., Watt, F.M., Elsasser, H.P., and Eilers, M. (2006). Myc regulates keratinocyte adhesion and differentiation via complex formation with Miz1. J Cell Biol *172*, 139-149.

Gu, T., Zhang, Z., Wang, J., Guo, J., Shen, W.H., and Yin, Y. (2011). CREB is a novel nuclear target of PTEN phosphatase. Cancer Res *71*, 2821-2825.

Lamb, L.E., Knudsen, B.S., and Miranti, C.K. (2010). E-cadherin-mediated survival of androgen-receptor-expressing secretory prostate epithelial cells derived from a stratified in vitro differentiation model. J Cell Sci *123*, 266-276.

Lyu, J., Yu, X., He, L., Cheng, T., Zhou, J., Cheng, C., Chen, Z., Cheng, G., Qiu, Z., and Zhou, W. (2015). The protein phosphatase activity of PTEN is essential for regulating neural stem cell differentiation. Mol Brain *8*, 26.

Paulsen, M.T., Veloso, A., Prasad, J., Bedi, K., Ljungman, E.A., Magnuson, B., Wilson, T.E., and Ljungman, M. (2014). Use of Bru-Seq and BruChase-Seq for genome-wide assessment of the synthesis and stability of RNA. Methods *67*, 45-54.

Yan, R., He, L., Li, Z., Han, X., Liang, J., Si, W., Chen, Z., Li, L., Xie, G., Li, W., Wang, P., Lei, L., Zhang, H., Pei, F., Cao, D., Sun, L., and Shang, Y. (2015). SCF(JFK) is a bona fide E3 ligase for ING4 and a potent promoter of the angiogenesis and metastasis of breast cancer. Genes Dev *29*, 672-685.

Cancer Research

Transient Induction of ING4 by Myc Drives Prostate Epithelial Cell Differentiation and Its Disruption Drives Prostate Tumorigenesis

Penny L. Berger, Sander B. Frank, Veronique V. Schulz, et al.

Updated version	Access the most recent version of this article at: doi:10.1158/0008-5472.CAN-13-3076
Supplementary Material	Access the most recent supplemental material at: http://cancerres.aacrjournals.org/content/suppl/2014/04/24/0008-5472.CAN-13-3076.DC1.html

Cited Articles	This article cites by 47 articles, 19 of which you can access for free at: http://cancerres.aacrjournals.org/content/74/12/3357.full.html#ref-list-1

E-mail alerts	Sign up to receive free email-alerts related to this article or journal.
Reprints and Subscriptions	To order reprints of this article or to subscribe to the journal, contact the AACR Publications Department at pubs@aacr.org.
Permissions	To request permission to re-use all or part of this article, contact the AACR Publications Department at permissions@aacr.org.

Transient Induction of ING4 by Myc Drives Prostate Epithelial Cell Differentiation and Its Disruption Drives Prostate Tumorigenesis

Penny L. Berger[1], Sander B. Frank[1,5], Veronique V. Schulz[1], Eric A. Nollet[1,4], Mathew J. Edick[1], Brittany Holly[2], Ting-Tung A. Chang[2], Galen Hostetter[3], Suwon Kim[6], and Cindy K. Miranti[1]

Abstract

The mechanisms by which Myc overexpression or Pten loss promotes prostate cancer development are poorly understood. We identified the chromatin remodeling protein, ING4, as a crucial switch downstream of Myc and Pten that is required for human prostate epithelial differentiation. Myc-induced transient expression of ING4 is required for the differentiation of basal epithelial cells into luminal cells, while sustained ING4 expression induces apoptosis. ING4 expression is lost in >60% of human primary prostate tumors. ING4 or Pten loss prevents epithelial cell differentiation, which was necessary for tumorigenesis. Pten loss prevents differentiation by blocking ING4 expression, which is rescued by ING4 re-expression. Pten or ING4 loss generates tumor cells that co-express basal and luminal markers, indicating prostate oncogenesis occurs through disruption of an intermediate step in the prostate epithelial differentiation program. Thus, we identified a new epithelial cell differentiation switch involving Myc, Pten, and ING4, which when disrupted leads to prostate tumorigenesis. Myc overexpression and Pten loss are common genetic abnormalities in prostate cancer, whereas loss of the tumor suppressor ING4 has not been reported. This is the first demonstration that transient ING4 expression is absolutely required for epithelial differentiation, its expression is dependent on Myc and Pten, and it is lost in the majority of human prostate cancers. This is the first demonstration that loss of ING4, either directly or indirectly through loss of Pten, promotes Myc-driven oncogenesis by deregulating differentiation. The clinical implication is that Pten/ING4 negative and ING4-only negative tumors may reflect two distinct subtypes of prostate cancer. *Cancer Res; 74(12); 3357–68. ©2014 AACR.*

Introduction

Normal prostate glands contain prostatic ducts composed of two distinct layers of epithelial cells: luminal cells that express androgen receptor (AR) and secrete prostate-specific antigen (PSA) and basal cells that express nuclear p63. It is thought that the stem or progenitor cells within or in proximity of the basal layer differentiate and give rise to the luminal cells (1, 2). Prostate tumors are often devoid of the cell layer distinction and express both luminal and basal cell markers, suggesting deregulated cell differentiation. That prostate can-

cer arises from deregulated differentiation is also supported by mouse models. The most notable example is loss of Nkx3.1, a known prostate-specific differentiation gene, which predisposes mice to develop prostate cancer in the context of additional oncogenic events (3). Two other well characterized oncogenic events linked with prostate cancer are loss of Pten or overexpression of Myc (4, 5). Both of which lead to downregulation of Nkx3.1 expression, but are also sufficient to induce prostate cancer in mice (6, 7). The prostate-specific oncogene, TMPRSS2-Erg, when overexpressed in mouse prostates leads to prostate intraepithelial neoplasia (PIN), with a corresponding change in differentiation, where progenitor cell markers Sca1 and integrin α6 are increased, whereas basal cell keratin is diminished and AR is expressed (8, 9). In addition, overexpression of Erg upregulates Myc expression and produces an expression profile consistent with a change in differentiation (10). A recent mouse study where Pten was deleted in either basal or luminal cells, demonstrated the appearance of $K5^+/K8^+$ intermediate tumor cells, further supporting the idea that deregulated differentiation is a hallmark of prostate cancer (11). However, the mechanism by which differentiation is deregulated is unknown.

We recently reported on an *in vitro* differentiation model in which AR-negative human basal prostate epithelial cells can be differentiated into AR-positive and androgen-responsive

Authors' Affiliations: [1]Laboratory of Integrin Signaling; [2]Laboratory of Translational Imaging; and [3]Laboratory of Analytical Pathology; and [4]Van Andel Institute Graduate School, Grand Rapids; [5]Genetics Graduate Program, Michigan State University, Lansing, Michigan; and [6]Tranlational Genomics Research Institute and University of Arizona College of Medicine, Phoenix, Arizona

Corresponding Author: Cindy K. Miranti, Laboratory of Integrin Signaling, Van Andel Research Institute, 333 Bostwick Avenue NE, Grand Rapids, MI 49503. Phone: 616-234-5358; Fax: 616-234-5359; E-mail: cindy.miranti@vai.org

postmitotic secretory cells (12). Based on known prostate and epithelial differentiation markers, and the demonstration that PSA can be secreted into the medium from the differentiated cells, this model recapitulates the biology and physiology of the human prostate gland *in vivo*. A major step in the differentiation process is the loss of integrin expression and cell–matrix adhesion, which is crucial to generate stable AR-expressing cells. This is accompanied by a dramatic shift in survival signaling pathways, whereby basal cells, which survive primarily through integrin-mediated activation of the Erk signaling pathway, give rise to secretory cells that depend on E-cadherin based cell–cell adhesion and activation of Akt for survival.

The separation of AR and integrin functions in the two different epithelial populations is wholly consistent with what is observed *in vivo*; that integrin expression is limited to the basal cells and AR is only in the secretory cells (13, 14). In prostate cancer this distinction is lost, whereby AR and integrin $\alpha6\beta1$ are coexpressed in the tumors, where integrin $\alpha6\beta1$ cooperates with AR to promote the survival of prostate cancer cells (15). Other markers typically associated with basal or intermediate cells, such as receptor tyrosine kinases EGFR and Met, bcl-2, and coexpression of basal and secretory keratins K5 and K8, are also found in tumor cells that express AR-dependent differentiation genes (14, 16, 17). Thus, the majority of the primary tumor population in prostate cancer resembles a potential differentiation intermediate. In addition, the unexplained loss of basal cells in prostate cancer points to altered differentiation as a major factor in prostate cancer (18).

Myc is overexpressed in up to 90% of primary prostate tumors, presenting itself as a major driver in prostate cancer (4). Recent studies have unraveled the function of Myc in reprogramming of somatic cells into pluripotent stem cells and the maintenance of self-renewal in stem cells (19), and is consistent with the idea that deregulated Myc prevents full differentiation of prostate epithelial cells, leading to prostate cancer when given additional molecular lesions. ING4 is a tumor suppressor whose expression is lost in several cancers; but whose role in prostate cancer is unknown (20). ING4 is a plant homeodomain–containing transcriptional regulator, which binds trimethylated histone H3 and recruits the HBO1 acetyltransferase to increase histone acetylation (21). ING4 was shown to block Myc-induced anchorage-independence and mammary hyperplasia in a mouse model of breast cancer, suggesting ING4 may function to suppress Myc (22, 23). We hypothesized there would be an interplay between Myc and ING4 in prostate epithelial cell differentiation that would be disrupted in prostate tumorigenesis. In this study, we determine how Myc, Pten, and ING4 are involved in normal prostate epithelial differentiation and demonstrate the importance of ING4 loss in promoting prostate oncogenesis through suppressing differentiation.

Materials and Methods

Cell lines

Primary basal prostate epithelial cells were isolated from clinical prostectomies as previously described (24, 25). Cultures were validated to be Mycoplasma-free and express only basal epithelial cell markers (12, 25). Cells were immortalized with retroviruses expressing HPV E6/E7 and hTert, selected in 150 μg/mL neomycin for 3 days, and the resulting population pooled. Cells retain all the basal markers of primary cells. Immortalized cells (iPrEC) were transformed by retroviruses expressing Erg and Myc (EM), and lentivirus expressing Pten shRNA (EMP) or ING4 shRNA (EMI), then selected and maintained in 0.35 μg/mL puromycin. All lines were maintained and passaged as previously described (24, 25).

Differentiation protocol

Differentiation and layer separation protocols were detailed previously (12). Briefly, iPrECs at confluency were treated in complete growth medium with 10 ng/mL keratinocyte growth factor (KGF; Cell Sciences) and 5 nmol/L R1881 (PerkinElmer) every other day for up to 21 days. For biochemical analysis, the suprabasal differentiated layer was separated from the basal layer as previously described (12).

Constructs

The wild-type retroviral pBabe-Myc construct was obtained from Dr. B. Knudsen. pLPCX-Erg was generated by subcloning the *ERG* cDNA *Not*I/*Spe*I fragment from pMax Dest ΔN-Erg (9), supplied by Dr. Vasioukhin, into *Not*I/*Xho*I of pLPCX. The wild-type (pMIG-ING4) and C-terminal deletion mutant (pMIG-ING4-ΔC1) of ING4 were described previously (23). The ING4 shRNA construct was generated by subcloning the oligo 5'-CCGGGCTAGGTGTGATCAACACTTTCTCGAGAAAGTGTT-GATCACACCTAGCTTTTTTG-3', complementary to the 3'-UTR of ING4, into a lentiviral vector to generate pLKO.1-shING4. The pLKO vector containing Pten shRNA was generated by first creating a pCR8-GW-TOPO-shLEGO shuttle vector. A 344bp PCR product containing a multicloning site, *Eco*RV/*Xba*I/*Sal*I/*Pst*I, the pLKO U6 promoter, an *Age*I site, a *Hin*dIII site, followed by a reverse multicloning site, *Pst*I/*Sal*I/*Xba*I/*Eco*RV, and an *Eco*RI site was TA cloned into pCR8-GW-TOPO. Oligo shPten2, 5'-CCGGTCCACAGCTAGAACTTAT-CAAACTCGAGTTTGATAAGTTCTAGCTGTGGTTTTTA-3', was cloned into the *Age*I/*Hin*dIII site of the pCR8-GW-TOPO-shLEGO shuttle vector. The *Age*I/*Eco*RI fragment was subcloned into pLKO to generate pLKO-shPten2.

Virus generation and infection

Lentivirus shRNAs were generated by transfecting a packaging cell line, harvesting virus 3 days later and immediately infecting iPrECs. Cells were selected and pools maintained in 0.35 μg/mL puromycin. Retroviruses expressing ING4 or Myc were generated by transfecting Phoenix cells (National Gene Vector Biorepository), harvesting 2 days later and immediately infecting iPrECs. Myc expressing cells were selected and maintained in 0.35 μg/mL puromycin. ING4 construct has no selectable marker and cells were generated *de novo* as needed.

siRNA transfection

A pool of siRNAs against Myc and a nontargeting sequence were purchased from Origene. ON-Targetplus SMARTpool targeted to Bnip3, came from Dharmacon. Differentiated cultures were serially transfected every 2 days with Myc or

control siRNA using siLentFect lipid reagent (Bio-Rad) following manufacturer's directions. Cells were placed in differentiation medium 18 hours after transfection.

Antibodies

Immunofluorescence. AR (C-19), Nkx3.1 (H-50), and TMPRSS2 (H-50) were purchased from Santa Cruz. ITGα6 (GoH3) was purchased from BD Pharmingen, and PSA (18127) from R&D Systems. Keratin 8 (M20) came from Abcam and Keratin 5 (AF-138) came from Covance. ING4 monoclonal antibody was generated as previously described (26) and a polyclonal antibody was obtained from Proteintech. Cleaved caspase-3 (Asp175)(5A1E) was purchased from Cell Signaling.

Immunoblotting. Myc (o6–340) was purchased from Millipore, Erg (C-20) from Santa Cruz, Pten (138G6) and p27 (Kip1) from Cell Signaling, and ING4 (EP3804) from GeneTex. Tubulin antibody (DM1A) was purchased from Sigma and GAPDH (6CS) from Millipore. Polyclonal integrin α6 (AA6A) antibody was a gift from Dr. A. Cress (University of Arizona; ref. 27).

Immunostaining and microscopy

Differentiated cultures were fixed in 4% paraformaldehyde and permeabilized with 0.2% Triton-X 100. After washing, cells were blocked with 2% normal goat serum for 2 hours. Primary antibodies, diluted in 1% BSA/PBS, were applied to samples overnight at 4°C. After washing, secondary conjugated antibodies diluted in 1% BSA/PBS were incubated for 1 to 2 hours. Nuclei were stained with Hoechst 33258 (Sigma) for 10 minutes at room temperature. Coverslips were mounted using Fluoromount-G (SouthernBiotech). Epifluorescent images were acquired on a Nikon Eclipse TE300 fluorescence microscope using OpenLab v5.5.0 image analysis software (Improvision). Confocal images were acquired by sequential detection on an Olympus FluoView 1000 LSM using FluoView software v5.0.

Immunoblotting

Total cell lysates were prepared for immunoblotting as previously described (24). Briefly, cells were lysed in RIPA buffer, 30 to 50 μg of total cell lysates were run on SDS polyacrylamide gels and transferred to PVDF membranes. Membranes were blocked in 5% BSA in TBST overnight at 4°C then probed with primary antibody, and HRP-conjugated secondary antibodies (Bio-Rad) in TBST + 5% BSA. Signals were visualized by chemiluminescence reagent with a CCD camera in a Bio-Rad Chemi-Doc Imaging System using Quantity One software v4.5.2 (Bio-Rad).

RT-PCR

Total RNA was isolated using Qiagen's RNeasy Kit. RNA was purified with RNase-free DNase and RNeasy Mini Kits (Qiagen). For qRT-PCR, 0.5 μg RNA was reversed transcribed using a reverse transcription system (Promega). Synthesized cDNA was amplified for qRT-PCR using SYBR Green Master Mix (Roche) with gene-specific primers and an ABI 7500 RT-PCR system (Applied Biosystems). Gene expression was normalized to 18s rRNA by the $2^{-\Delta\Delta Ct}$ method (28). Primers for ING4 and Myc were as follows: ING4: 5′-TCGGAAGTTGCTTTGTTTTGC-3′, Myc: 5′-TTCGGGTAGTGGAAAACCAG-3′.

Mouse tumorigenesis

Half a million iPrEC, EM, EMP, EMI, or EM-vector cells were injected orthotopically into the prostates of 8-week nude mice. Mice were monitored by ultrasound between 8 and 18 weeks for the development of tumors. Mice were sacrificed between 16 and 18 weeks and prostate glands analyzed histologically for tumors. In one cohort of EMPs, 5 mice with tumors were castrated 16 weeks postorthotopic transplantation and measured by ultrasound for regression of tumors. All animal work was carried out following Institutional Animal Care and Use Committee approval at an Association for Assessment and Accreditation of Laboratory Animal Care-accredited facility.

Histology

Prostates isolated from mice were formalin-fixed and paraffin-embedded. Sections were analyzed following hematoxylin and eosin or immunohistochemical (IHC) staining. Human-specific MHC class I was purchased from Abcam, polyclonal ING4 was purchased from ProteinTech, and AR (N-20) was purchased from Santa Cruz. IHC was performed using automated immunostaining (Ventana Discovery XT). A human prostate tumor survey tissue microarray (TMA) was constructed as previously described (29). The prostate survey TMA contained 52 de-identified unique prostate carcinomas ranging from Gleason 6 to 9 and 23 control cores, including 14 cases of benign prostatic hypertrophy (BPH). TMA sectioned at 5 μm thicknesses was stained using standard DAB. IHC was performed with ING4 antibody as previously described (26, 30). For validation, sections were also stained with a commercial ING4 antibody (ProteinTech). Negative control was nonimmune rabbit antiserum without primary antibody. TMA staining was scored manually with IHC assigned to each core as composite scores of 0, 1, 2, or 3 with 0 to 1 representing complete to major loss of protein, and 2 to 3 near normal to wild-type levels.

Results

Myc and ING4 are transiently expressed during differentiation

When grown to confluency and treated with KGF plus androgen, primary cultures of basal prostate epithelial cells (PrEC) undergo differentiation such that a second suprabasal layer forms on top of the basal layer in about 2 weeks (12). An immortalized primary prostate epithelial cell line (iPrEC) was established by expressing the E6/E7 viral oncogenes and hTert. Treatment of confluent iPrEC cultures with 10 ng/mL KGF and 5 nmol/L R1881, a synthetic AR agonist, for 18 days resulted in a distinct top layer of cells that no longer expressed integrin α6, K14, or p63 but expressed AR and AR-dependent targets, such as TMPRSS2 and Nkx3.1 (Fig. 1A and Supplementary Figs. S1 and S2). These data indicate iPrECs retain the ability to differentiate.

ING4 expression was low to undetectable in untreated iPrECs, but by as early as 8 days of differentiation, distinct nuclear staining was detected in the newly forming suprabasal layer of differentiated cells (Fig. 1B). The initial increase in
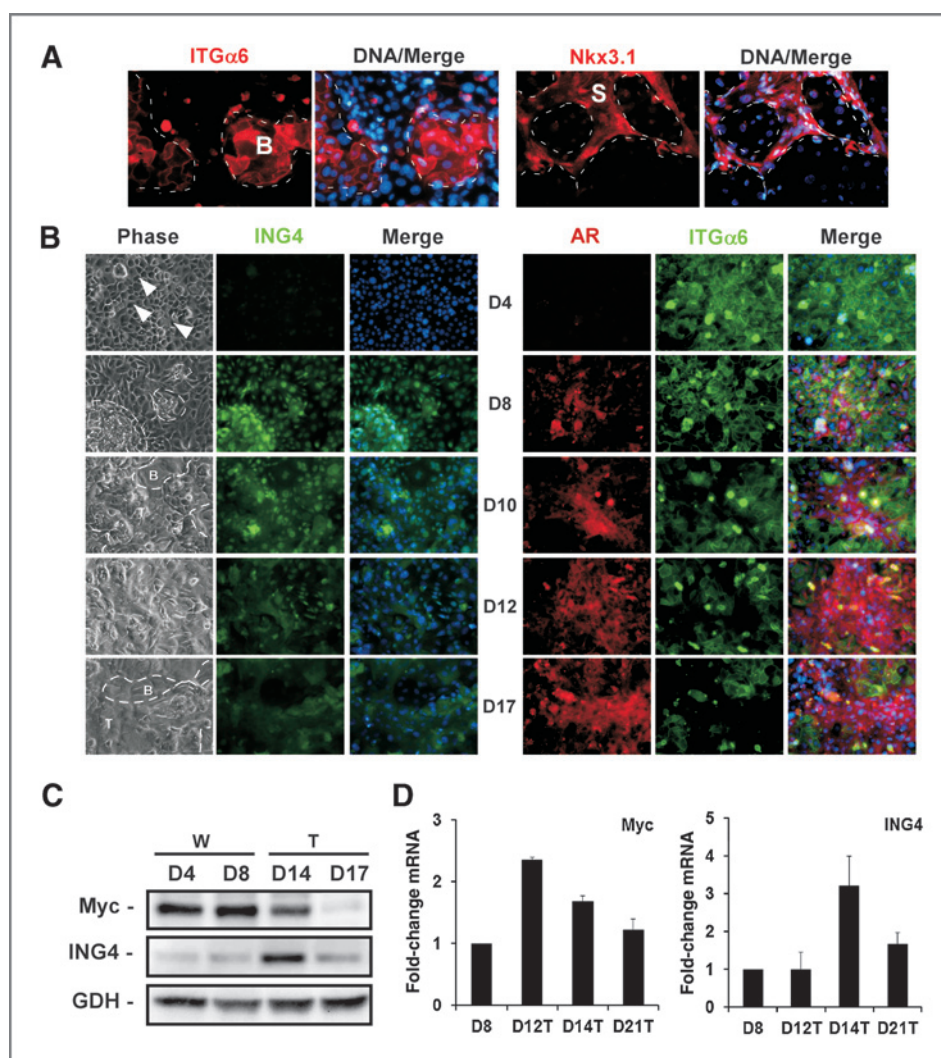
Figure 1. ING4 is transiently expressed in differentiated immortalized prostate epithelial cells. Confluent immortalized prostate epithelial cells (iPrEC) were induced to differentiate with 10 ng/mL KGF and 5 nmol/L R1881 for 4 to 21 days. A, terminally differentiated iPrECs were immunostained (red) and counterstained with Hoechst (blue), then imaged by confocal microscopy. Suprabasal cells (S) express NKX3.1, whereas only basal cells (B) express integrin α6. Dashed lines demarcate suprabasal and basal layer cells. B, iPrECs were immunostained 4 to 17 days after differentiation to detect ING4 (green), AR (red), or integrin α6 (green). C and D, protein or RNA was isolated from whole (W) differentiated cultures at days 4 to 8 or only the suprabasal (T, top) cells at days 12 to 21. C, ING4, Myc, and GAPDH (GDH) were detected by immunoblotting. D, ING4 and Myc mRNA were measured by qRT-PCR. Data are normalized to 18S rRNA and are mean ± SD.

ING4 expression was coincident with the increase in AR expression and the loss of integrin α6 expression, two hallmarks of differentiation (Fig. 1B and Supplementary Fig. S1B). At no time point were we able to dissociate ING4 expression from changes in AR or integrin α6 expression; nor were we able to separate loss of basal keratin K14 from integrin α6 loss (Supplementary Fig. S2), suggesting ING4 controls a major differentiation switch. Although AR persisted in the differentiated layer, ING4 expression was transient and no longer nuclear at later time points.

Once a sufficient number of cells have differentiated, typically between day 12 and 14, it is possible to separate the top layer of differentiated cells from the bottom layer (12). Immunoblot analysis of whole cultures from days 4 and 8, and the top layers from days 14 and 17 indicated a transient increase in ING4 protein expression at day 14, which returned to basal level expression by day 17 (Fig. 1C). ING4 mRNA expression also peaked at day 14 (Fig. 1D). The apparent lag in ING4 expression seen biochemically, compared with the immunostaining data, is most likely because of the low number of differentiated cells within the culture relative to the basal cells at early time points.

Over the same time course, Myc protein and mRNA expression were also transiently elevated (Fig. 1C and D). Myc expression preceded that of ING4 expression, suggesting a concerted temporal regulation of Myc and ING4 during iPrEC differentiation.

Myc-induced ING4 expression is required for differentiation

Cells were engineered to overexpress ING4, Myc, and/or ING4 shRNA (Fig. 2A). Although ING4 expression levels did not affect Myc expression, most notable was the increase in ING4 expression in the Myc overexpressing cells (Fig. 2A and B). These results suggest that Myc is responsible for the increase in ING4 expression during iPrEC differentiation.

Overexpression of ING4 or Myc accelerated the emergence of differentiated cells compared with the control iPrECs. The appearance of suprabasal layer cells, loss of integrin α6, and gain in Nkx3.1 expression was more robust between days 8 and

Figure 2. Myc-induced ING4 expression is required for differentiation. iPrECs were engineered to overexpress ING4, Myc, ING4 and Myc, ING4 shRNA (shING4), or Myc with shING4. A, ING4, Myc, and tubulin (Tub) expression in basal cells were measured by immunoblotting. B, cells differentiated for 8 days were immunostained for ING4 (green) and imaged by fluorescent microscopy. C, cells differentiated for 12 days were immunostained (red) to detect NKX3.1 or ITGα6, counterstained with Hoechst (blue), and imaged by fluorescent microscopy. D–F, one day after inducing differentiation, iPrECs (iPr) or iPrECs overexpressing ING4 (ING4) were serially transfected with Myc siRNA (siMyc) or a scrambled sequence (Scr) on days 2, 4, and 6. D, ING4 and Myc expression were detected in undifferentiated (iPr) or in siRNA-treated differentiated cells on day 8 by immunoblotting. E and F, differentiated iPrECs (iPr) or ING4-overexpressing cells were immunostained for ING4 (red), AR (red), or ITGα6 (green) on day 9.
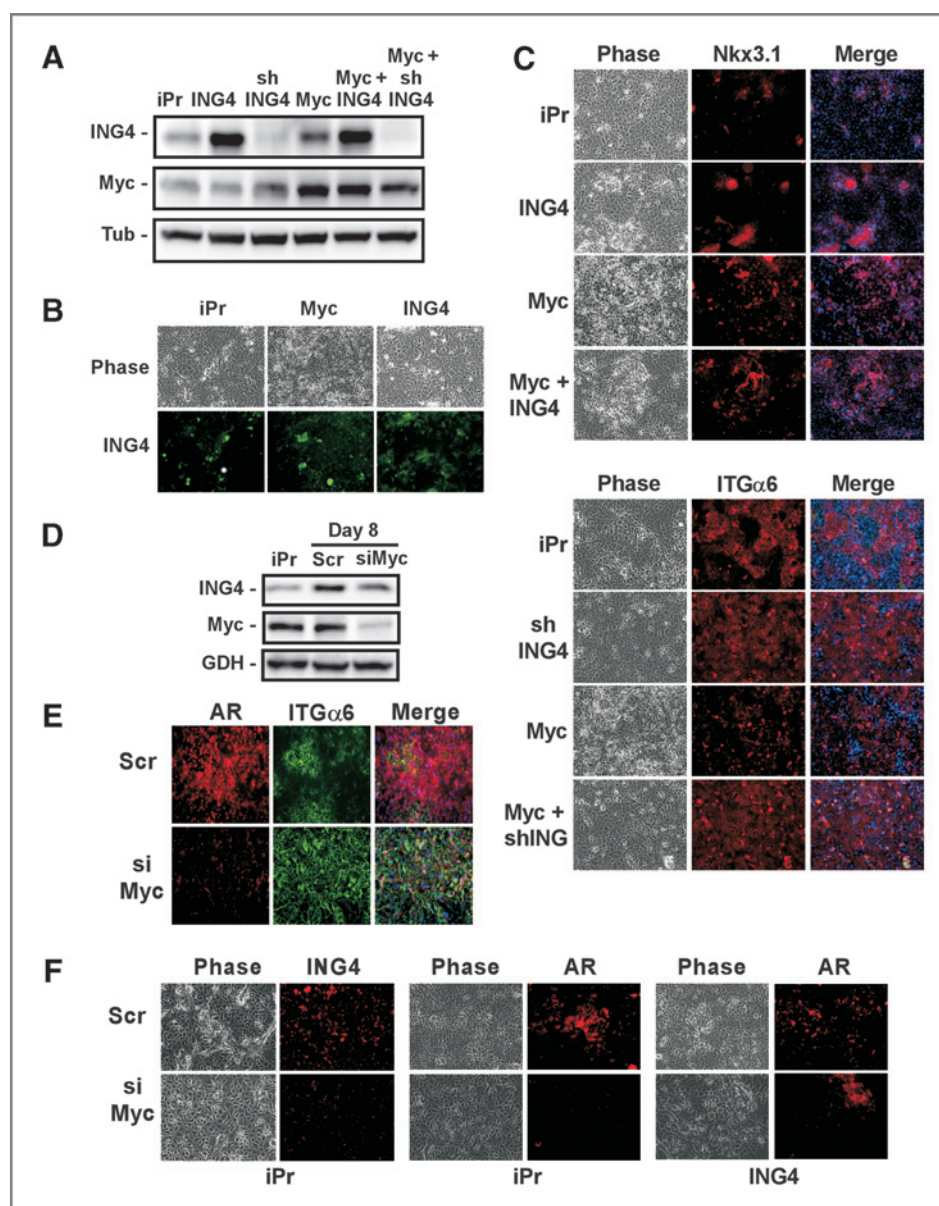
12 in the ING4 or Myc overexpressing cells, whereas the control iPrECs do not robustly express the same set of differentiation markers until days 14 to 16 (day 12 shown in Fig. 2C). Combined overexpression of Myc and ING4 did not exert an additive effect on accelerating differentiation compared with cells overexpressing either Myc or ING4 alone (Fig. 2C). However, it should be noted that the higher levels of ING4 expression in the Myc+ING4 cell line (Fig. 2A) was not always observed; most likely it is not tolerated because of enhanced cell death (see Fig. 3). Thus, it is possible we did not achieve levels of ING4 overexpression required for an additive effect. Downregulation of ING4 expression by shRNA (shING4) severely retarded the emergence of differentiated cells (Fig. 2C). Reduced ING4 expression prevented cells from appearing in the suprabasal layer, and the con-

comitant loss of integrin α6 (Fig. 2C) and gain of AR, indicating an absolute necessity for ING4 to suppress integrin α6 and permit AR expression.

The ability of Myc to accelerate differentiation was blocked by shING4 (Fig. 2C), indicating ING4 functions downstream of Myc during differentiation. This epistatic relationship is further supported by the fact that transient inhibition of Myc expression between days 2 to 6 failed to induce ING4 expression (Fig. 2D and F) and completely blocked differentiation (Fig. 2E and F). Furthermore, ING4 overexpression rescued the differentiation blocked by siMyc (Fig. 2F). Taken together, our results indicate that a temporal peak in Myc expression is required for the subsequent induction and transient expression of ING4 during iPrEC differentiation.
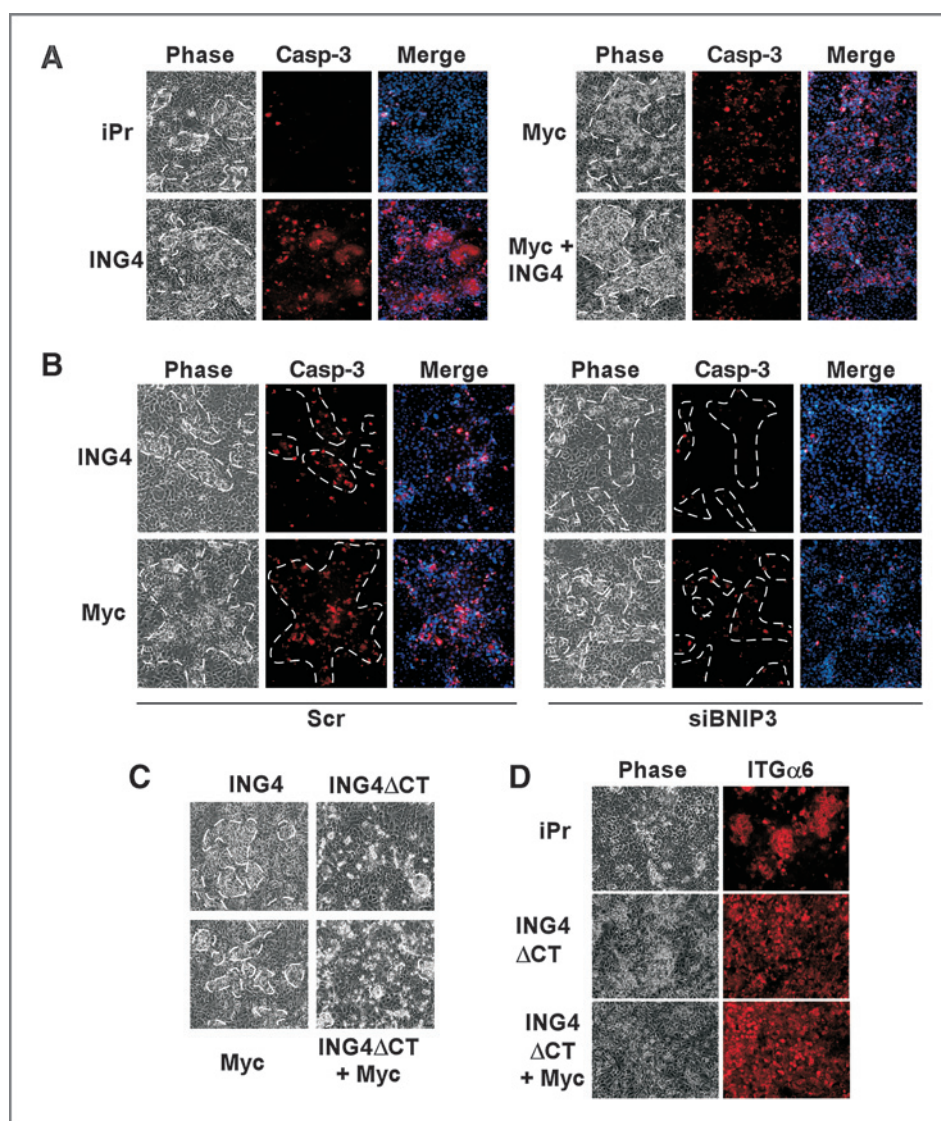
Figure 3. Constitutive Myc and ING4 expression leads to cell death. A, cell death was measured in cells differentiated for 12 days by immunostaining for caspase-3 activity (red). Nuclei were counterstained with Hoechst (blue). B, after 6 days of differentiation, Myc or ING4 overexpressing cells were transfected with Bnip3 siRNA (siBnip3) or a scrambled sequence (Scr) and immunostained 72 hours later for caspase-3 activity (red) and counterstained with Hoechst (blue). White dashes demarcate top layer. C, the C-terminal truncation mutant of ING4 was overexpressed in iPrECs (ING4ΔCT) or in Myc overexpressing cells and compared 8 days after differentiation by phase contrast to cells overexpressing wild-type ING4. D, after 12 days of differentiation, iPrECs (iPr), ING4ΔCT, and Myc plus ING4ΔCT expressing cells were immunostained for integrin α6 (red) and imaged by fluorescent microscopy.

Constitutive Myc and ING4 expression leads to cell death of the differentiated cells via Bnip3

Although Myc or ING4 overexpression initially accelerated iPrEC differentiation, the differentiated cells eventually became disorganized and dissociated from the basal cells, resulting in the loss of the differentiated cell layer (not shown). Differentiated cells from the control iPrEC cultures remained healthy and viable. At day 12, many more apoptotic cells were detected in the differentiating Myc or ING overexpressing cultures as evidenced by increased cleaved caspase-3 (Fig. 3A) and TUNEL staining (not shown) specifically in the suprabasal layer. The basal cell layer remained intact and displayed no evidence of cell death. Thus, sustained overexpression of Myc or ING4, specifically in the differentiated cells, ultimately causes their death.

A qRT-PCR screen for cell death effectors identified elevated expression of Bnip3 (not shown), which encodes a BH3-only proapoptotic protein. Inhibiting Bnip3 expression with siRNA blocked the death induced by ING4 or Myc overexpression, as measured by a reduction in caspase-3–positive cells (Fig. 3B). Blocking Bnip3 expression did not inhibit differentiation (Supplementary Fig. S3), indicating death occurs after differentiation. Thus, the death induced by Myc and ING4 overexpression in differentiated cells is mediated by elevated Bnip3 expression, leading to apoptosis.

The C-terminal domain of ING4 is required for iPrEC differentiation

Myc promotes the trimethylation of H3 at K4 (H3K4me3; ref. 31). ING4 functions in chromatin remodeling complexes by binding to histone H3K4me3 sites via its C-terminal PHD motif and recruiting the HBO1 acetyltransferase via the N-terminal domain (21, 32). Deletion of the PHD motif generates a dominant inhibitory mutant (23). The ability of ING4 to accelerate differentiation was abrogated when the C-terminal domain of ING4 (ING4ΔCT) was deleted (Fig. 3C). This is

further evidenced by the failure to suppress integrin α6 expression (Fig. 3D) in the cells expressing ING4ΔCT. Furthermore, ING4ΔCT blocked the ability of Myc to induce differentiation. Cells that did appear in the suprabasal layer were dying as determined by caspase-3 immunostaining (not shown). Thus, the C-terminus of ING4 containing the PHD domain is required for iPrEC differentiation and survival of the emerging cells, suggesting that the Myc-ING4 differentiation program depends on ING4-dependent chromatin remodeling.

ING4 expression is lost in patient with prostate cancer tumors

To determine whether ING4 expression is altered in prostate cancer, a tissue microarray containing 50 malignant prostate tumors and 12 noncancerous prostates was surveyed for ING4 and AR expression (Fig. 4A). ING4 expression was detected in the nuclei of the luminal cell population of noncancerous samples (Fig. 4B). ING4 expression levels were scored on a scale ranging from 0 to 3; 0 for no detectable expression and 3 for distinct nuclear expression in accordance with a previous

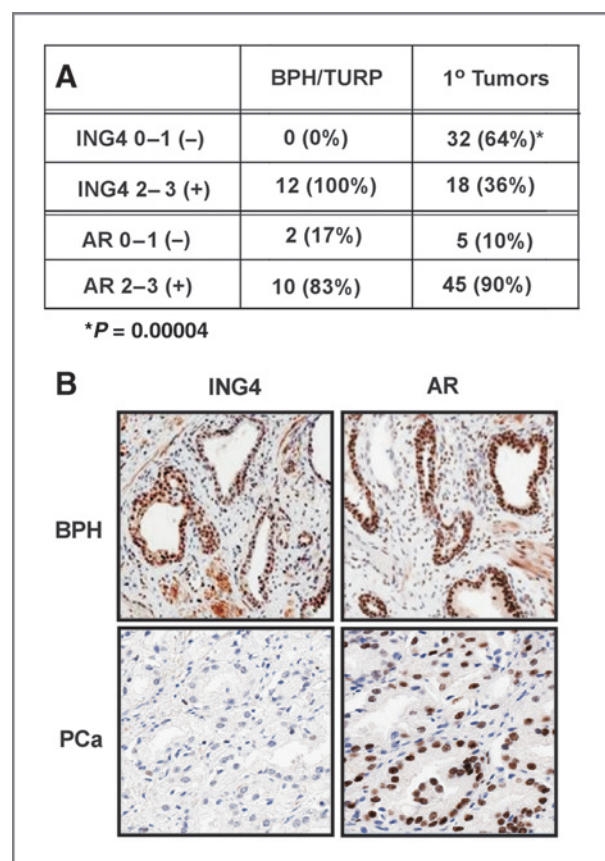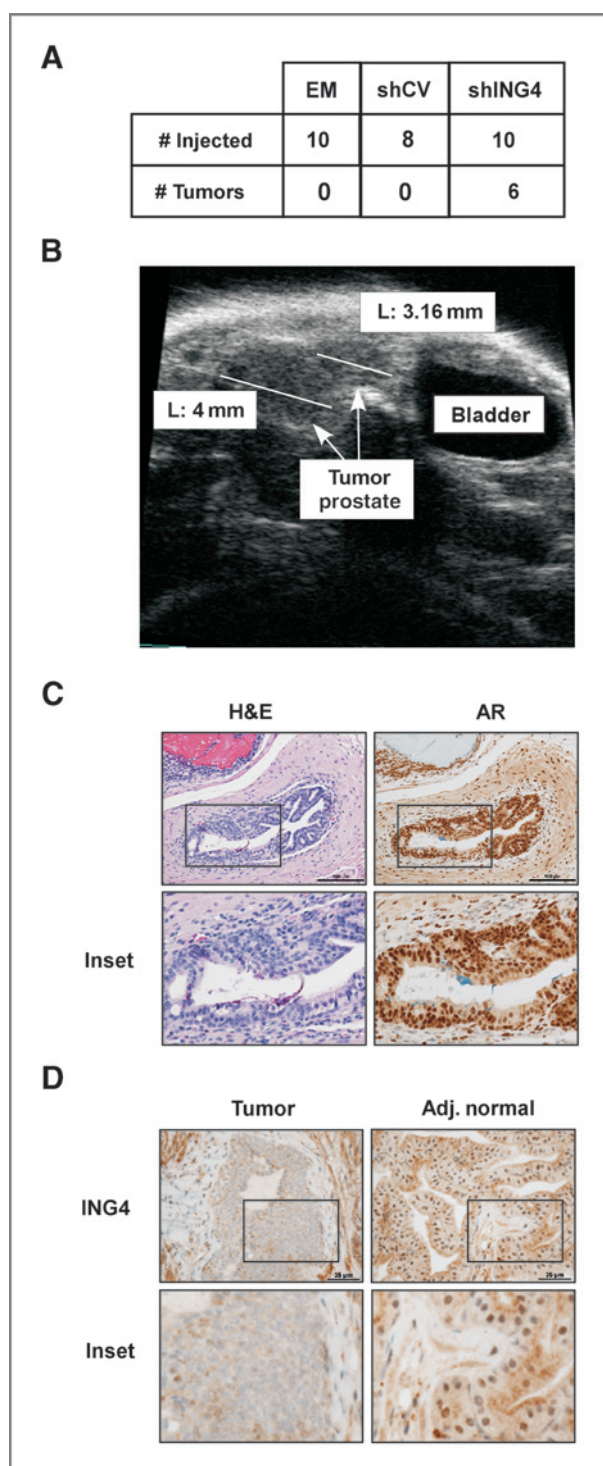| A	BPH/TURP	1° Tumors
ING4 0–1 (−)	0 (0%)	32 (64%)*
ING4 2–3 (+)	12 (100%)	18 (36%)
AR 0–1 (−)	2 (17%)	5 (10%)
AR 2–3 (+)	10 (83%)	45 (90%)

*P = 0.00004

Figure 4. ING4 expression is lost in patients with prostate cancer. A tissue microarray of 50 cancerous and 12 noncancerous human prostate samples was immunostained for ING4 or AR. A, table of ING4 and AR histologic grading (scale 0–3; 3 being highest expression) comparing benign prostate hyperplasia/transurethral resection (BPH/TURP) and primary tumors (1°). *, P = 0.0004; n = 50. B, IHC staining of ING4 and AR in benign hyperplastic prostate tissue (BPH) and prostate cancer (PCa) tissue.

study (30). Although 100% of control (BPH or TURP) samples were positive for ING4, only 36% of tumor samples (18/50) were positive for nuclear ING4 expression (Fig. 4A). In contrast, 83% benign lesion sample (10/12) and 90% of the tumors were positive for AR (Fig. 4A). These results demonstrate that more than 60% of prostate tumors downregulate ING4 expression and this loss occurs in AR-positive cancer, indicating that ING4 loss may be a main event in prostate tumorigenesis.

Loss of ING4 expression cooperates with Myc/Erg in prostate tumorigenesis

As reported previously, Myc overexpression alone in human iPrECs was not sufficient to generate a cell line that is tumorigenic in mice (33). Combined overexpression of Myc and the prostate-specific oncogene, Erg (10), was also not sufficient to generate human tumors. To test whether loss of ING4 is also required, we orthotopically injected iPrECs overexpressing Erg and Myc (EM) with or without shING4 (EMI), or a nontargeting shRNA (EMshCV) into prostates of nude mice. Cells overexpressing the two oncogenes Myc and Erg (EM) or in conjunction with a nontargeting shRNA (EMshCV) did not produce tumors in the mice 18 weeks following orthotopic injection. However, EMI cells produced tumors in 60% of the mice (Fig. 5A). Ultrasound imaging of tumors in mice 18 weeks following orthotopic injection is shown in Fig. 5B. Tumors were positive for AR, but negative for ING4 expression when compared with adjacent normal tissue (Fig. 5C and D). Thus, loss of ING4 is required in human cells to cooperate with Myc and Erg to produce prostate tumors.

Pten loss prevents ING4 expression

To further develop prostate cancer models, Pten expression was silenced by overexpressing Pten shRNA in the EM cells (EMP). Overexpression of Myc and Erg and knockdown of Pten was verified in EMP cells by immunoblotting (Fig. 6A). In EMP cells, the expression of integrin α6 was increased whereas the expression of the p27 cell-cycle inhibitor was reduced (Fig. 6A), consistent with changes observed in prostate cancer (13, 34).

Orthotopic injection of EMP, but not iPrECs, into the prostates of nude mice produced tumors that were detectable by ultrasound imaging as early as 8 weeks after injection. At 16 weeks, the tumors averaged 2.85 mm in diameter, ranging from 2.11 to 3.68 mm (Fig. 6B). The tumor penetrance was 60%, as 17 of 30 injections resulted in prostate tumor formation (Fig. 6C). IHC with human-specific MHC class I antibody revealed the presence of human cells demarcating the tumorigenic foci. The EMP tumors stained positive for AR (Fig. 6D) and castrating the mice 16 weeks after the tumors were established resulted in complete tumor regression, indicating a dependence on androgen for tumor maintenance (Fig. 6C).

When subjected to the differentiation protocol, EM cells were completely competent at differentiating as evidenced by the formation of distinct layers, loss of integrin α6, and gain of AR in the suprabasal layer (Fig. 7A). In contrast, the EMI cells failed to differentiate as evidenced by reduced numbers of suprabasal cells, poor AR expression, and retention of integrin α6 in all the cells. EMP cells also failed to differentiate, as evidenced by the lack of a suprabasal layer, and failure to lose

Figure 5. Loss of ING4 expression is required for tumorigenesis. A, iPrECs were engineered to stably overexpress Myc and Erg (EM) with or without shING4 (EMshING4) or a nontargeting shRNA (shCV). Number of mice in which tumors formed following orthotopic injection of EMshING4 compared with control EM and EMshCV cells 18 weeks postinjection. B, tumor measured by ultrasound imaging 18 weeks after orthotopic injection of EMshING4 into the prostates of nude mice. C, hematoxylin and eosin (H&E) and IHC staining of a tumor sample with AR. D, IHC staining of ING4 in normal mouse prostate and tumor sample.
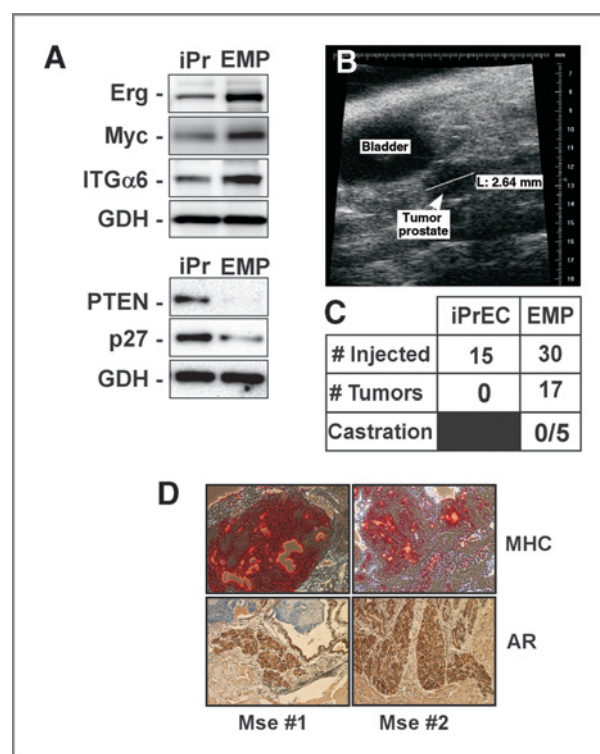
Figure 6. Pten loss promotes tumorigenesis. A, iPrECs (iPr) were engineered to stably overexpress Myc and Erg, along with Pten shRNA (EMP). Immunoblotting confirmed overexpression of Myc, Erg, integrin α6 (ITGα6), and loss of Pten and p27Kip. B, tumor measured by ultrasound imaging 16 weeks after orthotopic injection of EMP cells into the prostates of nude mice. C, number of mice in which tumors formed following orthotopic injection of EMP cells compared with control iPrECs 16 weeks postinjection. Sixteen weeks postinjection, 5 mice harboring EMP tumors were castrated and 11 weeks later the number of tumors that regressed was recorded. D, IHC staining of different tumor samples with human-specific MHC class I or AR.

integrin expression (Fig. 7A). However, in contrast to EMI cells, the EMP cells induced high AR and integrin α6 expression in the basal layer (Fig. 7A). Elevated integrin α6 expression in EMP cells was also observed by immunoblotting (Fig. 6A). This resulted in a population of cells coexpressing AR and integrin α6; reproducing the histopathology observed in clinical samples (13). The inability of EMI and EMP cells to differentiate, correlated with a failure of Myc to induce ING4 expression (Fig. 7A and B). The small clusters of AR-positive cells in the EMI culture are cells in which shING4 was poorly expressed, as evidenced by ING4 positivity in those clusters. Analysis of the keratin subtypes further revealed that EMP cells coexpress both basal keratin K5 and secretory keratin K8 (16) compared with normal iPrECs, where each keratin was distinctively expressed in their respective cell types (Fig. 7C). Thus, EMP cells have a dysfunctional differentiation program that prevents ING4 expression in the presence of Myc, resulting in tumorigenic cells with an intermediate differentiation phenotype. Re-expression of ING4 in EMP cells completely rescued the differentiation defect, restoring the suprabasal layer, AR expression, loss of integrin (Fig. 7B), and separation of the K5

Figure 7. Pten-mediated loss of ING4 and altered differentiation in tumorigenic cells. A, iPrECs (iPr), EM, EMI, or EMP cells differentiated for 12 to 14 days were immunostained for AR (red), ITGα6 (green), or ING4 (red), counterstained with Hoechst (blue), and imaged by fluorescent microscopy. B, ING4, Myc, Erg, and Pten expression in undifferentiated iPrECs (iPr), EM, EMP, EMP+ING4, or EMI cells detected by immunoblotting. EMP or EMP-ING4 cells differentiated for 12 to 14 days were immunostained for ING4 (green), ITGα6 (red), or Nkx3.1 (red). Dashed lines demarcate supra (T) and basal cell layers. C, cultures of iPrECs, EMP, or EMP-ING4 cells were differentiated for 17 days, immunostained for keratins K8 (green) and K5 (red), counterstained with Hoechst (blue), and imaged by confocal microscopy.
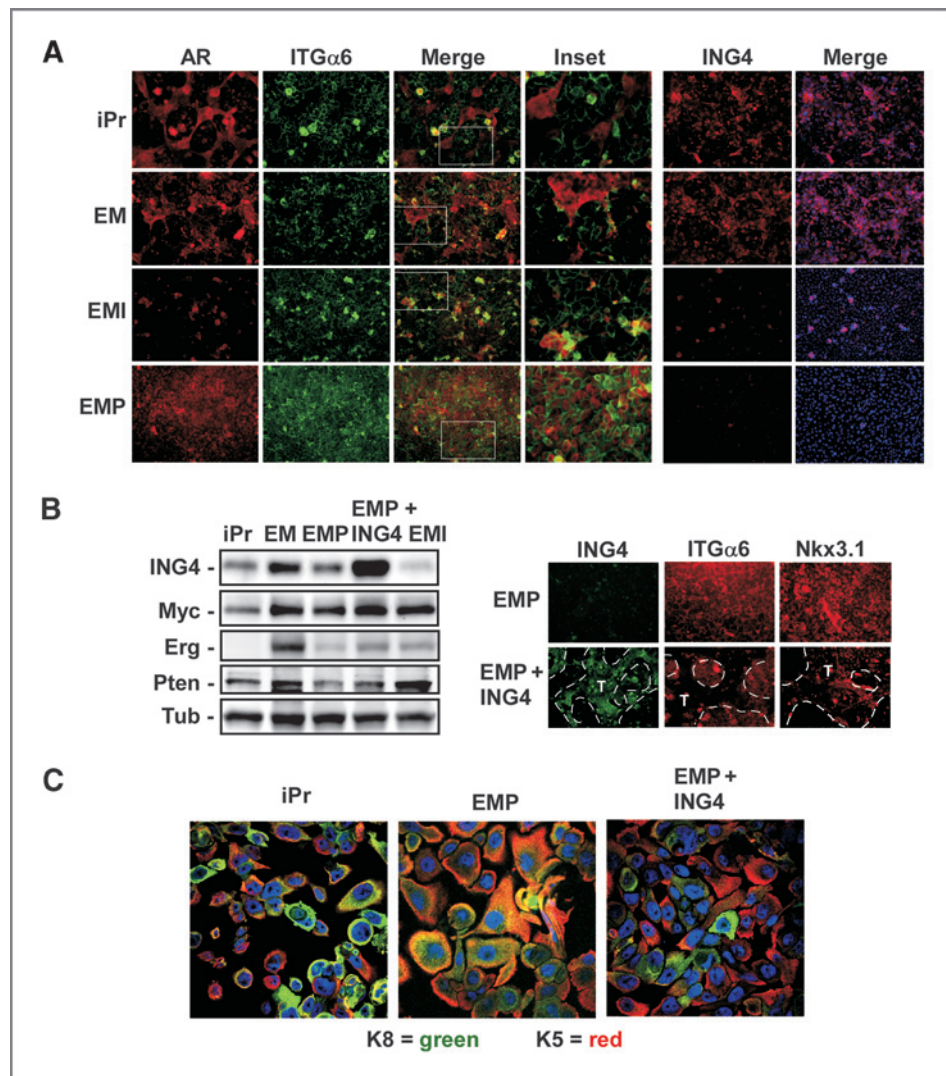
and K8 populations (Fig. 7C). Expression of the ING4ΔCT mutant in EMP cells did not rescue the differentiation defect (not shown). Thus, the Myc-ING4 differentiation relay is no longer functional in the oncogenic EMP cells and Pten loss is responsible. Together our results support the conclusion that ING4 is required for differentiation of iPrECs and suggest that one of the major oncogenic events in prostate cancer is the uncoupling of the Myc-ING4 differentiation program.

Discussion

In immortalized human prostate epithelial cells with the capacity to differentiate *in vitro*, transient ING4 expression, dependent on Myc, is required for prostate epithelial differentiation. ING4 expression coincides with loss of matrix-based adhesion, downregulation of integrin, and acquisition of AR; blocking ING4 prevents the initiation of these processes. In normal differentiating iPrECs, the acquisition of AR expression and androgen responsiveness is observed only in cells in which integrin expression is lost (12). We found that neither AR nor

androgen is required for ING4 expression (not shown), nor were we able to demonstrate any influence of ING4 on AR expression or its ability to activate its transcriptional targets in cells expressing AR. Thus, the role of ING4 in prostate epithelial differentiation lies at least in part within its capacity to target integrins. This is consistent with the observations in the Myc breast cancer mouse model, where overexpression of the C-terminal deletion mutant of ING4 (ING4ΔCT) restored integrin expression in the tumors (unpublished results; ref. 23). This is also consistent with the established role for Myc in directly suppressing integrin α6 and β1 transcription during differentiation (35). Our data indicate that ING4 is an essential component of the Myc-dependent effect on integrin expression, because removal of ING4 prevents Myc from suppressing integrin expression.

Myc or ING4 overexpression in basal cells is sufficient to accelerate differentiation toward luminal cells; however, improper prolonged expression of Myc or ING4 leads to cell death. Thus, the temporal, that is, Myc expression preceding ING4, and transient nature of Myc and ING4 expression is

crucial for normal epithelial cell differentiation. The molecular mechanism of this concerted transcriptional relay is currently unclear. Previous ChIP analysis identified Myc bound to the ING4 promoter, suggesting ING4 is a direct target of Myc (36). However, we failed to detect an increase in ING4 mRNA in undifferentiated basal cells overexpressing Myc (not shown). Similarly, Myc overexpression in breast epithelial cells also did not increase ING4 expression (unpublished results). Thus, our results point to an indirect action of Myc in ING4 induction, or requiring additional factor(s) during the course of differentiation.

Differentiation is dependent on the ING4 C-terminal domain containing the PHD motif required for H3K4me3 binding (21). ING4 overexpression alters chromatin modifications (not shown), suggesting ING4 association with chromatin is required for differentiation. To our knowledge, this is the first time that the chromatin remodeling properties of ING4 have been linked to differentiation. Once bound, ING4 recruits the HBO1 acetyltransferase (21, 37), facilitates histone H3/H4 acetylation, and activates gene transcription (21, 38). Like ING4, Myc is extensively involved in chromatin remodeling (39, 40). In addition, recent studies have brought to light the chromatin remodeling activity of Myc in the maintenance of pluripotent stem cells (19, 41). Taken together, the relay from Myc to ING4 is likely to install epigenetic changes that govern differential transcription and ultimately prostate epithelial cell differentiation.

Myc overexpression alone often fails to transform normal human cells because of induction of cell death (33, 42). Myc or ING4 overexpression specifically induces death of the differentiated cells, but not the underlying basal cells. This supports the current paradigm that Myc activity manifests in a context-dependent manner such that Myc induces cell death in more differentiated cells, but maintains the proliferative and self-renewal capacity of less differentiated stem or progenitor cells. The death phenotypes induced by Myc overexpression are mediated in part by p53 and ING4 enhances p53 function (43). However, the death induced by Myc or ING4 overexpression in iPrECs is likely p53-independent, because the iPrECs express E6 that blocks p53 function. In iPrECs, Bnip3 is responsible for the observed cell death. Although p53 is reported to regulate Bnip3 (44, 45), our results describe an alternate mechanism of Bnip3 activation that is p53 independent. Nonetheless, ING4 may be part of the mechanism by which p53 regulates Bnip3. In prostate cancer, p53 loss is rare and associated with a small subset of late stage disease (46). Thus, loss of ING4 may be a mechanism by which prostate cancer cells escape the tumor suppressive effects of p53 when Myc is overexpressed. This idea is further supported when contrasting the prostate cancer tissue data, which demonstrate a 60% loss of ING4, with that of breast cancer where p53 loss is more highly prevalent and only 34% of the samples lack ING4.

ING4 expression is lost in more than 60% of prostate tumors, suggesting for the first time a significant contribution of ING4 loss to prostate tumorigenesis. The high prevalence of Myc overexpression in prostate cancer and its tendency to induce cell death suggests loss of ING4 is necessary for Myc-dependent prostate oncogenesis. Indeed, only Myc-overexpressing cells without ING4 are capable of generating tumors in mice. Moreover, loss of ING4 blocked tumor cell differentiation generating cells coexpressing both basal and luminal markers, a phenotype often seen in prostate cancer. The mechanism by which ING4 is lost in prostate cancer needs more investigation, but LOH at 12p13, the genomic region that contains the ING4 gene, has been reported in 10% to 20% of primary and up to 45% of metastatic prostate tumors (47, 48). Our data demonstrate loss of Pten is another mechanism that leads to ING4 loss. The molecular mechanism of Pten in the regulation of ING4 expression is presently unknown and likely to be indirect.

We have established a genetic link between Myc and ING4 in prostate epithelial differentiation and prostate cancer. Our data demonstrate that a Myc-ING4 temporal relay is required for normal prostate cell differentiation and when this relay is missing, it leads to prostate cancer. Whether the Myc-ING4 relay also governs cell differentiation in other cell types, including breast epithelia, needs to be addressed. We propose that ING4 dictates the downstream program driven by Myc toward differentiation, and in its absence Myc is directed toward targets that promote tumorigenesis. Pten loss resulting in the loss of ING4 expression, disruption of the Myc-ING4 relay, a block in differentiation, and susceptibility to tumorigenesis, reinforces the idea that ING4 plays a pivotal role in determining prostate epithelial cell fate.

Disclosure of Potential Conflicts of Interest

Authors' Contributions
Conception and design: P.L. Berger, E.A. Nollet, G. Hostetter, S. Kim, C.K. Miranti
Development of methodology: P.L. Berger, S.B. Frank, T.-T.A. Chang, G. Hostetter, C.K. Miranti
Acquisition of data (provided animals, acquired and managed patients, provided facilities, etc.): S.B. Frank, B. Holly, T.-T.A. Chang, G. Hostetter, S. Kim, C.K. Miranti
Analysis and interpretation of data (e.g., statistical analysis, biostatistics, computational analysis): P.L. Berger, B. Holly, T.-T.A. Chang, C.K. Miranti
Writing, review, and/or revision of the manuscript: P.L. Berger, B. Holly, T.-T.A. Chang, G. Hostetter, S. Kim, C.K. Miranti
Administrative, technical, or material support (i.e., reporting or organizing data, constructing databases): P.L. Berger, V.V. Schulz, C.K. Miranti
Study supervision: T.-T.A. Chang, C.K. Miranti

Acknowledgments

Grant Support

References

1. Burger PE, Xiong X, Coetzee S, Salm SN, Moscatelli D, Goto K, et al. Sca-1 expression identifies stem cells in the proximal region of prostatic ducts with high capacity to reconstitute prostatic tissue. Proc Natl Acad Sci U S A 2005;102:7180–5.

2. Lawson DA, Xin L, Lukacs RU, Cheng D, Witte ON. Isolation and functional characterization of murine prostate stem cells. Proc Natl Acad Sci U S A 2007;104:181–6.

3. Gao H, Ouyang X, Banach-Petrosky W, Borowsky AD, Lin Y, Kim M, et al. A critical role for p27kip1 gene dosage in a mouse model of prostate carcinogenesis. Proc Natl Acad Sci U S A 2004;101:17204–9.

4. Koh CM, Bieberich CJ, Dang CV, Nelson WG, Yegnasubramanian S, De Marzo AM. MYC and prostate cancer. Genes Cancer 2010;1: 617–28.

5. Schmitz M, Grignard G, Margue C, Dippel W, Capesius C, Mossong J, et al. Complete loss of PTEN expression as a possible early prognostic marker for prostate cancer metastasis. Int J Cancer 2007;120: 1284–92.

6. Ellwood-Yen K, Graeber TG, Wongvipat J, Iruela-Arispe ML, Zhang J, Matusik R, et al. Myc-driven murine prostate cancer shares molecular features with human prostate tumors. Cancer Cell 2003;4:223–38.

7. Wang S, Gao J, Lei Q, Rozengurt N, Pritchard C, Jiao J, et al. Prostate-specific deletion of the murine Pten tumor suppressor gene leads to metastatic prostate cancer. Cancer Cell 2003;4:209–21.

8. Zong Y, Xin L, Goldstein AS, Lawson DA, Teitell MA, Witte ON. ETS family transcription factors collaborate with alternative signaling pathways to induce carcinoma from adult murine prostate cells. Proc Natl Acad Sci U S A 2009;106:12465–70.

9. Klezovitch O, Risk M, Coleman I, Lucas JM, Null M, True LD, et al. A causal role for ERG in neoplastic transformation of prostate epithelium. Proc Natl Acad Sci U S A 2008;105:2105–10.

10. Sun C, Dobi A, Mohamed A, Li H, Thangapazham RL, Furusato B, et al. TMPRSS2-ERG fusion, a common genomic alteration in prostate cancer activates C-MYC and abrogates prostate epithelial differentiation. Oncogene 2008;27:5348–53.

11. Choi N, Zhang B, Zhang L, Ittmann M, Xin L. Adult murine prostate basal and luminal cells are self-sustained lineages that can both serve as targets for prostate cancer initiation. Cancer Cell 2012;21:253–65.

12. Lamb LE, Knudsen BS, Miranti CK. E-cadherin-mediated survival of androgen-receptor-expressing secretory prostate epithelial cells derived from a stratified in vitro differentiation model. J Cell Sci 2010;123:266–76.

13. Cress AE, Rabinovitz I, Zhu W, Nagle RB. The $\alpha6\beta1$ and $\alpha6\beta4$ integrins in human prostate cancer progression. Cancer Metastasis Rev 1995;14:219–28.

14. Litvinov IV, De Marzo AM, Isaacs JT. Is the Achilles' heel for prostate cancer therapy a gain of function in androgen receptor signaling? J Clin Endocrinol Metab 2003;88:2972–82.

15. Lamb LE, Zarif JC, Miranti CK. The androgen receptor induces integrin $\alpha6\beta1$ to promote prostate tumor cell survival via NF-κB and Bcl-xL independently of PI3K signaling. Cancer Res 2011;71: 2739–49.

16. Myers RB, Grizzle WE. Changes in biomarker expression in the development of prostatic adenocarcinoma. Biotech Histochem 1997;72: 86–95.

17. Verhagen AP, Aalders TW, Ramaekers FC, Debruyne FM, Schalken JA. Differential expression of keratins in the basal and luminal compartments of rat prostatic epithelium during degeneration and regeneration. Prostate 1988;13:25–38.

18. Nagle RB, Ahmann FR, McDaniel KM, Paquin ML, Clark VA, Celniker A. Cytokeratin characterization of human prostatic carcinoma and its derived cell lines. Cancer Res 1987;47:281–6.

19. Buganim Y, Faddah DA, Jaenisch R. Mechanisms and models of somatic cell reprogramming. Nat Rev Genet 2013;14:427–39.

20. Coles AH, Jones SN. The ING gene family in the regulation of cell growth and tumorigenesis. J Cell Physiol 2009;218:45–57.

21. Hung T, Binda O, Champagne KS, Kuo AJ, Johnson K, Chang HY, et al. ING4 mediates crosstalk between histone H3 K4 trimethylation and H3 acetylation to attenuate cellular transformation. Mol Cell 2009;33: 248–56.

22. Kim S, Chin K, Gray JW, Bishop JM. A screen for genes that suppress loss of contact inhibition: identification of ING4 as a candidate tumor suppressor gene in human cancer. Proc Natl Acad Sci U S A 2004;101:16251–6.

23. Kim S, Welm AL, Bishop JM. A dominant mutant allele of the ING4 tumor suppressor found in human cancer cells exacerbates MYC-initiated mouse mammary tumorigenesis. Cancer Res 2010;70:5155–62.

24. Edick MJ, Tesfay L, Lamb LE, Knudsen BS, Miranti CK. Inhibition of integrin-mediated crosstalk with epidermal growth factor receptor/Erk or Src signaling pathways in autophagic prostate epithelial cells induces caspase-independent death. Mol Biol Cell 2007;18:2481–90.

25. Gmyrek GA, Walburg M, Webb CP, Yu HM, You X, Vaughan ED, et al. Normal and malignant prostate epithelial cells differ in their response to hepatocyte growth factor/scatter factor. Am J Pathol 2001;159: 579–90.

26. Tapia C, Zlobec I, Schneider S, Kilic E, Güth U, Bubendorf L, et al. Deletion of the inhibitor of growth 4 (ING4) tumor suppressor gene is prevalent in human epidermal growth factor 2 (HER2)-positive breast cancer. Hum Pathol 2011;42:983–90.

27. Pawar SC, Demetriou MC, Nagle RB, Bowden GT, Cress AE. Integrin $\alpha6$ cleavage: a novel modification to modulate cell migration. Exp Cell Res 2007;313:1080–9.

28. Livak KJ, Schmittgen TD. Analysis of relative gene expression data using real-time quantitative PCR and the 2($-\Delta\Delta$C)T Method. Methods 2001;25:402–8.

29. Watanabe A, Hostetter G. Tissue microarray applications in drug discovery for pancreatic cancer. In: Han H, Grippo P., editors. Drug discovery in pancreatic cancer, models and techniques. New York: Springer; 2010. pg. 205–222.

30. Byron SA, Min E, Thal TS, Hostetter G, Watanabe AT, Azorsa DO, et al. Negative regulation of NF-κB by the ING4 tumor suppressor in breast cancer. PLoS One 2012;7:e46823.

31. Lin CH, Lin C, Tanaka H, Fero ML, Eisenman RN. Gene regulation and epigenetic remodeling in murine embryonic stem cells by c-Myc. PLoS One 2009;4:e7839.

32. Palacios A, Munoz IG, Pantoja-Uceda D, Marcaida MJ, Torres D, Martin-Garcia JM, et al. Molecular basis of histone H3K4me3 recognition by ING4. J Biol Chem 2008;283:15956–64.

33. Berger R, Febbo PG, Majumder PK, Zhao JJ, Mukherjee S, Signoretti S, et al. Androgen-induced differentiation and tumorigenicity of human prostate epithelial cells. Cancer Res 2004;64:8867–75.

34. De Marzo AM, Meeker AK, Zha S, Luo J, Nakayama M, Platz EA, et al. Human prostate cancer precursors and pathobiology. Urology 2003;62:55–62.

35. Gebhardt A, Frye M, Herold S, Benitah SA, Braun K, Samans B, et al. Myc regulates keratinocyte adhesion and differentiation via complex formation with Miz1. J Cell Biol 2006;172:139–49.

36. Zhou L, Picard D, Ra Y-S, Li M, Northcott PA, Hu Y, et al. Silencing of thrombospondin-1 is critical for Myc-induced metastatic phenotypes in medulloblastoma. Cancer Res 2010;70:8199–210.

37. Doyon Y, Cayrou C, Ullah M, Landry AJ, Cote V, Selleck W, et al. ING tumor suppressor proteins are critical regulators of chromatin acetylation required for genome expression and perpetuation. Mol Cell 2006;21:51–64.

38. Coles AH, Gannon H, Cerny A, Kurt-Jones E, Jones SN. Inhibitor of growth-4 promotes IκB promoter activation to suppress NF-κB signaling and innate immunity. Proc Natl Acad Sci U S A 2010;107:11423–8.

39. Pellakuru LG, Iwata T, Gurel B, Schultz D, Hicks J, Bethel C, et al. Global levels of H3K27me3 track with differentiation in vivo and are deregulated by MYC in prostate cancer. Am J Pathol 2012;181:560–9.

40. Secombe J, Eisenman RN. The function and regulation of the JARID1 family of histone H3 lysine 4 demethylases: the Myc connection. Cell Cycle 2007;6:1324–8.

41. Soufi A, Donahue G, Zaret KS. Facilitators and impediments of the pluripotency reprogramming factors' initial engagement with the genome. Cell 2012;151:994–1004.

42. Larsson LG, Henriksson MA. The Yin and Yang functions of the Myc oncoprotein in cancer development and as targets for therapy. Exp Cell Res 2010;316:1429–37.

43. Shiseki M, Nagashima M, Pedeux RM, Kitahama-Shiseki M, Miura K, Okamura S, et al. p29ING4 and p28ING5 bind to p53 and p300, and enhance p53 activity. Cancer Res 2003;63:2373–8.

44. Jafarnejad S, Li G. Regulation of p53 by ING family members in suppression of tumor initiation and progression. Cancer Metastasis Rev 2011;31:1–19.

45. Feng X, Liu X, Zhang W, Xiao W. p53 directly suppresses BNIP3 expression to protect against hypoxia-induced cell death. EMBO J 2011;30:3397–415.

46. Markert EK, Mizuno H, Vazquez A, Levine AJ. Molecular classification of prostate cancer using curated expression signatures. Proc Natl Acad Sci U S A 2011;108:21276–81.

47. Kawana Y IT, Suzuki H, Ueda T, Komiya A, Ichikawa Y, Furuya Y, et al. Loss of heterozygosity at 7q31.1 and 12p13-12 in advanced prostate cancer. Prostate 2002;53:60–4.

48. Kibel AS, Faith DA, Bova GS, Isaacs WB. Loss of heterozygosity at 12P12-13 in primary and metastatic prostate adenocarcinoma. J Urol 2000;164:192–6.

Miz1, a Novel Target of ING4, Can Drive Prostate Luminal Epithelial Cell Differentiation

Penny L.[Q1] Berger,[1] Mary E. Winn,[2] and Cindy K. Miranti[1]*

[1]*Laboratory of Integrin Signaling, Van Andel Research Institute, Grand Rapids, Michigan*
[2]*Bioinformatics and Biostatistics Core, Van Andel Research Institute, Grand Rapids, Michigan*

BACKGROUND. How prostate epithelial cells differentiate and how dysregulation of this process contributes to prostate tumorigenesis remain unclear. We recently identified a Myc target and chromatin reader protein, ING4, as a necessary component of human prostate luminal epithelial cell differentiation, that is, often lost in primary prostate tumors. Furthermore, loss of ING4 in the context of oncogenic mutations is required for prostate tumorigenesis. Identifying the gene targets of ING4 can provide insight into how its loss disrupts differentiation and leads to prostate cancer.
METHODS. Using a combination of RNA-Seq, a best candidate approach, and chromatin immunoprecipitation (ChIP), we identified Miz1 as a new ING4 target. ING4 and Miz1 overexpressions, shRNA knock-down, and a Myc-binding mutant were used in a human in vitro differentiation assay to assess the role of Miz1 in luminal cell differentiation.
RESULTS. ING4 directly binds the Miz1 promoter and is required to induce Miz1 mRNA and protein expression during luminal cell differentiation. Miz1 mRNA was not induced in shING4 expressing cells or tumorigenic cells, which fail to express ING4. Miz1 dependency on ING4 was unique to differentiating luminal cells; Miz1 mRNA expression was not induced in basal cells. Although Miz1 is a direct target of ING4, and its overexpression can drive luminal cell differentiation, Miz1 was not required for differentiation.
CONCLUSIONS. Miz1 is a newly identified ING4-induced target gene which can drive prostate luminal epithelial cell differentiation although it is not absolutely required. *Prostate 9999: 1–11, 2016.* © 2016 Wiley Periodicals, Inc.

KEY WORDS: chromatin; integrins; RNA-Seq; Myc; human

INTRODUCTION

The manner in which prostate epithelial cells differentiate, that is, how cells in the prostate epithelium transition from basal to secretory luminal cells, still remains to be fully elucidated. The process is one that demands attention since dysregulated differentiation is implicated in prostate oncogenesis [1]. Several different models have been used to investigate prostate epithelial differentiation, the most common being in vivo mouse models [2–4]. We developed an in vitro differentiation model using human basal epithelial cells to better assess both differentiation and oncogenesis in a human model [5]. Stimulation of human basal cells with KGF and DHT for 14–18 days results in a bilayer culture with fully differentiated AR-positive secretory luminal cells sitting atop basal cells that mimics human prostate histology. Utilizing this model, we identified the chromatin binding protein and Myc target, ING4 [6–8], as a major luminal cell determinant [1]. ING4 is induced downstream of Myc and required for luminal differentiation, and its

induction is coincident with integrin loss within the luminal cell population.

Introduction of oncogenes, that is, overexpression of Erg and Myc and knock-down of Pten, into differentiating basal cells generated AR-positive luminal-like tumorigenic cells that retained some basal markers including integrin α6β1 analogous to what is seen in human tumors [1,9]. These same tumorigenic cells lost their ability to fully differentiate and this was shown to be due to loss of ING4. To better understand how ING4 drives integrin loss during normal differentiation, we sought to identify the gene targets of ING4.

The loss of integrin expression during epithelial cell differentiation has been studied in other contexts including mammary and skin [10,11]. In addition to Notch being a strong suppressor of both integrins and matrix [11], a Myc/Miz1 (*ZBTB17*) repressive complex, which binds integrin α6 and β1 promoters, was shown to be necessary for Myc-induced differentiation of keratinocytes [10]. Miz1 is also necessary in the mammary gland for proper transitioning from late stage pregnancy to early lactation [12]. ING4 expression is also lost in some breast cancers [13] where it may suppress NF-κB signaling [14], and elevated expression of an ING4 E3-ligase, SCF(JFK), promotes breast cancer metastasis [15]. Interestingly, expression of an ING4 mutant unable to bind chromatin induced integrin expression in a mouse breast cancer model [8]. Thus, we hypothesized that Miz1 might be the link between ING4 and α6β1 integrin that could explain its loss during normal differentiation and its retention in tumor cells.

MATERIALS AND METHODS

Cell Lines

Immortalized human basal prostate epithelial cells (iPrEC) were generated from primary clinical prostectomies as previously described [1,5]. Cultures were validated to be Mycoplasma-free and express only basal epithelial cell markers [5]. Tumorigenic iPrEC-EMP (Erg/Myc/shPten overexpression) and ING4 or shING4 overexpressing (iPrEC-ING4; iPrEC-shING4) cells were generated as previously described [1,8]. All lines were maintained and passaged in keratinocyte serum-free media (Invitrogen) [1,5].

Differentiation Protocol

Differentiation and layer separation protocols were detailed previously [5]. Briefly, iPrECs at confluency were treated in complete growth medium with 2 ng/ml keratinocyte growth factor (KGF) (Cell Sciences) and 5 nM R1881 (PerkinElmer) every other day for up to 18 days. For biochemical analysis, the differentiated luminal layer was separated from the basal layer using disassociation buffer (Invitrogen) as previously described [5].

Constructs

The pLKO vector containing Pten shRNA was generated by subcloning the oligo 5′- CCGGTGGGCT TTAACTGTAGTATTTGTACTAGTCAAATACTACA GTTAAAGCCCTTTTTG-3′, complementary to the 3′-UTR of Pten, into a lentiviral vector to generate pLKO.1-shPten. The shPten in the iPrEC-EMP cells reported here contain the above targeting sequence, which is more stable and generated subsequent to the initial report on iPrEC-EMP [1]. The pLKO vector containing ING4 shRNA was purchased from Sigma–Aldrich (Clone ID:NM_016162.3-522s21c1) and used to generate the iPrEC-shING4 cells. ING4 shRNA targeting sequence: 5′-CCGGTTAAAG CTCGTGCGCACAAGTCTCGAGACTTGTGCGCAC-GAGCTTTAATTTTTTG-3′. The pLKO-TetON-shMiz1 constructs were generated by subcloning each of two oligos into the pLKO-TetON vector purchased from Addgene [16]. The Tet-pLKO-Puro vector was first modified, EZ-Tet-pLKO-Puro, to contain a shortened stuffer region by inserting an EcoRI site at base 222 of the stuffer (primer 5′-GCTACTCCACCACTT-GAATTCCTAAGCGGTCAGC-3′). The vector was then digested with EcoRI and re-ligated. Mutagenesis was then used to mutate the AgeI site to NheI (primer 5′-TATCAGTGATAGAGACGCTAGCGTGTTGTAAA TGAGCA-—3′). shMiz1 oligo sequences were as follows: 5′-CTAGTGTCCAAGCACATCATCATT-CAACTAGTGAGAATGATGATGTGCTTGGACATT TTT-3′ (5730), 5′-CTAGGTTC ACTTTAAGG CTCAT AAAAACTAGTGATTTATGAGCCTTAAAGTGAAC TTTTT-3′ (5729). Wild-type Miz1 (pLenti-Myc-DDK-ZBTB17)(PS100064) was purchased from OriGene Technologies (Rockville, MD). Wild-type c-Myc (pMSCV-c-Myc-GFP) and Myc-Miz1 binding mutant (pMSCV-c-Myc-V394D-RFP) were generous gifts from Dr. Martine Roussel [10,17].

Virus Generation and Infection

Lentiviruses expressing shRNAs or Miz1 cDNA were generated by co-transfecting the 293FT packaging cell line with 6 μg each of the lentiviral packaging plasmids, pVSVG, pLP1, and pLP2 with Lipofectamine 2000 (ThermoFisher) following manufacturers recommended protocol. Virus was harvested 3 days later and immediately used to infect iPrECs. Pooled cells were selected and maintained in 0.75 μg/ml puromycin.

Retroviruses expressing Myc or MycV394D were generated by transfecting Phoenix cells (National Gene Vector Biorepository) using Lipofectamine 2000 following manufacturers recommended protocol, harvesting 2 days later and immediately infecting iPrECs. Pools of Myc expressing cells were selected and maintained in 0.75 μg/ml puromycin.

Antibodies

Immunofluorescence: AR (C-19) and Miz1 (H-190) were purchased from Santa Cruz. ITGα6 (GoH3) antibody was purchased from BD Pharmingen. Immunoblotting: Myc (N-term) and ING4 (EP3804) antibodies were purchased from Abcam. Polyclonal Miz1 antibody was purchased from GeneTex. Tubulin antibody (DM1A) was purchased from Sigma and GAPDH (6CS) from Millipore.

Immunostaining and Microscopy

Differentiated cultures were fixed in 4% paraformaldehyde and permeabilized with 0.2% Triton-X 100 for 5 min. After washing with PBS, cells were blocked with 4% normal goat serum for 2 hr. Primary antibodies, diluted in 1% BSA/PBS, were applied to samples overnight at 4°C. After washing, secondary conjugated antibodies diluted in 1% BSA/PBS were incubated for 1–2 hr. Nuclei were stained with Hoechst 33258 (Sigma) for 10 min at room temperature. Coverslips were mounted using Fluoromount-G (SouthernBiotech). Epifluorescent images were acquired on a Nikon Eclipse TE300 fluorescence microscope using OpenLab v5.5.0 image analysis software (Improvision).

Immunoblotting

Total cell lysates were prepared for immunoblotting as previously described [18]. Briefly, cells were lysed in RIPA buffer and 30–50 μg total protein was separated on SDS polyacrylamide gels and transferred to PVDF membranes. Membranes were blocked in 5% BSA in TBST overnight at 4°C then probed with primary antibody, and HRP-conjugated secondary antibodies (Bio-Rad) in TBST + 5% BSA. Signals were visualized by chemiluminescence reagent with a CCD camera in a Bio-Rad Chemi-Doc Imaging System using Quantity One software v4.5.2 (Bio-Rad).

qRT-PCR

Total RNA was isolated and purified using RNase-free DNase and Life Technology's RNeasy PureLink Kits. For qRT-PCR, 0.5 μg RNA was reversed transcribed using a reverse transcription system (Promega). Synthesized cDNA was amplified for qRT-PCR using SYBR green master mix (Roche) with gene-specific primers and an ABI 7500 RT-PCR system (Applied Biosystems). Gene expression was normalized to 18 sec rRNA by the 2-ΔΔCt method (Livak, 2001). qRT-PCR primers for Miz1 were as follows: Miz1 Fwd: 5′-CTACTCTTTTCTGACAGTTTGCC-3′, Miz1 Rev: 5′-CCTTTGTCTGCTCTGGAGT-3′.

Chromatin Immunoprecipitations

Cells (3.0×10^6) were fixed in 1% formaldehyde (Thermo Scientific) for 1–5 min and washed 3× with ice cold calcium-magnesium free PBS (CMF-PBS) supplemented with protease inhibitors: pepstatin, aprotinin, leupeptin, and phenylmethylsulfonyl (PMSF). Cells were scraped and pelleted at 2,000 rpm for 8 min at 4°C. Pellet was resuspended in swelling buffer (5 mM PIPES pH 8.0, 85 mM KCl, 0.5% IGEPAL, and incubated on ice for 30 min). Nuclei were dounce homogenized and then pelleted at 4,000 rpm for 10 min, 4°C. Nuclei were resuspended in sonication buffer (0.1% SDS, 10 mM EDTA, 50 mM Tris–HCl pH 8.1) and incubated on ice for 10 min prior to sonication. Chromatin was sheared at 4°C using the Covaris E220 Ultra Sonicator following manufacturer's suggested settings of 2% Duty Cycle, 105 Watt Peak Intensity, 200 Cycles/Burst. Chromatin was sonicated for 10 min to achieve 300–500 bp fragments.

Chromatin immunoprecipitations (ChIPs) were performed with 1 million cells/IP using magnetic beads (NEB). The following antibodies were used: ING4 (EP3804) and anti-HBO1 (ab70183) from Abcam. Chromatin was incubated with 6 μg of appropriate antibody overnight at 4°C with rotation. Following incubation, magnetic beads blocked with 1% BSA supplemented with 10 μg/ml salmon sperm, were added to samples and incubated at 4°C with rotation for 6 hr. Following immunoprecipitations, beads were washed in the following buffers at 4°C for 10 min with rotation: Triton Wash Buffer (50 mM Tris–HCl pH 7.4, 150 mM NaCl, 1% Triton X-100), followed by Lysis Buffer 500 (0.1% NaDOC, 1 mM EDTA, 50 mM HEPES pH 7.5, 500 mM NaCl, 1% Triton X-100), LiCl Detergent buffer (0.5% NaDOC, 1 mM EDTA, 250 mM LiCl, 0.5% IGEPAL, 10 mM Tris–HCl pH 8.1), and Tris–EDTA pH 8.1. Chromatin was eluted from beads in Elution Buffer (10 mM EDTA, 1% SDS, Tris–HCl pH 8.0) for 30 min at 65°C. Samples were then treated with 20 μg proteinase K, and 10 μg RNase A, and NaCl (200 mM) was added and incubated at 65°C overnight to reverse cross-links. DNA was purified using phenol/chloroform extraction followed by ethanol precipitation.

ChIP Primer Sequences

Primers were designed referencing the UCSC Genome Browser to determine transcriptional start sites of promoters, and in the case of ING4-ChIP, regions within the promoter region with high H3K4me3 were used to design targeting primers. Primer sequences are as follows: Miz1: Fwd: 5′-AACAGTCTCCCC ACTGCATA-3′, Rev: 5′-GTAGCTCTAGGCCACTG ACT-3′; Histone 3: Fwd: 5′-TTTTGTTTTCCA AAGCGCCC-3′, Rev: 5′-TCAGATTGTTCC CTTTC CGC-3′; SAT2: Fwd: 5′-ATCGAATGGAAATGAAAG- GAGTCA-3′, Rev: 5′-GACCATTGGATGATTGCAG TCA-3′.

RNA-Sequencing

The iPrEC and EMP lines were grown and differentiated as described above and harvested at days 0 (basal), 4, 8, 11, 14, and 17. At day 14 and 17, iPrEC differentiated cultures were treated with CFM-PBS supplemented with 1 mM EDTA and dissociation buffer for 40–45 min to isolate the luminal cells. Total RNA was isolated and purified using Life Technologies RNeasy and Purelink RNA mini kits. TruSeq mRNA libraries were prepared for sequencing using standard Illumina protocols from PolyA-enriched RNA. Illumina RNAseq—single read, 50 bp, approximately 30 million reads per sample. Sequenced reads were mapped to the hg19 whole genome using the Subread aligner (v1.4.3). Reads were assigned to genes using featureCounts. Raw read counts were voom transformed and differential expression performed using limma.

NCBI GEO Database Access to RNA-Sequencing

[release date: upon publication]. http://www.ncbi. nlm.nih.gov/geo/query/acc.cgi?token=utahcoigpd ubpcj&acc=GSE77460

RESULTS

Miz1 Expression Is Increased During Prostate Luminal Cell Differentiation

When grown to confluency and treated with KGF plus androgen, basal prostate epithelial cells (iPrEC) undergo differentiation such that a second suprabasal luminal layer forms on top of the basal layer in 14–18 days [1,5]. To identify genes associated with luminal cell differentiation, iPrECs differentiated for 0–17 days were subjected to RNA sequencing. Miz1 (*ZBTB17*) transcript levels first dropped and then increased over the course of differentiation, peaking at day 14 in the luminal cells (Fig. 1A top panel).

ING4 expression (Fig. 1A bottom panel) followed a similar trend, except that it peaked earlier at day 11. This trend of increased Miz1 mRNA expression over time was further validated by qRT-PCR (Fig. 1B), with a 1.8-fold peak in expression occurring after 14 days of differentiation in the luminal cells; paralleling the RNA-Seq data. There was a similar steady and significant increase in Miz1 protein expression over time, subsequent to the induction of ING4 expression (Fig. 1C). Highest expression of Miz1 was at day 14, mirroring the mRNA. Immunofluorescence imaging at day 3 versus day 12 revealed Miz1 was dramatically induced in the luminal cells (Fig. 1D). It should be noted that Miz1 expression is not restricted to the luminal cells; Miz1 staining is also seen in the basal cells of differentiated cultures, where its expression also increased but less dramatically.

ING4 Induces MIz1 Expression in Prostate Luminal Cells and Binds Directly to its Promoter

Because Miz1 was induced subsequent to ING4, we tested the effect of constitutive ING4 expression on Miz1. ING4 overexpression (iPrEC-ING4), resulted in an earlier and more robust induction of Miz1 expression around day 8 of differentiation, compared to a modest increase at day 12 in normal iPrECs (Fig. 2A). Constitutive ING4 expression also resulted in a sustained ~1.8-fold induction in Miz1 mRNA over the course of differentiation (Fig. 2B), which peaked at 2.5-fold in the luminal cells. Despite ING4 overexpression in the basal cells, Miz1 mRNA was not constitutively expressed in basal cells. Thus, the effect of ING4 on Miz1 is limited to luminal cells. We previously demonstrated that ING4 overexpression accelerates luminal cell differentiation [1] and as seen before there is significantly more luminal cells at day 8 in the ING4 overexpressing cells compared to normal iPrECs (Fig. 2C). There is also a concomitant increase in Miz1 expression in this luminal population as seen by immunostaining (Fig. 2C). These data indicate that ING4 overexpression in the luminal population enhances induced Miz1 expression.

Since constitutive ING4 expression was able to enhance the induction of Miz1 expression in luminal cells, we tested whether Miz1 is a direct target of ING4 using chromatin immunoprecipitation (ChIP). For these experiments, we compared iPrEC, iPrEC-ING4, and iPrEC-shING4 cells. Cell lines were differentiated for 3 days (low ING4) or 10 days (high ING4). ChIP of ING4 in normal iPrECs revealed that after 10 days of differentiation, ING4 was inducibly bound to the Miz1 promoter (Fig. 2D). ING4 overexpression resulted in its constitutive association at the Miz1 promoter at day 3. Cells lacking ING4
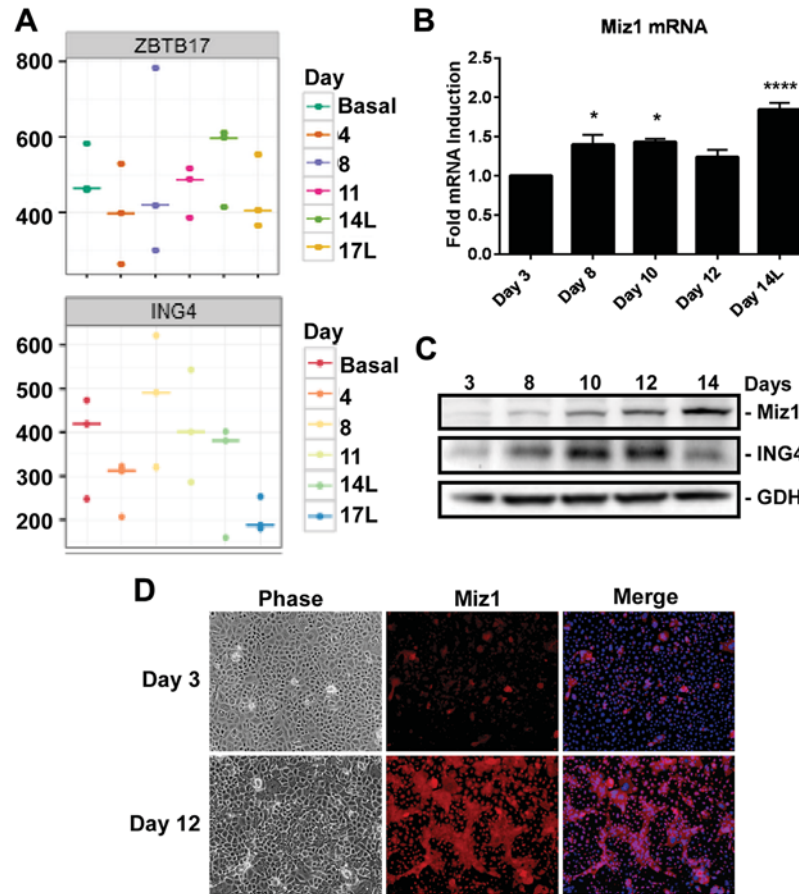
Fig. 1. Miz1 expression increasing during prostate luminal cell differentiation. Confluent immortalized prostate basal epithelial cells (iPrECs) were induced to differentiate with 2 ng/ml KGF and 5 nM R1881 for 0–17 days. ``L'' denotes isolated luminal-specific cells. (**A**) RNA sequencing was performed on samples isolated at the specified time points during iPrEC differentiation. Raw transcript counts are shown for Miz1 (*ZBTB17*) and ING4. (**B**) qRT-PCR was used to validate Miz1 mRNA expression. Data is normalized to 18 sec rRNA and expressed as fold induction relative to day 3 of differentiation. Error bars denote S.D. One-way ANOVA multiple comparisons *t*-test was used to calculate significance relative to day 3; *$P < 0.05$; ****$P < 0.0001$. (**C**) Miz1 and ING4 protein levels were measured by immunoblotting. GAPDH (GDH) served as a loading control. (**D**) iPrECs differentiated for 3 or 12 days were immunostained for Miz1 (red), nuclei stained with Dapi (blue), and imaged by phase and epifluorescence microscopy.

ablated its ChIP at the Miz1 promoter (Fig. 2D) and ING4 did not bind the Histone 3 promoter. ING4 is thought to recruit the histone acetyltransferase HBO1 to chromatin [7]; however, we found HBO1 to be constitutively bound to the Miz1 promoter independent of ING4 (Fig. 2E). On the other hand, a gene known to be repressed during differentiation, SAT2 [19], lost HBO1 association at day 10 of normal differentiation and at day 3 in ING4 overexpressing cells (Fig. 2E).

ING4 is Necessary for Miz1 mRNA Induction in Luminal Cells

To determine if ING4 is necessary for Miz1 induction, we utilized two cell lines that do not express ING4 and do not differentiate; iPrEC-shING4 and

tumorigenic iPrEC-EMP [1]. RNA-Seq data from iPrEC-EMP cells indicated Miz1 mRNA was not induced during the differentiation time course (not shown), and this was similarly observed by qRT-PCR (Fig. 3A). Miz1 mRNA also was not significantly induced in the iPrEC-shING4 cells (Fig. 3B). Thus, ING4 expression is necessary for Miz1 mRNA induction during luminal cell differentiation.

Miz1 Protein is Stabilized in Basal Cells

Despite the lack of significant Miz1 mRNA induction, Miz1 protein was still induced by the differentiation conditions in the undifferentiated "basal-like" EMP and shING4 cells in absence of ING4 (Fig. 3C). We attempted to measure Miz1 protein stability in iPrEC-shING4 cells by treating
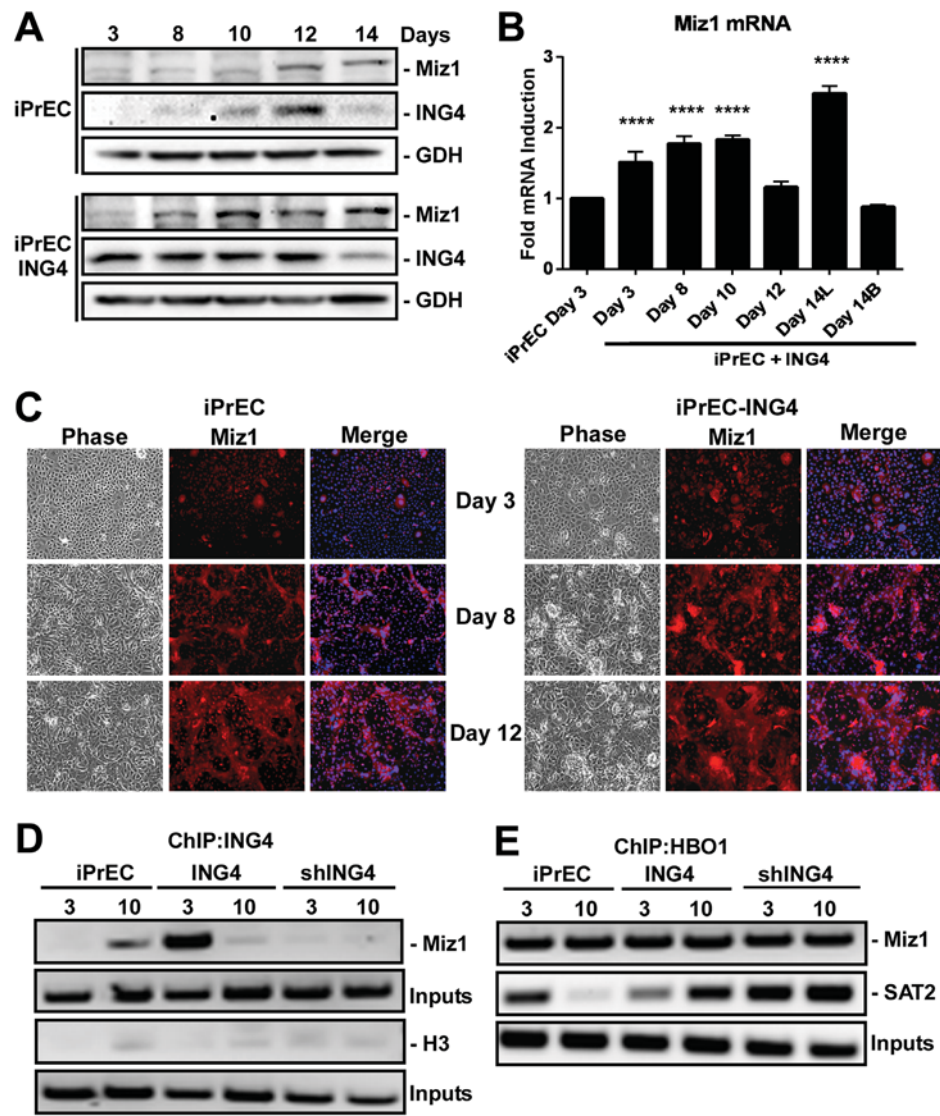
Fig. 2. ING4 is sufficient to induce Miz1 expression in prostate luminal cells and binds directly to its promoter. Confluent iPrEC, iPrEC-ING4, and shING4-iPrEC cell lines were induced to differentiate with 2 ng/ml KGF and 5 nM R1881 for 3–14 days. (**A**) Miz1 and ING4 protein levels were measured by immunoblotting. GAPDH (GDH) served as a loading control. (**B**) qRT-PCR analysis of Miz1 mRNA isolated from iPrECs + ING4 over the indicated time course of differentiation. Data normalized to 18sec rRNA and expressed as fold induction relative to day 3 of iPrEC differentiation. (L and B) denotes isolated luminal and basal cell populations. Error bars denote S.D. One-way ANOVA multiple comparisons t-test was used to calculate significance relative to day 3 of iPrEC differentiation; $****P < 0.0001$. (**C**) Cells differentiated for indicated times were immunostained for Miz1 (red), nuclei stained with Dapi (blue), and imaged by phase and epifluorescence microscopy. (**D**) Chromatin immunoprecipitation (ChIP) of ING4 on the Miz1 promoter at day 3 or 10 of differentiation. Histone 3 served as a negative control and shING4 controlled for antibody specificity. (**E**) ChIP of HBO1 on the Miz1 and SAT2 promoters at day 3 or 10 of differentiation.

with cycloheximide for different times. Regardless of the length of time of CHX treatment (up to 6 hr), we were unable to detect a change in Miz1 protein expression (Fig. 3E), suggesting Miz1 protein in basal cells is very stable. Under the same conditions, Myc protein was rapidly lost. Thus, ING4 expression is necessary for Miz1 mRNA induction in luminal cells, but Miz1 protein

stability may be enhanced independent of ING4 in basal cells.

Constitutive Miz1 Expression Is Sufficient to Drive Luminal Cell Differentiation

If Miz1 is a primary target of ING4 required for differentiation, then overexpression of Miz1 could be
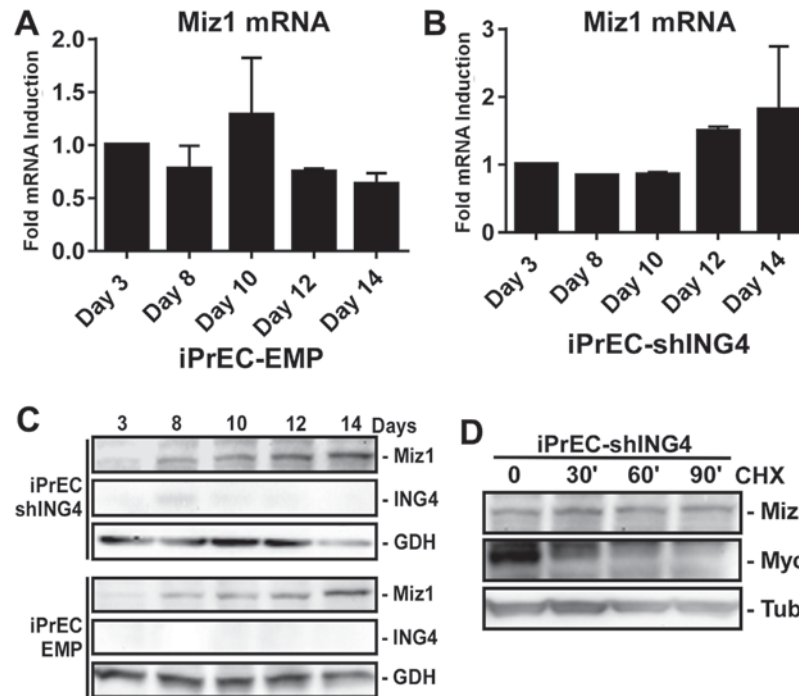
Fig. 3. ING4 is necessary for Miz1 induction in luminal cells, while Miz1 protein is stabilized in basal cells. iPrECs, iPrEC-shING4, and EMP-iPrECs were induced to differentiate with 2 ng/ml KGF and 5 nM R1881 for 3–17 days. (**A** and **B**) qRT-PCR analysis of Miz1 mRNA isolated from iPrEC-shING4 and EMP cells. Error bars denote S.D. No statistical difference between time points. (**C**) Miz1 and ING4 protein levels were measured by immunoblotting. GAPDH (GDH) served as a loading control. (**D**) iPrEC-shING4 cells were differentiated for 12 days and then treated with 50 μg/ml cycloheximide (CHX) for 0–90 min and levels of Miz1 and Myc protein measured by immunoblotting. Tubulin (Tub) served as a loading control.
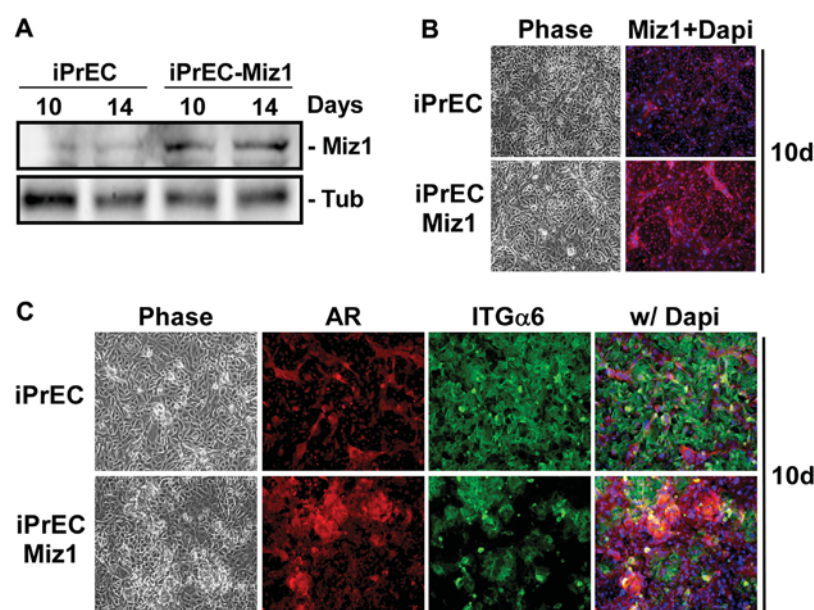
sufficient to drive iPrEC differentiation. To address Miz1 sufficiency, we generated iPrECs that constitutively overexpress Miz1 (iPrEC-Miz1) as assessed by immunoblotting and immunostaining (Fig. 4A and B). Compared to normal iPrECs differentiated for 10 days, when a few AR-positive, integrin α6-negative luminal cells appear, there was considerably more of these luminal cells in the iPrEC-Miz1 cultures (Fig. 4C). This is the same phenotype that is observed in ING4 overexpressing cells (see Fig. 2C). Thus, overexpression of Miz1 is sufficient to induce luminal cell differentiation equivalent to that observed when ING4 is overexpressed.

Miz1 Is Not Required for Luminal Cell Differentiation

To determine if Miz1 is necessary for luminal cell differentiation, we generated cells that express a Tet-inducible shRNA targeting Miz1. This allowed us to selectively inhibit Miz1 expression late in differentiation, when it is maximally induced in the luminal cells. To test Miz1 knock-down, iPrEC-TetON-shMiz1 cells were differentiated for 10 days, and Miz1 expression suppressed by Dox induction

of Miz1 shRNA during the last 5 or 3 days of differentiation. Miz1 expression was significantly reduced in as little as 3 days (Fig. 5A). To test the dependency on Miz1, iPrEC-TetON-shMiz1 cells were differentiated for 8, then treated with doxycycline for an additional 6 days of differentiation (14 days total). Miz1 expression was effectively inhibited under these conditions (Fig. 5B). The same amount of AR-positive, integrin α6-negative luminal cells were induced in the presence or absence of Miz1 (Fig. 5B), indicating that the cells were fully able to differentiate without Miz1. This was observed with two different shRNAs (not shown).

This lack of necessity was surprising given previous findings indicating Miz1 is required for differentiation in other models [10,12,20]. Furthermore, one of these studies indicated Miz1 interaction with Myc was required for differentiation and a Myc mutant which cannot bind Miz1, MycV394D, blocked differentiation [10]. We previously showed that Myc is required for ING4 induction and luminal cell differentiation [1]. Therefore, we generated iPrECs that overexpress Myc-GFP or Myc-V394D-RFP (Fig. 5D). Expression of MycV394D had no impact on the ability of these cells to differentiate; inducing comparable

Fig. 4. Constitutive Miz1 expression is sufficient to drive luminal cell differentiation. iPrECs overexpressing Miz1 (iPrEC-Miz1) were induced to differentiate with 2 ng/ml KGF and 5 nM R1881 for 10–14 days. (**A**) Level of Miz1 expression was measured by immunoblotting. Tubulin (Tub) served as a loading control. (**B**) Cells differentiated for 10 days were immunostained for Miz1 (red) and nuclei were stained with Dapi (blue). (**C**) Differentiation was measured after 10 days by immunostaining of basal cells for integrin α6 (ITGα6; green) and luminal cells for AR (red), and nuclei were stained with Dapi (blue). All cells were visualized by phase and epifluorescence microscopy.

levels of AR-positive and integrin α6-negative luminal cells (Fig. 5E).

DISCUSSION

We set out to determine how ING4 induction during prostate luminal cell differentiation leads to the suppression of integrin expression by defining ING4 target genes that might control integrin expression. Our studies successfully identified Miz1 as a direct downstream target of ING4 in luminal cells, and demonstrated that Miz1 overexpression is sufficient to mimic the differentiation phenotype induced by ING4 including loss of integrin α6 expression. However, Miz1 is not necessary for luminal cell differentiation as determined by shRNA knock-down or expression of a dominant Myc-Miz1 binding mutant and therefore is not absolutely necessary for integrin loss during luminal cell differentiation.

ING4 is a chromatin binding protein that specifically recognizes and binds the H3K4me3 chromatin mark [21]. It has been shown to recruit HBO1, an acetyltransferase that can acetylate histone H4 or H3 to promote transcription of target genes [7,22]. However, the exact targets that ING4 actually binds have largely not been identified, and are limited to Smc4, Egln1, Ext1 in HT1080 cells [22], and few NF-κB targets such as Cox2 and MMP9 [23]. Using RNA-Seq, a best candidate approach, and ChIP, we identified the Miz1

promoter as a binding target of ING4 during prostate luminal epithelial differentiation. We further demonstrate that genetically increasing or decreasing ING4 expression results in a concomitant increase or decrease in Miz1 mRNA expression, respectively. However, this coordinated expression is not present in basal cells, even when ING4 is constitutively overexpressed, being restricted to the luminal cells. Thus, there are likely to be other "competency" factors required, that is, a signal that defines a pre-luminal state induced by the differentiation conditions of KGF and androgen. Similarly, we demonstrate that overexpression of Miz1 is sufficient to robustly accelerate luminal cell differentiation to the same degree seen with ING4 overexpression. However, this effect is still dependent on the differentiation factors; constitutive Miz1 overexpression in the absence of KGF and androgen is not sufficient to induce differentiation on its own.

Given the reported ability of ING4 to specifically recruit HBO1 to H3K4me3 marked promoters [7,21,22], we were surprised to find that HBO1 was constitutively bound to the Miz1 promoter. This was not true for all genes, as we saw HBO1 loss at SAT2, a gene that is down regulated upon luminal cell differentiation in our model. We noted that Miz1 is also expressed in basal cells, where it is not subject to ING4 regulation. These data are consistent with Miz1 being an already active gene in prostate epithelial cells. Thus, ING4 may be acting to enhance transcription via recruitment of
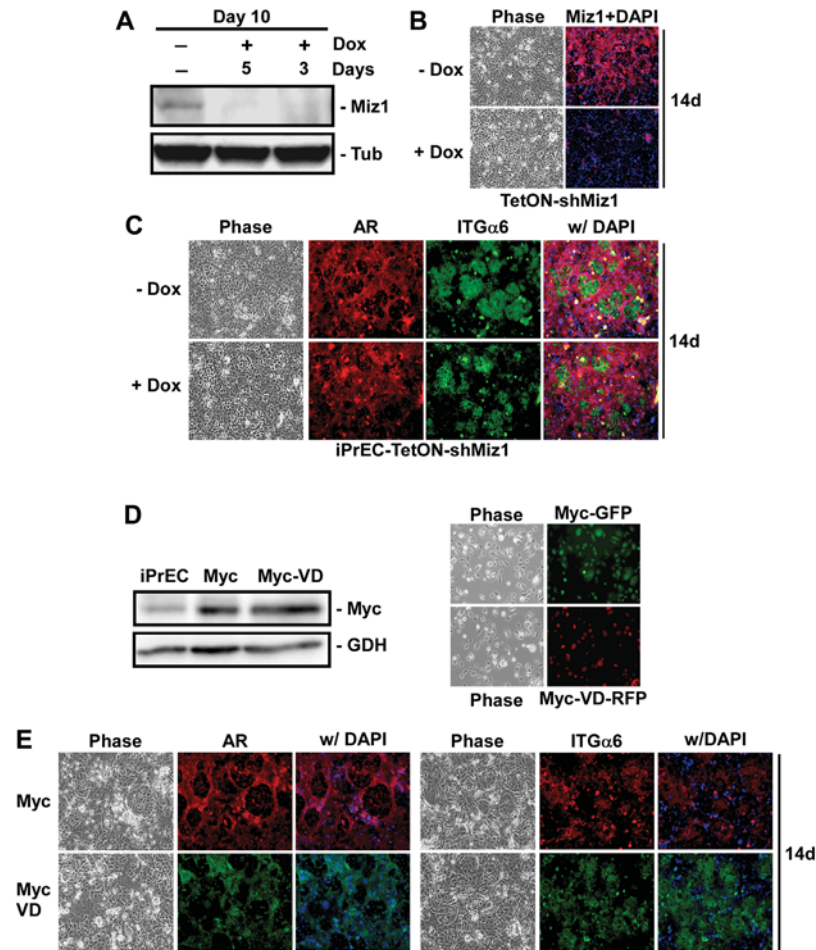
Fig. 5. Miz1 is not required for luminal cell differentiation. iPrECs overexpressing Miz1 Tet-inducible shRNA (iPrEC-TetON-shMiz1), Myc (Myc-GFP), or MycV394D mutant (Myc-V394D-RFP) were induced to differentiate with 2 ng/ml KGF and 5 nM R1881 for 10–14 days. (**A**) Cells were differentiated for 10 days and treated with 100 ng/ml doxycycline (Dox) during the last 5 or 3 days of differentiation. Miz1 and tubulin (Tub) expression were measured by immunoblotting. (**B** and **C**) Cells were differentiated for 14 days and treated with Dox during the last 6 days of differentiation. (**B**) Control cultures were immunostained for Miz1 (red) and nuclei stained with Dapi (blue). (**C**) Differentiation was measured by immunostaining of basal cells for integrin α6 (ITGα6; green) and luminal cells for AR (red), and nuclei were stained with Dapi (blue). All cells were imaged by phase and epifluorescence microscopy. (**D**) Myc-GFP or Myc-VD-RFP expression was assessed in undifferentiated cells by western blot (left panel), with GAPDH (GDH) as a loading control, and epifluorescence microscopy (right panel). (**E**) Differentiation was measured after 14 days by immunostaining of luminal cells for AR (red-Myc; green-MycVD) and basal cells for integrin α6 (ITGα6; red-Myc; green-MycVD), and nuclei were stained with Dapi (blue). All cells were visualized by phase and epifluorescence microscopy.

other factors specifically during luminal cell differentiation. ChIP-Seq experiments are underway to define other ING4 targets and associated chromatin modifiers.

We previously showed that oncogenic conversion of human iPrECs by Erg, Myc, and shPten overexpression (EMP cells), generates tumorigenic cells that are arrested in differentiation and fail to induce ING4 expression [1]. We also demonstrated Erg/Myc overexpressing cells are not tumorigenic, but loss of ING4 is sufficient to transform them and that ING4 is lost in over 60% of human primary prostate tumors [1]. Consistent with Miz1 dependency on ING4 expression, the EMP cells also did not induce

Miz1 expression in response to the differentiation conditions. Correspondingly, these cells do not properly differentiate as defined by a lack of a distinct AR-positive and integrin α6-negative population.

Loss of Miz1 expression per see is not likely to be a good distinguishing marker for prostate cancer as basal cells and EMP cells still express Miz1; it is just not induced or regulated by ING4. Nonetheless, this allowed us to identify at least two mechanisms by which Miz1 expression is regulated. However, the most striking finding was the apparent lack of dependency on Miz1 for luminal cell differentiation. Despite the presence of distinct mechanisms for

regulating Miz1 mRNA and protein expression, cells were still capable of differentiating without Miz1. This indicates there are other, potentially compensatory, factors that control differentiation, and integrin expression in particular. It also indicates there are other ING4 targets required for luminal cell differentiation. One potential target could be Notch signaling [24]. Studies are currently underway to determine the relationship between ING4, Notch, and luminal cell differentiation.

CONCLUSIONS

The Myc repressor, Miz1, is a direct target of the chromatin binding protein ING4, whose induction during luminal cell differentiation is dependent on ING4. Miz1 is capable of accelerating luminal cell differentiation when overexpressed, but is not absolutely required for differentiation.

ACKNOWLEDGMENTS

REFERENCES

1. Berger PL, Frank SB, Schulz VV, Nollet EA, Edick MJ, Holly B, Chang TT, Hostetter G, Kim S, Miranti CK. Transient induction of ING4 by Myc drives prostate epithelial cell differentiation and its disruption drives prostate tumorigenesis. Cancer Res 2014;74(12):3357–3368.

2. Li X, Wang Y, Sharif-Afshar AR, Uwamariya C, Yi A, Ishii K, Hayward SW, Matusik RJ, Bhowmick NA. Urothelial transdifferentiation to prostate epithelia is mediated by paracrine TGF-beta signaling. Differentiation 2009;77(1):95–102.

3. Wu CT, Altuwaijri S, Ricke WA, Huang SP, Yeh S, Zhang C, Niu Y, Tsai MY, Chang C. Increased prostate cell proliferation and loss of cell differentiation in mice lacking prostate epithelial androgen receptor. Proc Natl Acad Sci USA 2007;104(31):12679–12684.

4. Luo W, Rodriguez M, Valdez JM, Zhu X, Tan K, Li D, Siwko S, Xin L, Liu M. Lgr4 is a key regulator of prostate development and prostate stem cell differentiation. Stem cells 2013;31(11):2492–2505.

5. Lamb LE, Knudsen BS, Miranti CK. E-cadherin-mediated survival of androgen-receptor-expressing secretory prostate

6. Coles AH, Jones SN. The ING gene family in the regulation of cell growth and tumorigenesis. J Cell Physiol 2009;218(1):45–57.

7. Doyon Y, Cayrou C, Ullah M, Landry A-J, Côté V, Selleck W, Lane WS, Tan S, Yang X-J, Côté J. ING tumor suppressor proteins are critical regulators of chromatin acetylation required for genome expression and perpetuation. Mol Cell 2006;21(1):51–64.

8. Kim S, Welm AL, Bishop JM. A dominant mutant allele of the ING4 tumor suppressor found in human cancer cells exacerbates MYC-initiated mouse mammary tumorigenesis. Cancer Res 2010;70(12):5155–5162.

9. Cress AE, Rabinovitz I, Zhu W, Nagle RB. The α6β1 and α6β4 integrins in human prostate cancer progression. Cancer Metastasis Rev 1995;14(3):219–228.

10. Gebhardt A, Frye M, Herold S, Benitah SA, Braun K, Samans B, Watt FM, Elsässer H-P, Eilers M. Myc regulates keratinocyte adhesion and differentiation via complex formation with Miz1. J Cell Biol 2006;172(1):139–149.

11. Mazzone M, Selfors LM, Albeck J, Overholtzer M, Sale S, Carroll DL, Pandya D, Lu Y, Mills GB, Aster JC, Artavanis-Tsakonas S, Brugge JS. Dose-dependent induction of distinct phenotypic responses to Notch pathway activation in mammary epithelial cells. Proc Natl Acad Sci USA 2010;107(11):5012–5017.

12. Sanz-Moreno A, Fuhrmann D, Wolf E, von Eyss B, Eilers M, Elsässer H-P. Miz1 deficiency in the mammary gland causes a lactation defect by attenuated stat5 expression and phosphorylation. PloS ONE 2014;9(2):e89187.

13. Tapia C, Zlobec I, Schneider S, Kilic E, Guth U, Bubendorf L, Kim S. Deletion of the inhibitor of growth 4 (ING4) tumor suppressor gene is prevalent in human epidermal growth factor 2 (HER2)-positive breast cancer. Hum Pathol 2011;42(7):983–990.

14. Byron SA, Min E, Thal TS, Hostetter G, Watanabe AT, Azorsa DO, Little TH, Tapia C, Kim S. Negative regulation of NF-kappaB by the ING4 tumor suppressor in breast cancer. PloS ONE 2012;7(10):46823.

15. Yan R, He L, Li Z, Han X, Liang J, Si W, Chen Z, Li L, Xie G, Li W, Wang P, Lei L, Zhang H, Pei F, Cao D, Sun L, Shang Y. SCF(JFK) is a bona fide E3 ligase for ING4 and a potent promoter of the angiogenesis and metastasis of breast cancer. Genes Dev 2015;29(6):672–685.

16. Wiederschain D, Susan W, Chen L, Loo A, Yang G, Huang A, Chen Y, Caponigro G, Yao Y-m, Lengauer C, Sellers WR, Benson JD. Single-vector inducible lentiviral RNAi system for oncology target validation. Cell Cycle 2009;8(3):498–504.

17. Herold S, Wanzel M, Beuger V, Frohme C, Beul D, Hillukkala T, Syvaoja J, Saluz HP, Haenel F, Eilers M. Negative regulation of the mammalian UV response by Myc through association with Miz-1. Mol Cell 2002;10(3):509–521.

18. Edick MJ, Tesfay L, Lamb LE, Knudsen BS, Miranti CK. Inhibition of integrin-mediated crosstalk with epidermal growth factor Receptor/Erk or src signaling pathways in autophagic prostate epithelial cells induces caspase-independent death. Mol Biol Cell 2007;18(7):2481–2490.

19. Chen Y, Vujcic S, Liang P, Diegelman P, Kramer DL, Porter CW. Genomic identification and biochemical characterization of a second spermidine/spermine N1-acetyltransferase. Biochem J 2003;373(Pt 3):661–667.

20. Kerosuo L, Bronner ME. Biphasic influence of Miz1 on neural crest development by regulating cell survival and apical adhesion complex formation in the developing neural tube. Mol Biol Cell 2014;25(3):347–355.

21. Culurgioni S, Munoz IG, Moreno A, Palacios A, Villate M, Palmero I, Montoya G, Blanco FJ. Crystal structure of inhibitor of growth 4 (ING4) dimerization domain reveals functional organization of ING family of chromatin-binding proteins. J Biol Chem 2012;287(14):10876–10884.

22. Hung T, Binda O, Champagne KS, Kuo AJ, Johnson K, Chang HY, Simon MD, Kutateladze TG, Gozani O. ING4 mediates crosstalk between histone H3 K4 trimethylation and H3 acetylation to attenuate cellular transformation. Mol Cell 2009;33(2): 248–256.

23. Nozell S, Laver T, Moseley D, Nowoslawski L, De Vos M, Atkinson GP, Harrison K, Nabors LB, Benveniste EN. The ING4 tumor suppressor attenuates NF-kappaB activity at the promoters of target genes. Mol Cell Biol 2008;28(21):6632–6645.

24. Chakrabarti R, Wei Y, Romano RA, DeCoste C, Kang Y, Sinha S. Elf5 regulates mammary gland stem/progenitor cell fate by influencing notch signaling. Stem Cells 2012;30(7): 1496–1508.

BMC Biotechnology

A Streamlined Method for the Design and Cloning of shRNAs into an Optimized Dox-inducible Lentiviral Vector
--Manuscript Draft--

Manuscript Number:	
Full Title:	A Streamlined Method for the Design and Cloning of shRNAs into an Optimized Dox-inducible Lentiviral Vector
Article Type:	Methodology article
Section/Category:	RNAi mechanisms and applications

| Abstract: | ABSTRACT
Background: Short hairpin RNA (shRNA) is an established and effective tool for stable knock down of gene expression. Lentiviral vectors can be used to deliver shRNAs, thereby providing the ability to infect most mammalian cell types with high efficiency, regardless of proliferation state. Furthermore, the use of inducible promoters to drive shRNA expression allows for more thorough investigations into the specific timing of gene function in a variety of cellular processes. Moreover, inducible knockdown allows the investigation of genes that would be lethal or otherwise poorly tolerated if constitutively knocked down. Lentiviral, inducible shRNA vectors are readily available, but unfortunately the process of cloning, screening, and testing shRNAs can be time-consuming and expensive. Therefore, we sought to refine a popular vector (Tet-pLKO-Puro) and streamline the cloning process with efficient protocols so that researchers can more efficiently utilize this powerful tool.
Results: First, we modified the Tet-pLKO-Puro vector to make it more amenable for molecular cloning (EZ-Tet-pLKO-Puro). Our primary modification was to shrink the stuffer region, which allows vector purification via polyethylene glycol precipitation thereby avoiding the need to purify DNA through agarose. In addition, we generated EZ-Tet-pLKO vectors with hygromycin or blasticidin resistance to provide greater flexibility in cell line engineering. Furthermore, we provide a detailed guide for utilizing these vectors, including shRNA design strategy and simplified screening methods. Notably, we emphasize the importance of loop sequence design and demonstrate that the addition of a single mismatch in the loop stem can greatly improve shRNA efficiency. Lastly, we display the robustness of the system with a doxycycline titration and recovery timecourse.
Conclusions: Our aim was twofold: first, to take a very useful shRNA vector and make it more amenable for molecular cloning and, secondly, to provide a streamlined protocol and rationale for cost-effective design, cloning, and screening of shRNAs. With this knowledge, anyone can take advantage of this powerful tool to inducibly knockdown any gene of their choosing. |

| Corresponding Author: | Cindy K Miranti
Van Andel Research Institute
UNITED STATES |
Corresponding Author Secondary Information:	
Corresponding Author's Institution:	Van Andel Research Institute
Corresponding Author's Secondary Institution:	
First Author:	Sander B Frank
First Author Secondary Information:	

Order of Authors:	Sander B Frank
	Veronique V Schulz
	Cindy K Miranti
Order of Authors Secondary Information:	
Opposed Reviewers:	

A Streamlined Method for the Design and Cloning of shRNAs into an Optimized

Dox-inducible Lentiviral Vector

Sander B. Frank[1,2], Veronique V. Schulz[1], and Cindy K. Miranti[1]

[1]Laboratory of Integrin Signaling and Tumorigenesis, Van Andel Research Institute Grand Rapids, MI

USA

[2]Genetics Program, Michigan State University, East Lansing, MI USA

Short Title: Streamlined Method for Tet-inducible shRNA

Keywords: pLKO, shRNA, lentivirus, inducible, Tet-On

Email addresses:

sander.frank@vai.org

veronique.schulz@vai.org

cindy.miranti@vai.org

Corresponding Author:

Cindy K. Miranti

Laboratory of Integrin Signaling and Tumorigenesis

Van Andel Research Institute

333 Bostwick Ave NE

Grand Rapids, MI 49503

Cindy.miranti@vai.org

616-234-5358

ABSTRACT

Background: Short hairpin RNA (shRNA) is an established and effective tool for stable knock down of gene expression. Lentiviral vectors can be used to deliver shRNAs, thereby providing the ability to infect most mammalian cell types with high efficiency, regardless of proliferation state. Furthermore, the use of inducible promoters to drive shRNA expression allows for more thorough investigations into the specific timing of gene function in a variety of cellular processes. Moreover, inducible knockdown allows the investigation of genes that would be lethal or otherwise poorly tolerated if constitutively knocked down. Lentiviral, inducible shRNA vectors are readily available, but unfortunately the process of cloning, screening, and testing shRNAs can be time-consuming and expensive. Therefore, we sought to refine a popular vector (Tet-pLKO-Puro) and streamline the cloning process with efficient protocols so that researchers can more efficiently utilize this powerful tool.

Results: First, we modified the Tet-pLKO-Puro vector to make it more amenable for molecular cloning (EZ-Tet-pLKO-Puro). Our primary modification was to shrink the stuffer region, which allows vector purification via polyethylene glycol precipitation thereby avoiding the need to purify DNA through agarose. In addition, we generated EZ-Tet-pLKO vectors with hygromycin or blasticidin resistance to provide greater flexibility in cell line engineering. Furthermore, we provide a detailed guide for utilizing these vectors, including shRNA design strategy and simplified screening methods. Notably, we emphasize the importance of loop sequence design and demonstrate that the addition of a single mismatch in the loop stem can greatly improve shRNA efficiency. Lastly, we display the robustness of the system with a doxycycline titration and recovery timecourse.

Conclusions: Our aim was twofold: first, to take a very useful shRNA vector and make it more amenable for molecular cloning and, secondly, to provide a streamlined protocol and rationale for cost-effective design, cloning, and screening of shRNAs. With this knowledge, anyone can take advantage of this powerful tool to inducibly knockdown any gene of their choosing.

BACKGROUND

Knockdown of gene expression at the mRNA level via RNA interference (RNAi) is a common method for investigating gene function. For transient knockdown in mammalian cell culture, small interfering RNA (siRNA) is often favored. The benefits of siRNA include commercially available RNA oligos which can be transfected into cells for quick and efficient knockdown. However, siRNA becomes less useful when working with cell types with low transfection efficiency or in experiments that require prolonged gene knockdown [1]. Another common method for utilizing RNAi is short-hairpin RNA (shRNA), which are synthetic non-coding RNA genes that share microRNA machinery used by cells for post-transcriptional regulation. Though not as simple to utilize as siRNA, shRNA can avoid concerns of low transfection efficiency and temporary knockdown by using retroviral delivery and selection for stable genomic integration [2-4].

Lentiviral shRNA vectors are popular due to their ability to infect nearly any cell type and integrate into the genome of both dividing and non-dividing cells. In 2006, the BROAD institute established the RNAi Consortium to identify and clone multiple shRNA candidate sequences for every gene in the mouse and human genomes [5]. The consortium cloned the shRNA sequences into the pLKO lentiviral vector backbone and has made them available for distribution from Fisher Thermo Scientific and Sigma-Aldrich. The shRNAs were not all functionally validated but were given a computationally calculated score for predicated efficiency and specificity.

In 2009, Dmitri Wiederschain and colleagues built upon the pLKO vector and made multiple changes, the two most significant of which were the inclusion of the Tet-Repressor gene (TetR) and an H1 promoter containing the TetOperator (TetO) sequence to drive shRNA expression. Together, these modifications allow transcription of shRNA upon the addition of tetracycline, or its analogue doxycycline (Dox), to sequester TetR and relieve repression at the TetO [5, 6]. This vector combines the benefits of lentiviral delivery and inducible gene knockdown, providing many advantages over siRNA or constitutive shRNA including the ability to use the same pool of cells as its own negative control, thereby eliminating concerns of transfection/infection efficiency or unintentional clonal variation. By combining inducible

vectors with the list of candidate shRNA sequences from the RNAi consortium it is now possible to induce knockdown of nearly any gene in virtually any cell type.

The Tet-pLKO-Puro vector is a potentially powerful tool, but the process of designing and cloning shRNAs into the vector is not without challenge. In an effort to improve this tool even further we made some modifications to make it more amenable for cloning. Furthermore, we establish clear and efficient protocols for designing and cloning shRNAs into the vector. In addition, we demonstrate the importance of loop design including using a single mismatch to improve shRNA efficiency. Finally, we generated hygromycin and blasticidin resistance genes to expand the tool box and to allow for selection of several different shRNAs in one cell. With our modified vector (EZ-Tet-pLKO) and a detailed description for designing and cloning shRNAs, we aim to make it easy for anyone to quickly adopt and utilize this tool.

RESULTS

Modifications to the Tet-pLKO-Puro vector

We started with the Tet-pLKO-Puro vector and modified it to make it more amenable for molecular cloning, terming our version EZ-Tet-pLKO-Puro. First, we used mutagenesis to delete the large stuffer region (~1.9 kb), leaving a smaller stuffer of ~200 bp (**Fig. 1a**). Second, we mutated the 5' AgeI cloning site to an NheI sequence to ameliorate occasional difficulties with inefficient AgeI+EcoRI co-digestion. Additionally, we generated matching vectors with mammalian selection markers for hygromycin (Hygro) or blasticidin (Blast) resistance (**Fig. 1a**). The smaller stuffer makes it possible to purify cut vector by size-selective DNA precipitation with polyethylene glycol (PEG). To compare precipitation methods, cut DNA was precipitated by isopropanol, 8% PEG, or 6% PEG. The 6% PEG precipitation removed nearly all of the 200 bp stuffer **(Fig. 1b).** Together, the combination of vector modifications and utilization of PEG precipitation provides a simplified method for preparing cut vector.

shRNA oligo design

4

Developing functional shRNA constructs often requires testing many targeting sequences; therefore, a process for designing shRNAs quickly and efficiently is quite valuable. Targeting sequences were selected as described in the methods section and used to generate sense and antisense shRNA oligos. shRNA oligos contain the following elements: 5' overhang, targeting sequence, loop, reverse-complement targeting sequence, transcriptional terminator sequence, and 3' overhang **(Fig. 2a)**. The antisense oligo (bottom strand) is a reverse complement of the sense oligo with complementary overhangs. Without a mismatch, a 6 nt palindrome loop is predicted to collapse to a 4 nt loop and shift the targeting sequence by one base **(Fig. 2b)**. Immortalized prostate epithelial cells (iPrECs) were infected with shRNA lentivirus (sh.p38δ or sh.Creb1) and pools were selected containing the same targeting sequence with or without a single mismatch. Immunoblot showed very efficient knockdown of p38δ with the 7 nt loop and no knockdown with the 6 nt loop **(Fig. 2c)**. Probing for TetR showed that both pools were infected with the lentivirus and had similar expression levels of the lentiviral construct. A similar test was performed using cells containing the sh.Creb1 construct and produced similar results **(Fig. 2d)**. Thus, when designing shRNA sequences it is crucial to consider not only the targeting sequence, but also a mismatch in the loop stem.

Streamlined colony screening

Colony-PCR is a quick way to use small amounts of bacteria directly as template in a PCR reaction to screen bacterial colonies for the desired construct. We designed primers to span the stuffer/shRNA insert region, producing a ~450 bp band for positive clones and a ~620 bp band for background vector with retained stuffer **(Fig 3a)**. PCR product was visualized by agarose gel electrophoresis, which produced clearly identifiable bands for true clones and background colonies **(Fig. 3b)**. Additionally, clones can be further validated by restriction enzyme (RE) digest screening of isolated DNA. The original Tet-pLKO-Puro protocol recommended using an XhoI loop in the hairpin [6, 7]. When running an RE screen with XhoI, the primary indication of a positive clone is the loss of a ~400 bp band and gain of very small bands (~1-2% of total DNA) that are difficult to visualize on agarose **(Fig. 3c).** To

resolve this issue we used a SpeI site for loop design. When visualized on agarose, a SpeI screen produces a clear band at ~500 bp, which is ~5% of total DNA **(Fig. 3c,d).** This shift from a negative screen to a positive screen is more reliable and easier to analyze. Positive clones can then be sent for Sanger sequencing as final validation using the same pLKO-fwd primer as used in the PCR screen. Thus, the combination of colony-PCR as a cheap and quick primary screen and SpeI-based digest as a secondary screen creates a streamlined process for identifying positive shRNA clones.

Dox Titration and recovery time courses

Next, we validated the efficacy of the EZ-Tet-pLKO-Puro vector in cell culture. Cells were infected with lentivirus and pools were selected with puromycin. We performed a titration with Dox (0.5 to 50 ng/mL) and found that as little as 10 ng/mL was sufficient to induce target (p38α) knockdown **(Fig. 4a)**. Furthermore, the target protein can be recovered after removal of Dox. Cells with sh.p38α were treated with Dox for 72 h and then split. Dox was removed and samples were harvested over a recovery time course **(Fig. 4b)**. Recovery of protein began four days after removal of Dox. Thus, the EZ-Tet-pLKO system is both inducible and reversible.

DISCUSSION

The EZ-Tet-pLKO vector together with our detailed methods provides a descriptive guide to efficiently utilize inducible shRNAs. Though we have focused on a modified pLKO vector, the principles of shRNA design and screening could be applied to many other cloning scenarios. Our primary modification to the vector was to shrink the stuffer region, which allows for size-selective precipitation of cut vector via PEG [8]. Compared to alcohol precipitation and gel extraction, PEG precipitation is faster, provides cleaner DNA, and avoids concerns of potential DNA damage from UV exposure [9, 10]. We also emphasized the importance of using proper loop design for shRNAs by adding a stem mismatch [11]. The inclusion of a mismatch in the loop region can aid hairpin formation by preventing loop collapse and thus shifting the targeting sequence, which can disrupt proper DICER binding and

target mRNA cleavage [12, 13]. The mismatch was not always necessary for proper shRNA function (not shown), but in at least the two cases reported here it was crucial and should always be included to maximize the chances of developing a successful shRNA construct.

One important caveat with the Dox-inducible system is that at high doses (>1 μg/mL), Dox can have detrimental effects on cell viability via disruption of mitochondrial function [14]. In our experience, we observed viability effects from prolonged treatment (>4 days) at 500 ng/mL but saw no effects from a 2-week treatment at 50 ng/mL (not shown). As an extra control, the parent cell line (without lentiviral infection) can be treated with Dox to check specifically for effects on cell viability. In most cases a 10-50 ng/mL dose of Dox should be well tolerated but that should be tested by the end user in their particular cell line as a precaution.

A good control to include when testing new pools is to probe an immunoblot for the TetR protein to confirm that the selected pool of cells has robust expression of the lentiviral vector. Likewise, if comparing pools or clones, those with highest TetR expression often show the greatest knockdown (not shown). When targeting a new gene, we recommend starting with at least three different targeting sequences with the expectation that one or two will work efficiently.

The timing of gene knockdown and recovery is not universal. For most genes 72 h is sufficient to see knockdown at the protein level. However, this is highly dependent on protein stability. Longer-lived proteins (e.g. membrane-bound receptors, housekeeping proteins) may take up to a week for proper knockdown. We observed p38α knockdown at 72 h, but Creb1 knockdown was not observed until at least day five of Dox induction. Likewise, protein recovery will be highly dependent on the transcription rate of the gene so that lower expressed genes will take longer to recover. Furthermore, cell confluency and proliferation rate will also affect the rate of protein synthesis and turnover, thus affecting Dox knockdown and recovery timing. All these factors need to be considered when designing temporally-sensitive experiments and will be cell and context specific.

Lastly, we also sought to aid researchers by designing hygromycin and blasticidin resistant variants of the EZ-Tet-pLKO vector, thus providing more flexibility in creating multiple genetically

7

engineered cell lines. By combining all three vectors in one cell line it would be possible to knockdown two or three targets simultaneously upon Dox treatment. In addition to the Tet inducible system, there are other inducible shRNA vectors that can prove useful and are commercially available, such as cumate or IPTG-inducible vectors [15, 16]. With some creativity and strategy it would also be possible to create cells with multiple shRNAs, each activated by different inducers. Moreover, inducible shRNAs could be combined with inducible cDNA expression systems to test overexpression and knockdown simultaneously or sequentially [17]. Use of inducible vectors with various selection markers opens the door for greater quantity and variety of questions that can be addressed with molecular biology.

CONCLUSIONS

Inducible shRNAs are a very powerful tool when used properly. We sought to provide a guide to allow more people to more easily use this system with our EZ-Tet-pLKO vector. There are lots of ways to manipulate gene expression, including the recent advent of CRISPR/Cas9 technologies. Though the potential of CRISPR is great, it is not without serious limitations, including inability to study genes with lethal knockdown phenotypes and the reliance on selecting clonal populations for cell culture studies [18]. In addition to the cell culture uses shown here, the pLKO system is also useful *in vivo*, for example with tumor xenografts which can be induced to knockdown a gene upon addition of Dox to the animal food or water [19]. Our goal with this report was to take the useful Tet-pLKO-Puro system and refine it further. With these new EZ-Tet-pLKO vectors and protocols, researchers will find this tool to be more versatile and user-friendly than ever.

METHODS

pLKO vector modifications

The Tet-pLKO-Puro plasmid was ordered from Addgene (Plasmid 21915) [6, 7]. Mutagenesis was performed using the QuikChange II Site Directed Mutagenesis kit (Aligent). Bases 222-1869 of the stuffer region between the AgeI and EcoRI cloning sites were deleted. The deletion was performed by

8

179 inserting an EcoRI site at base 222 of the stuffer (primer 5'-GCTACTCCACCACTTGAATTCCTAAGCGGTCAGC). The vector was then digested with EcoRI, re-ligated, and clones were screened for those that ligated the new EcoRI site directly to the 3' cloning site, thus excising the bulk of the stuffer region and preserving the 3' cloning site. Mutagenesis was then used to mutate the AgeI restriction site to an NheI sequence (primer 5'-TATCAGTGATAGAGACGCTAGCGTGTTGTAAATGAGCA). The EZ-Tet-pLKO-Hygro vector was made by PCR subcloning the Hygro resistance gene from the pGL4.15 vector (Promega) using the following primers: 5'-ATTATGGATCCATGAAGAAGCCCGAACTC and 5'-ATTATGACGTCTTAAACTCGACCTACCTC. The EZ-Tet-pLKO-Blast construct was made by PCR subcloning the Blast resistance gene from pLenti-CMV-rtTA3-Blast (Addgene 26429). For PCR cloning, inserts were amplified with Q5 high fidelity polymerase (NEB) and ligated into Tet-pLKO-Puro between the BamHI and AatII RE sites.

Vector digest and PEG precipitation

Vector was prepared by co-digesting EZ-Tet-pLKO-Puro DNA with NheI and EcoRI (NEB). A typical digest consisted of 5 µg of vector DNA with 20 u of each enzyme in a 50 µL digest volume for at least 3 h at 37°C. Cut vector was then dephosphorylated with Antarctic Phosphatase (NEB) using the manufacturer's protocol and supplementing the 50 µL digest reaction with AP buffer, enzyme, and water to make a 60 µL reaction volume. Cut vector was then diluted with water to a 200 µL volume in a 1.5 mL Eppendorf tube. PEG was used to precipitate the DNA and exclude the 200 bp excised stuffer. We first prepared 2X stock of 12% (w/v) PEG-8000 and 20 mM Magnesium Chloride. The 2X stock was then added 1:1 to the cut and dephosphorylated DNA sample. The DNA/PEG mixture was gently mixed by inverting the tube a few times and left to sit at room temperature for 1 h. After the incubation, the DNA was centrifuged at 15,000 RCF in a bench top centrifuge (Eppendorf 5415D) for 40 min. The length of the incubation and spin are critical; any less time can greatly decrease recovery. After centrifugation, the supernatant was carefully decanted leaving a small volume of liquid behind to avoid sucking up the

9

204 DNA pellet (which may or may not be visible). Next, 500 µL of 70% ethanol was added to wash the

205 DNA pellet, which was then spun again for 5-10 min. The ethanol was then aspirated and the wash was

206 repeated once more. After the second wash the DNA pellet was allowed to air dry and then suspended

207 in water (typically ~50 µL). DNA was then quantified by Qubit kit (Q32850, ThermoFisher). Accurate

208 quantification is important for successful cloning. Typically DNA recovery following 6% PEG

209 precipitation is ~50%.

shRNA oligo design and loop prediction

211   shRNA targeting sequences were chosen from the BROAD RNAi Consortium database [20].

212 shRNA targeting sequences (with RNAi consortium ID) are as follows: p38α (TRCN0000196472), p38δ

213 (TRCN0000197043), Creb1 (TRCN0000226466). Oligos were designed as described in Fig. 2 and

214 ordered from Integrated DNA Technologies. The RNA folding probability values in Fig. 2 were calculated

215 using RNAstructure software (v5.7) by Reuter et al. [21, 22].

shRNA oligo preparation

217   Sense and antisense shRNA oligos were suspended at 100 µM in duplex buffer (100 mM

218 Potassium Acetate, 30 mM HEPES, pH 7.5). Next, 20 µL (2 µ-mol) of each oligo were combined and

219 annealed using a thermalcycler (Labnet TC9600-G) with a program set to start at 95°C and drop 5

220 degrees every minute down to room temperature. Alternately, DNA can be annealed by placing in a

221 beaker of boiling water and moved off the heater to cool slowly to room temperature. The annealed

222 oligos were then diluted with water to 360 µL total and precipitated with ethanol (added 40 µL of 3 M

223 sodium acetate and 1 mL ethanol). DNA was centrifuged for 30 min at 15,000 RCF in a bench top

224 centrifuge, washed twice with 70% ethanol, and suspended in 500 µL water. Annealed oligo DNA was

225 then quantified by Qubit (Q32850, ThermoFisher). Synthesized oligos do not contain phosphorylated

226 overhangs, so annealed oligo was treated with T4 poly-nucleotide kinase (M0201, NEB) and heat

227 inactivated, according to the manufacturer's protocol.

Ligation and transformation

Prepared vector (cut, dephosphorylated, and PEG purified) was diluted to a working concentration of ~20-100 ng/μL if needed. Phosphorylated oligos were diluted (from the heat-inactivated PNK reaction) to a 1 ng/μL working concentration. Ligations were performed using the LigateIT rapid ligase kit (78400, Affymetrix) with 100 ng vector DNA and an 8:1 insert:vector molar ratio. A vector-only ligation was also prepared to control for incompletely digested and/or re-ligated vector derived colonies. 2 μL of the ligation reactions were transformed into Stbl3 (Life Technologies) or NEB-Stable (NEB) chemically competent *E. coli*. These strains are recommended for their ability to minimize unwanted recombinations due to lentiviral LTR sequences. Competent cells were incubated on ice for 30 min with the ligation DNA, then heat shocked at 42°C for 40 sec and returned to ice for 1 min. 1 mL of LB media was then added to the cells and they were allowed to recover at 37°C for 30 min, after which time 100-200 μL was plated on LB-agar plates containing 100 μg/mL ampicillin and incubated 12-16 h at 37°C.

PCR screen

Colony-PCR was used to screen bacteria for successfully ligated clones. Primers used were as follows: pLKO-Fwd 5'- ATTAGTGAACGGATCTCGACGG; pLKO-rev 5'- AACCCAGGGCTGCCTTGG. Successful clones will produce a 624 bp product while background colonies that retain the stuffer region amplify a 456 bp product. To set up the PCR reactions, first 15 μL of water was added to PCR tubes. Colony inoculation was performed by touching a p10 pipette tip to a colony, then mixing it in the desired PCR tube with the water, and then dotting ~1 uL on a labeled fresh LB agar (+amp) plate to keep track of the colony. A positive control is always included by adding ~ 1-10 ng of EZ-Tet-pLKO-Puro plasmid to 15 μL water. PCR was performed using Emprical Bioscience Taq and buffer (TP-MG-500). A master mix was made containing (per reaction): 2.5 μL of 10X Taq Buffer, 0.2 μL of Taq enzyme, 2 μL of 25 mM magnesium chloride, 0.2 μL of each primer (fwd and rev, 100 μM stocks), and 3.9 μL water. Optimal conditions may vary with other Taq reagents. 10 μL of the master mix was then added to the 15 μL of inoculated water which served as the template. Thermalcycler settings used were as follows: 1x [95°C

11

for 2 min], 35x [95° for 30 sec, 68°C for 45 sec], 1x [72°C for 1 min]. DNA was then run on 2% agarose

for visualization with a DNA ladder (N3231 or N3232, NEB). Positive clones can then be further

validated by RE screening or sent directly for Sanger sequencing using the pLKO-Fwd primer. A

cautionary note on sequencing: shRNA hairpin sequences can sometimes cause early termination

when read by Sanger sequencing and may (but not always) require the use of specialized sequencing

protocols for dealing with RNAi constructs [23, 24].

Restriction enzyme digest screen

Clones were minipreped by alkaline lysis. DNA was digested using the SpeI restriction enzyme

(NEB). A standard reaction condition was ~3 µg of DNA digested with 10 u of enzyme in a 50 µL reaction

for at least 1 h at 37°C. 10-20 µL of digest was then run out on a 1.2% agarose gel. Background plasmid

with stuffer intact will be cut once by SpeI and create a band at ~9 kb, while clones with shRNA oligos

properly ligated and containing a SpeI sequence in their loop will produce bands at ~8.5 kb and ~500

bp.

Cell culture

iPrEC cells were grown in KSFM with included supplements (17005042, Gibco) and 30 u/mL

Pen/Strep (Gibco). For shRNA induction 50-100 ng/mL Dox (Sigma) was used. HEK293FT cells were

used for lentivirus production and maintained in DMEM (11995, Gibco) with 2 mM L-glutamine, 10%

fetal bovine serum (FBS), and 30 u/mL Pen/Strep. During transfection and infection, cells were grown

without antibiotics and for infection were grown with heat inactivated serum (30 min at 56°C) to avoid

immune complement interference. Cells were maintained at 37°C with 5% CO_2.

Virus production / infection

pLKO constructs were used to make lentivirus in HEK293FT cells using the ViraPower system

(K497500, Invitrogen). One T75 flask was needed per viral construct, which were first coated with 2

µg/mL PolyD lysine in PBS for 1 h at 37°C. 5 million cells were then seeded per T75 and left overnight.

The next day, cells were switched to antibiotic-free media with heat-inactivated serum and transfected (Lipofectamine2000, ThermoFisher) with packaging plasmids (5 µg each: pLP1, pLP2, pVSV-G) and the desired pLKO construct or a GFP lentiviral vector as control. 24 h following transfection, media was changed to the target cell media (without antibiotics), i.e. the media for the cells you wish to infect. HEK293FT cells were then returned to 37°C for 48 h to produce viral particles. Viral media was collected in 15 mL conical tubes and centrifuged for 10 min at 1500 RPM in a swinging bucket centrifuge (Megafuge 1.0R) to pellet cell debris. Next, the viral media was filtered by syringe through a 0.45 µM, low protein binding filter (28145-505, VWR). Cells were typically infected by first adding half the volume with normal growth media (no antibiotics, heat inactivated serum) and half volume with the filtered viral media plus polybrene to a 5 µg/mL final concentration to improve infection rate. Infected cells were incubated 48-72 h and then given fresh growth media for 24-48 h before beginning selection. If a GFP lentivirus control was used, those infected cells can be imaged to see the rough percent of infected cells. Remaining virus can be snap frozen in liquid nitrogen and stored at -80ºC. Thawed virus is still effective but loses ~50% infectivity each thaw cycle.

Immunoblot

Cells were lysed in MAPK lysis buffer (50 mM Tris, pH 7.5, 0.5 mM EDTA, 50 mM NaF, 100 mM NaCl, 50 mM β-glycerol phosphate, 5 mM Sodium Pyrophosphate, 1% TritonX100) or RIPA lysis buffer (10 mM Tris, pH 7.5, 1 mM EDTA, 158 mM NaCl, 0.1% SDS, 1% Sodium Deoxycholate, 1% TritonX100). Cells were chilled, washed, and then lysis buffer was added and plates sat for 30 min on ice. Cells were then scrapped, centrifuged, and protein was quantified by BCA assay (Pierce). Equivalent amounts of 30-50 µg of denatured protein per sample was run on Novex SDS polyacrylamide tris-glycine gels (Life Technologies). Protein was then transferred onto PVDF membrane and blocked in 5% BSA/TBST for 1 h at room temp. Primary and secondary antibodies were diluted in blocking buffer. Primary antibodies were probed either 2-3 h at room temp or overnight at 4ºC while all secondary antibodies were probed 1 h at room temp. Luminol chemiluminescence was used with a Bio-Rad Chemi-

13

302   Doc imaging system with CCD camera to image blots and analyzed on Quantity One software v4.5.2.

303   Antibody info (vendor, catalog no., dilution) is as follows: p38α (CST, 9218, 1:2,000), p38δ (Santa Cruz,

304   sc-136063, 1:1,000), Tubulin (Sigma, T9026, 1:10,000), Creb1 (CST, 4820, 1:1,000), TetR (Clone Tech,

305   631131, 1:2,000).

306

14

DECLARATIONS

List of abbreviations

Dox: doxycycline / Tet: tetracycline / iPrEC: immortalized prostate epithelial cell / TetR: Tet Repressor / TetO: Tet operator / RE: restriction enzyme / PEG: polyethylene glycol / ISO: isopropanol / FBS: fetal bovine serum

Competing interests

The authors declare that they have no competing interests.

Availability of material

pEZ-Tet-pLKO-Puro, pEZ-Tet-pLKO-Hygro, and pEZ-Tet-pLKO-Blast are being deposited with Addgene to make them available to everyone.

Author's contributions

S.B.F. was responsible for experimental design, analysis, execution, and writing of the manuscript. V.V.S. generated and validated the iPrEC-sh.Creb1 cell lines. C.K.M was responsible for analysis, writing, communication, and supervising the project.

FIGURE LEGENDS

Figure 1. Vector maps and PEG purification. **(a)** Basic vector maps (not to scale) for the original Tet-pLKO-Puro vector and our modified versions. **(b)** Agarose gel electrophoresis comparing DNA precipitation methods. 10 µg of EZ-Tet-pLKO vector DNA was co-digested with NheI+EcoRI. The digest was split into three 3 µg aliquots and precipitated with isopropanol (Iso) or polyethylene glycol (PEG) at 6% or 8% concentration. 1 µg of control DNA (uncut and cut) was run alongside 1/3 of the precipitated DNA samples.

Figure 2. shRNA oligo design and loop comparison. (a) Format for shRNA oligo design. Upper strand is sense oligo, lower strand is anti-sense oligo. **(b)** Diagram of predicted shRNA loop structure with a basic SpeI sequence (6nt: ACUAGU) or including a single stem mismatch (7nt: UACUAGU). Colors represent calculated likely occurrence of the depicted pairing. See methods for details on prediction tool. **(c)** Immunoblot showing two different pools of iPrEC cells with shRNA against p38δ, with the only difference being a single mismatch in the loop sequence of the shRNA. Cells were treated -/+ Dox for 72 h. TetR was probed on a separate gel. p38α and Tubulin serve as loading controls. **(d)** Same experiment as (c) using a different pair of shRNAs targeting Creb1. Cells were treated -/+ Dox for 5 days.

Figure 3. Molecular cloning screening techniques. **(a)** Diagram showing expected products from PCR screening pLKO ligation-transformed colonies. **(b)** Agarose gel (2%) with a positive and negative PCR product. **(c)** Diagram showing expected DNA fragments and relative intensity on gel from an XhoI vs SpeI loop sequence restriction digest screen. **(d)** Agarose gel (1.5%) with XhoI or SpeI shRNAs screens. 2 µg of DNA was digested with the indicated enzyme and half the digest was run on agarose. The <200 bp fragments from the XhoI screen were very faint and just barely visible using a very high exposure (not shown).

Figure 4. Dox titration and recovery. (a) Immunoblot of p38α (the target), p38δ (non-target control), and tubulin (loading control) following Dox titration with iPrECs containing EZ-Tet-pLKO-sh.p38α. Cells were treated with Dox for 72 h before lysing. Note: the lower band (arrow) is p38α. Upper band is non-specific. **(b)** Cells were treated -/+ Dox (50 ng/mL) for 72 h. At that time, two samples were lysed (72 h pre-treated) while another plate of treated cells was split and allowed to recover without Dox for 1-8 days. Note: due to changes in confluency, the 'pre-treated' cells have higher basal level of p38 (α and δ) than at day 8.

REFERENCES

1. Davidson BL, McCray PB, Jr.: **Current prospects for RNA interference-based therapies**. *Nature reviews Genetics* 2011, **12**(5):329-340.

2. Hannon GJ: **RNA interference**. *Nature* 2002, **418**(6894):244-251.

3. Fellmann C, Lowe SW: **Stable RNA interference rules for silencing**. *Nature cell biology* 2014, **16**(1):10-18.

4. Singer O, Verma IM: **Applications of lentiviral vectors for shRNA delivery and transgenesis**. *Current gene therapy* 2008, **8**(6):483-488.

5. Moffat J, Grueneberg DA, Yang X, Kim SY, Kloepfer AM, Hinkle G, Piqani B, Eisenhaure TM, Luo B, Grenier JK *et al*: **A lentiviral RNAi library for human and mouse genes applied to an arrayed viral high-content screen**. *Cell* 2006, **124**(6):1283-1298.

6. Wiederschain D, Wee S, Chen L, Loo A, Yang G, Huang A, Chen Y, Caponigro G, Yao YM, Lengauer C *et al*: **Single-vector inducible lentiviral RNAi system for oncology target validation**. *Cell cycle* 2009, **8**(3):498-504.

7. Wee S, Wiederschain D, Maira SM, Loo A, Miller C, deBeaumont R, Stegmeier F, Yao YM, Lengauer C: **PTEN-deficient cancers depend on PIK3CB**. *Proceedings of the National Academy of Sciences of the United States of America* 2008, **105**(35):13057-13062.

8. Lis JT, Schleif R: **Size fractionation of double-stranded DNA by precipitation with polyethylene glycol**. *Nucleic acids research* 1975, **2**(3):383-389.

9. Cariello NF, Keohavong P, Sanderson BJ, Thilly WG: **DNA damage produced by ethidium bromide staining and exposure to ultraviolet light**. *Nucleic acids research* 1988, **16**(9):4157.

10. Grundemann D, Schomig E: **Protection of DNA during preparative agarose gel electrophoresis against damage induced by ultraviolet light**. *BioTechniques* 1996, **21**(5):898-903.

11. Li L, Lin X, Khvorova A, Fesik SW, Shen Y: **Defining the optimal parameters for hairpin-based knockdown constructs**. *Rna* 2007, **13**(10):1765-1774.

12. McIntyre GJ, Fanning GC: **Design and cloning strategies for constructing shRNA expression vectors**. *BMC biotechnology* 2006, **6**:1.

13. Gu S, Jin L, Zhang Y, Huang Y, Zhang F, Valdmanis PN, Kay MA: **The loop position of shRNAs and pre-miRNAs is critical for the accuracy of dicer processing in vivo**. *Cell* 2012, **151**(4):900-911.

14. Moullan N, Mouchiroud L, Wang X, Ryu D, Williams EG, Mottis A, Jovaisaite V, Frochaux MV, Quiros PM, Deplancke B *et al*: **Tetracyclines Disturb Mitochondrial Function across Eukaryotic Models: A Call for Caution in Biomedical Research**. *Cell reports* 2015.

15. Mullick A, Xu Y, Warren R, Koutroumanis M, Guilbault C, Broussau S, Malenfant F, Bourget L, Lamoureux L, Lo R *et al*: **The cumate gene-switch: a system for regulated expression in mammalian cells**. *BMC biotechnology* 2006, **6**:43.

16. Chen Q, Gao S, He W, Kou X, Zhao Y, Wang H, Gao S: **Xist repression shows time-dependent effects on the reprogramming of female somatic cells to induced pluripotent stem cells**. *Stem cells* 2014, **32**(10):2642-2656.

17. Hodkinson PS, Elliott PA, Lad Y, McHugh BJ, MacKinnon AC, Haslett C, Sethi T: **Mammalian NOTCH-1 activates beta1 integrins via the small GTPase R-Ras**. *The Journal of biological chemistry* 2007, **282**(39):28991-29001.

18. Zhang F, Wen Y, Guo X: **CRISPR/Cas9 for genome editing: progress, implications and challenges**. *Human molecular genetics* 2014, **23**(R1):R40-46.

19. Chin YR, Yoshida T, Marusyk A, Beck AH, Polyak K, Toker A: **Targeting Akt3 signaling in triple-negative breast cancer**. *Cancer research* 2014, **74**(3):964-973.

20. **The RNAi Consortium.** http://www.broadinstitute.org/rnai/trc. Accessed 7 June 2016.

21. Reuter JS, Mathews DH: **RNAstructure: software for RNA secondary structure prediction and analysis**. *BMC bioinformatics* 2010, **11**:129.

410   22.   Mathews DH. **RNAstructure.** http://rna.urmc.rochester.edu/RNAstructure.html. Accessed 7

411   June 2016.

412   23.   Guo Y, Liu J, Li YH, Song TB, Wu J, Zheng CX, Xue CF: **Effect of vector-expressed**

413   **shRNAs on hTERT expression**. *World journal of gastroenterology : WJG* 2005, **11**(19):2912-

414   2915.

415   24.   Devroe E, Silver PA: **Retrovirus-delivered siRNA**. *BMC biotechnology* 2002, **2**:15.

416

417

Figure 1

FIGURE 1

FIGURE 2

a

Target Seq.   Loop   Target Seq. (rev. comp.)   Term.   Overhang (EcoRI)

5'- CTAGCGAAACTCACAGTGGATGAATGTACTAGTCATTCATCCACTGTGAGTTTCTTTTTG

Overhang (NheI)

GCTTTGAGTGTCACCTACTTACATGATCAGTAAGTAGGTGACACTCAAAGAAAAACTTAA -5'

b

6nt

7nt

Probability

>95%   70-80%
90-95%   50-60%

c

TetON-sh.p38δ

6nt   7nt

Dox: −   +   −   +

p38α

p38δ

Tubulin

TetR

Tubulin

d

TetON-sh.Creb1

6nt   7nt

Dox: −   +   −   +

Creb1

TetR

Tubulin

FIGURE 3

a

624bp

pLKO-fwd → - - - - - - - - - - - - - - - - - - - ← pLKO-rev

Promoter | Stuffer

NheI | EcoRI

456bp

→ - - - - - - - - - - - - - - - ←

Promoter | shRNA

NheI EcoRI

b

pLKO-stuffer | pLKO-shRNA

600bp -
500bp -
400bp -

c

XhoI Screen | **SpeI Screen**

Vec | Vec+sh | Vec | Vec+sh | *% relative intensity*

10kb - | | | | *100%*

500bp - | | | | *5.5%*

| | | | *3.8%*

| | | | *2.2%*

| | | | *1.5%*

100bp - | | | | *0.05%*

d

XhoI Screen | **SpeI Screen**

Vec | Vec+sh | Vec | Vec+sh

10kb -

1kb -

500bp -

Figure 4

FIGURE 4

a

b

Human Prostate Luminal Cell Differentiation requires NOTCH3 Induction by p38α-MAPK and MYC

Sander B. Frank[1,2], Penny L. Berger[1], Mats Ljungman[3], and Cindy K. Miranti[1]

[1]Laboratory of Integrin Signaling and Tumorigenesis, Van Andel Research Institute, Grand Rapids, MI USA

[2]Genetics Program, Michigan State University, East Lansing, MI USA

[3]Translational Oncology Program, University of Michigan Medical School, Ann Arbor, MI USA

Short Title: NOTCH3 and MYC in Prostate Differentiation

Keywords: prostate, luminal cell differentiation, NOTCH, MYC, p38-MAPK, development

Corresponding Author:

Cindy K. Miranti

Laboratory of Integrin Signaling and Tumorigenesis

Van Andel Research Institute

333 Bostwick Ave NE

Grand Rapids, MI 49503

Cindy.miranti@vai.org

616-234-5358

SUMMARY STATEMENT

p38-MAPK signaling to NOTCH3 is required for prostate epithelial differentiation. Regulation of NOTCH3 is mediated in part via MYC and enhancer-driven transcription as well as enhanced mRNA stability.

ABSTRACT

Many pathways dysregulated in prostate cancer are also involved in epithelial differentiation. To better understand tumor initiation in prostate epithelium, we sought to investigate specific genes and mechanisms required for normal basal to luminal cell differentiation. Utilizing human prostate basal epithelial cells and an *in vitro* differentiation model, we tested the hypothesis that p38-MAPK regulation of NOTCH3, via MYC, is required for luminal differentiation. Inhibition (SB202190, BIRB796) or knockdown of p38α or p38δ prevented differentiation. Additionally, treatment with a γ-secretase inhibitor (RO4929097) or knockdown of NOTCH1 or NOTCH3 greatly impaired differentiation and caused luminal cell death. Constitutive p38-MAPK activation by MKK6(CA) increased NOTCH3 (but not NOTCH1) mRNA/protein levels and was diminished upon MYC inhibition (10058-F4) or knockdown. Furthermore, we validated two *NOTCH3* enhancer elements by a combination of eRNA detection, luciferase reporters, and ChIP. Lastly, we found that *NOTCH3* mRNA half-life increased during differentiation or upon acute p38-MAPK activation. These results reveal a new connection between p38-MAPK and NOTCH signaling, demonstrate two mechanisms of *NOTCH3* regulation, and provide evidence for NOTCH3 playing a specialized role in the prostate.

INTRODUCTION

The human prostate gland contains an epithelial bi-layer of basal and luminal cells. Within these layers resides a combination of uni- and bi-potent progenitors important for normal gland homeostasis (Kwon et al., 2016; Ousset et al., 2012; Uzgare et al., 2004). Basal and luminal cells display various mutually exclusive markers, such as Androgen Receptor (AR) and K8 in the luminal layer and integrins and K5 in the basal layer (Lamb et al., 2010). Human prostate tumors co-express basal and luminal markers, which suggests a defect in differentiation (Tokar et al., 2005). Moreover, many of the commonly altered genes in prostate cancer (e.g *MYC*, *AR*, *ERG*, *PTEN*) are also implicated in differentiation (Frank and Miranti, 2013). Previous work from our group demonstrated that manipulation of differentiation regulators (MYC, PTEN, ING4*)* in normal human prostate epithelial cells results in tumor formation when grafted into a mouse prostate (Berger et al., 2014). To better understand tumor initiation in prostate epithelium, we sought to investigate specific genes and mechanisms required for normal basal to luminal cell differentiation.

p38-MAPK is a known driver of epithelial differentiation in various tissues including skin and lung (Cuadrado and Nebreda, 2010). p38-MAPK regulates a wide range of targets, including other kinases/phosphatases, transcription factors, and RNA binding proteins (Cuadrado and Nebreda, 2010). Moreover, p38-MAPK is a downstream target of FGFR2b, a crucial receptor for epithelial differentiation in the skin and prostate (Belleudi et al., 2011; Heer et al., 2006; Lamb et al., 2010). Despite these findings, a specific role for p38-MAPK in prostate epithelial differentiation, including its relevant targets, remains poorly defined.

MYC positively regulates normal skin and prostate differentiation and is a major prostate cancer oncogene (Berger et al., 2014; Gebhardt et al., 2006; Koh et al., 2010). MYC potentially targets thousands of genes via its activity as a transcription factor and many of its targets are tissue and context specific (Conacci-Sorrell et al., 2014; Luscher and Vervoorts, 2012). Within the prostate, Myc is required for loss of cell adhesion and stimulation of chromatin remodeling (Berger et al., 2014). Moreover, regulation of *MYC* itself is complex, occurring at many different levels, including pre- and post-transcription and post-translational modification (McKeown and Bradner, 2014).

NOTCH controls cell fate, including stemness, survival, and differentiation (Deng et al., 2015). Mammals contain four NOTCH transmembrane receptors (NOTCH1-4), five canonical transmembrane ligands (JAG1/2, DLL1/3/5) and ten classic downstream targets (HES1-7, HEY1/2/L). Cell-cell contact joins ligand and receptor triggering proteolytic cleavage by the γ-secretase complex which releases the active intracellular domain (ICD) of the receptor into the

nucleus to activate transcription (Kopan and Ilagan, 2009). Work with mouse models has demonstrated the importance of the NOTCH pathway in prostate development (Kwon et al., 2014; Valdez et al., 2012). NOTCH can promote cell cycle arrest and de-adhesion from the matrix, both of which are essential for luminal differentiation (Hodkinson et al., 2007; Mazzone et al., 2010; Rangarajan et al., 2001). However, there are conflicting reports as to whether the NOTCH pathway is oncogenic or tumor suppressive in prostate cancer and specific functions for each NOTCH receptor have not been defined in prostate differentiation or oncogenesis (Carvalho et al., 2014).

We sought to understand how each of these differentiation factors work together in normal prostate basal-to-luminal cell differentiation. We utilized an established model of *in vitro* differentiation of human basal prostate epithelial cells (PrEC) (Berger et al., 2014; Lamb et al., 2010). This model allows considerable pharmacologic and genetic manipulation to study specific genes and their role in luminal differentiation. We tested the hypothesis that p38-MAPK upregulation of NOTCH3, via MYC, is required for prostate epithelial luminal cell differentiation. We identify two mechanisms of *NOTCH3* regulation by p38-MAPK, both at the transcriptional and post-transcriptional level, which is required for differentiation of prostate basal epithelial cells into luminal cells. This knowledge improves our understanding of prostate epithelial differentiation by tying together multiple pathways and elucidating new mechanisms for key differentiation regulators.

METHODS

Cell Culture. Primary PrECs and immortalized PrECs (Berger et al., 2014) were grown in KSFM media (Gibco) plus pen/strep at 30 µg/mL (Gibco). Differentiation was induced as previously reported with 2.5 ng/mL recombinant KGF/FGF7 (Cell Sciences) and 10 nM R1881 (Perkin Elmer) with fresh media every 24 h (Lamb et al., 2010). Luminal layer separation was achieved using Ca/Mg-free PBS with 1 mM EDTA as previously described (Lamb et al., 2010). HEK 293FT cells were used for lentivirus production (ViraPower, Invitrogen) and grown in DMEM (11995, Gibco) with 10% FBS (Gemini) and 2 mM L-glutamine (Gibco). Cell lines were tested via MycoAlert PLUS kit (Lonza) and confirmed to be mycoplasma free.

Molecular Cloning and Stable Cell Line Construction. Immortalized PrECs (iPrEC) were engineered with Dox-inducible shRNAs using the Tet-pLKO-Puro vector (Addgene plasmid 21915) (Wiederschain et al., 2009). shRNA sequences are listed in supplementary material Table S1. Expression cDNAs were PCR subcloned with Q5 polymerase (NEB) into the pENTR3C gateway vector (Invitrogen) between SalI and NotI sites and then recombined with LR Clonase II

4

(Invitrogen) into pLenti-CMV/TO-Puro-DEST (Addgene plasmid 17293) (Campeau et al., 2009). The constitutively active MKK6 mutant was a gift (MKK6-DD) from Angel Nebreda (Alonso et al., 2000). The MYC cDNA was subcloned from pBabe-Myc, a gift from Beatrice Knudsen. TetR lines were established using pLenti-CMV-TetR-Blast (Addgene plasmid 17492) (Campeau et al., 2009). iPrECs were selected in 5 µg/mL blasticidin and/or 1-2 µg/mL puromycin. Doxycycline (Sigma) was used at 50 ng/mL to induce shRNAs and 2-10 ng/mL to induce cDNA expression.

siRNA and Inhibitors. A mixed siRNA pool against *MYC* and non-targeting siRNA (siScram) were purchased from Origene (SR303025). Cells were transfected with siLentfect reagent (Bio-Rad). Cyclohexamide and was used at 10 µg/mL and ActinomycinD at 5 µg/mL (both from Calbiochem). SB202190, BIRB796/Doramapimod, and 10058-F4 were purchased from Cayman Chemical. RO4929097 was purchased from Apex Bio.

Immunoblotting. Cell lysates were prepared in RIPA as previously described (Edick et al., 2007). Protein loading was standardized by BCA assay (Pierce). 20-50 µg of denatured protein was run on Novex SDS polyacrylamide tris-glycine gels (Life Technologies) and transferred onto PVDF membrane (Fisher). Chemiluminescence was used to image blots with a Bio-Rad Chemi-Doc imaging system via CCD camera. Images were analyzed using Quantity One software (v4.5.2). Antibodies are in supplementary material Table S2.

qRT-PCR. RNA was harvested and extracted with Trizol following the manufacturer's protocol (Invitrogen). cDNA was synthesized with M-MuLV reverse transcriptase (NEB) using a 4:1 mix of poly-d(16)T and random hexamer primers. qRT-PCR was performed using SYBR Green Master Mix (Roche) and an ABI 7500 thermalcycler (Applied Biosystems). Data were standardized to *18S* plus *GAPDH* unless otherwise stated and were normalized (∆∆CT) and plotted as Log_2(Fold). Primers were synthesized by Integrated DNA Technologies. Primers are in supplementary material Table S3.

Immunostaining. Cells were fixed, permeabilized, and stained as previously described (Berger et al., 2014). ITGα6 (555734, BD) and AR (sc-815, Santa Cruz) were co-stained each at 1:200 dilution. For propidium iodide staining cells were fixed with 4% paraformaldahyde, treated with 100 ng/mL RNAseA (Thermo) for 10 min, and then stained with 100 ng/mL propidium iodide (Sigma) for 5 min. Nuclei were stained with 10 µg/mL Hoescht33258 (Sigma) for 10 min. Epifluorescence microscopy was performed on a Nikon TE300 using Nikon Elements software (v4.11.00).

Luciferase Assay and Constructs. Putative *NOTCH3* regulatory elements were PCR subcloned from the RP11-937H1 BAC library (Life Technologies) using Q5 or LongAmp polymerase (NEB). The *NOTCH3* 2kb promoter element was ligated into pGL4.15-Hygro

(Promega). Candidate regulatory elements were ligated into pNL1.1 (Promega) after first cloning in a miniTK promoter at the HindIII site. Deletion mutants were made using the QuickChange II Mutagenesis kit (200524, Stratagene). Cloning primers, miniTK sequence, and mutagenesis primers are in supplementary material Table S4.

Luciferase assays were performed using the NanoGlo kit (Promega) and a Synergy Neo II (Bio Tek) plate reader with Gen5 software (v2.04.). Cells were transfected with XtremeGeneHP reagent (Roche) as a pool and then split for different treatments. pNL1.1-miniTK served as the negative control. Luciferase assays were run 16 h after Dox and 48 h after transfection in biological replicates (n=8).

Chromatin Immunoprecipitation. Detailed protocol can be found in supplementary material. Antibodies used were: Myc (sc-764, Santa Cruz) and Rabbit IgG (CST). qRT-PCR was performed as described in the qRT-PCR methods section. ChIP primers are in supplementary material Table S5. Percent input was calculated as $2^{\Delta CT}$x100 divided by the ratio of chromatin per IP to input (75 µL per IP, 25 µL for input). *HIST3* was used as a control locus not reported to be regulated by MYC and *ODC1* was used as a positive control for MYC binding (Hogarty et al., 2008).

mRNA Half-life Measurement. Cells were treated with 5 µg/mL ActinomycinD for 0-8 h. RNA and cDNA were prepared as described in the qRT-PCR methods section. Data were standardized to *18S* rRNA and normalized as ΔΔCT values vs the Day1 or –Dox samples at 0 h. 18S rRNA has a very long half-life (1-7 days) and thus is suitable for standardization (Defoiche et al., 2009). Linear regression curves, line equations, r^2 values, and p-values were calculated with GraphPad PRISM software. Half-life was calculated as 1/m. Overall expression change was calculated as $2^{\wedge}(b_2-b_1)$. AU rich elements were identified using the ARE site (v1) online tool (http://nibiru.tbi.univie.ac.at/cgi-bin/AREsite/AREsite.cgi) (Gruber et al., 2011).

BruUV-seq. iPrEC-TetON-MKK6(CA) cells were treated ±5 ng/mL Dox for 10 h, then UV treated (100 J/m^2) using a Stratalinker UV Crosslinker 1800 (Stratagene) and labeled with 2 mM 5-Bromo-deoxyuridine (sc-256904, SantaCruz) for 30 min before washing with PBS and collecting RNA with Trizol (Life Technologies). BrU isolation, library prep, sequencing, and mapping was performed as previously described (Andrade-Lima et al., 2015; Paulsen et al., 2014). Data were exported (bin size = 300 bp) and graphed using GraphPad PRISM software.

Statistical analysis. Unless specified, p-values were calculated using paired, two-tailed t-tests on biological triplicates. For Tables 1 and 2 p-values were calculated by ANCOVA analysis using PRISM GraphPad software. Fig. S3B used paired one-way ANOVA with Greenhouse-Geisser correction and Dunnett's correction. Fig. 5C used paired, one-way ANOVA with Sidak

6

correction. Fig. 5E used two-way ANOVA with Turkey's multiple testing correction. n.s. = not significant.

RESULTS

MAPK isoforms p38α and p38δ are required for prostate epithelial differentiation. To induce differentiation of human basal prostate epithelial cells (PrEC) into luminal cells, we treat with KGF/FGF7 and synthetic androgen (R1881) for two weeks (Lamb et al., 2010). This results in a stratified epithelium consisting of luminal cells sitting atop basal cells. p38-MAPK is a known downstream target of KGF-FGFR2 signaling and this pathway has been implicated in epithelial differentiation in several tissue types, including prostate (Belleudi et al., 2011; Lamb et al., 2010). There are four different genes encoding p38: *MAPK14*/p38α, *MAPK11*/p38β, *MAPK12*/p38γ, and *MAPK13*/p38δ. p38α is the most ubiquitously expressed, while the other isoforms are typically more tissue specific (Cuadrado and Nebreda, 2010). From RNA-seq of basal cells and immunoblotting we found p38α and p38δ to be the predominantly expressed isoforms (Fig. 1A,B).

Lysates from differentiating cells were collected over a two week time course, then p38α activity was measured by immunoblotting with a phospho-specific antibody. In primary cells (PrEC), elevated p-p38α was detected at day 4 and remained elevated (Fig. 1C). In immortalized cells (iPrEC), which take 4 days longer to differentiate, p-p38α was elevated at day 8 (Fig 1D).

To determine if p38-MAPK is necessary for differentiation, iPrECs were differentiated in the presence of a p38 inhibitor (SB202190, BIRB796) or Dox-induced p38α or p38δ shRNA. Inhibitor concentrations were selected based on their ability to block CREB1 phosphorylation by constitutively active MKK6 (supplementary Fig. S1A). Effective knockdown of p38α or p38δ in shRNA lines was achieved at 72 hours with Dox treatment (Fig. 1B). Control cells differentiated normally as visualized by the presence of large patches of Integrin α6 (ITGα6)-negative and Androgen Receptor (AR)-positive luminal cells with underlying non-differentiated basal cells (ITGα6+) (Fig. 1E). Treatment with 1 µM SB202190 or 0.1 µM BIRB796 completely prevented formation of a luminal layer. Moreover, Dox-induced shRNA knockdown of p38α or p38δ also prevented luminal cell formation. Nuclear staining of non-permeabilized cells with propidium iodide detected minimal cell death, indicating a block in differentiation rather than decreased survival (supplementary Fig. S1B). Thus, both p38α and p38δ are required for PrEC differentiation.

NOTCH1 and NOTCH3 are induced during differentiation. A hallmark of luminal cell differentiation is the loss of integrin expression. NOTCH is known to negatively regulate integrin

expression and is generally required for epithelial differentiation (Frank and Miranti, 2013; Koh et al., 2010; Mazzone et al., 2010). Additionally, MYC suppresses integrin expression (Gebhardt et al., 2006) and was previously demonstrated to be required for prostate luminal cell differentiation (Berger et al., 2014). In some contexts MYC is a direct downstream target of NOTCH (Weng et al., 2006). To decipher the roles of MYC and NOTCH, lysates from differentiating iPrECs (Fig. 2A) or PrECs (supplementary Fig. S2A) were collected over a two-week time course and protein expression measured by immunoblotting. MYC expression and activation (phosphorylation) was initially elevated but waned as basal cell proliferation subsided and transiently elevated again around day 8 (Fig. 2A). A similar response was observed in primary cells but occurring 4 days earlier, as expected due to their faster differentiation (supplementary Fig. S2A).

Of the four NOTCH receptors, we were only able to detect significant expression of NOTCH1, 2, and 3 (Fig. 2A). Expression of NOTCH2 remained essentially unchanged during differentiation. NOTCH1 protein was initially elevated, then decreased and remained relatively constant. In contrast, NOTCH3 protein expression was very low in basal cells, then increased with time during differentiation; moreover, an inflection occurred around day 8, when p38α and MYC activity were also maximal (Fig. 2A). A similar pattern was observed in primary PrECs (supplementary Fig. S2A).

NOTCH1 and *NOTCH3* mRNA expression, as measured by qRT-PCR, paralleled protein expression; *NOTCH1* dipped and recovered to baseline, while *NOTCH3* increased dramatically and ended higher in the luminal layer (Fig. 2B). *NOTCH3* mRNA appeared to increase in two phases; a steady climb increasing ~10-fold over the first eight days followed by a more dramatic spike, up ~220-fold (vs day 1) in the luminal cells (Fig. 2B). NOTCH ligands displayed two distinct expression profiles; *JAG1* (Fig. 2B) and *DLL4* (supplementary Fig. S2B) showed initial decreases but then recovered by day 10, following the pattern of *NOTCH1* expression. Meanwhile, *DLL3* remained flat and began to increase after day 10, paralleling the increase in *NOTCH3* mRNA expression (Fig. 2B). *HEY2/L* (Fig. 2B), *HES1/6*, and *HEY1* (supplementary Fig. S2B) all increased during differentiation, with day 8 being a key inflection point. *HEY2* mRNA was unique in that it segregated into the luminal population (up 45-fold vs day 1) similar to *NOTCH3*. These data indicate that the day 8-10 window is critical for activation of the NOTCH pathway and correlates with the appearance of an emerging luminal layer and integrin mRNA downregulation (supplementary Fig. S2B).

NOTCH1 and NOTCH3 are required for differentiation. To examine the requirement of NOTCH1/3 for differentiation, iPrECs were differentiated and treated with either a γ-secretase inhibitor (RO4929097) or Dox to induce expression of NOTCH1 or NOTCH3 shRNA. Efficient

knockdown of NOTCH1/3 mRNA was achieved by 48 h (supplementary Fig. S2C) and protein at 96 h (Fig. 2C). NOTCH3 shRNA had some effect on NOTCH1 expression; however, this was not due an effect on *NOTCH1* mRNA (data not shown). Control cells differentiated normally as indicated by formation of an AR-positive/Integrin α6-negative luminal layer, while treatment with RO4929097 ablated differentiation (Fig. 2D). Knockdown of NOTCH1 or NOTCH3 by shRNA each led to disruption of the luminal layer, though some small clumps of cells were visible in the upper layer. Propidium iodide staining indicated that these clumps of cells were dead (supplementary Fig. S2D). Thus, NOTCH1 and NOTCH3 are each required for prostate differentiation. However, unlike with p38-MAPK inhibition, the NOTCH-antagonized cells began detachment to form a luminal layer but were unable to survive.

MKK6-induced p38-MAPK activation recapitulates differentiation-induced MYC and NOTCH3 expression. To determine the relationship between p38-MAPK and NOTCH3, we engineered an iPrEC line with a Dox-inducible constitutively active MKK6 mutant, MKK6(CA), which directly phosphorylates and activates p38-MAPK (Alonso et al., 2000). During differentiation p38-MAPK activation is moderately elevated over several days (see Fig 1A), but when MKK6(CA) is induced the signaling events that naturally occur over days are condensed into hours (Fig. 3A). Although prolonged constitutive p38-MAPK activation leads to stress and cell death, the Dox-inducible system allows us to tightly control induction and measure downstream signaling over a short time period. A 16 hour treatment of iPrEC-TetON-MKK6(CA) cells with Dox led to an ~18-fold increase in *NOTCH3* mRNA (Fig. 3B). Conversely, MKK6(CA) induction decreased *NOTCH1* by ~2.5-fold.

To establish a temporal order of events, iPrEC-TetON-MKK6(CA) cells were treated with Dox and lysates collected over 0-16 hours for immunoblotting (Fig. 3C). MKK6(CA) was detectable as early as 4 hours, at which time a corresponding increase in active p-p38α and MYC was observed; peaking around 7-8 hours. NOTCH3 levels began to increase at around 6-8 hours and continued upwards. *MYC* mRNA induction also preceded *NOTCH3* mRNA induction while *NOTCH1* decreased (Fig. 3D). Furthermore, a short pulse of Dox after one day of differentiation was sufficient to induce NOTCH3 at day 2 to a level even higher than seen at day 4 of normal (no Dox) differentiation (Fig. 3E). These results show that constitutive activation of p38-MAPK is sufficient to induce p38α, MYC, MYC phosphorylation, and NOTCH3, and downregulate NOTCH1. Thus, the MKK6(CA) model mimics regulation of these genes as observed in the standard differentiation assay. Moreover, differentiation of iPrECs for four days in the presence of a p38-MAPK inhibitor suppressed *MYC* induction and dampened *NOTCH3* upregulation (~7- vs ~28-fold), thus confirming their role downstream of p38-MAPK (Fig. 3F).

9

MYC is required for p38-MAPK regulation of NOTCH3. Induction of *NOTCH3* mRNA could be due to direct activation of an existing transcription factor or indirect, requiring synthesis of a new factor. iPrEC-TetON-MKK6(CA) cells were treated with Dox for 12 hours and CHX was added at 6, 8, or 10 hours to measure the dependency for new protein synthesis. Addition of CHX at 6 hours blocked *NOTCH3* mRNA upregulation, while addition at 8 hours or later did not (Fig. 4A, supplementary Fig. S3A). Thus, there is a requirement for the synthesis of an intermediate, which must be translated after 6 hours but before 8 hours; this matches the time of maximal MYC induction and activation (Fig. 3C).

To test if *NOTCH3* induction requires MYC, iPrEC-TO-MKK6(CA) cells were transfected with siRNA against MYC or a non-targeting control sequence and MKK(CA) induced with Dox for 12 hours. *MYC* mRNA was knocked down ~80% and *NOTCH3* mRNA induction was diminished ~50% compared to the control cells (5- vs 10-fold) (Fig. 4B). To further address the dependency of *NOTCH3* induction on MYC, we utilized a MYC-MAX antagonist, 10058-F4 (Huang et al., 2006). iPrEC-TO-MKK6(CA) cells were treated with Dox and increasing concentrations of 10058-F4 for 16 hours. Treatment with as little as 5 µM 10058-F4 suppressed the induction of NOTCH3 protein to the same level as control cells (Fig. 4C), whereas 20 µM was required to suppress *NOTCH3* mRNA (supplementary Fig. S3B). These doses are at or below common usage for 10058-F4 (Guo et al., 2009; Wang et al., 2014). Together these results demonstrate that MYC is required for full p38-MAPK-mediated induction of NOTCH3.

To determine whether MYC is sufficient for NOTCH3 upregulation, we generated a Tet-inducible MYC expressing cell line: iPrEC-TetON-Myc. MYC induction occurred within 2 hours of Dox treatment and NOTCH3 protein increased slightly by 6 hours (Fig. 4D). However, there was no change in *NOTCH3* mRNA (supplementary Fig. S3C). We also induced MYC after differentiating cells for 5 days and observed only a slight increase in NOTCH3 protein expression (supplementary Fig. S3D). Thus, MYC is not sufficient in this context to induce *NOTCH3* mRNA though it may have some slight effect on NOTCH3 protein expression.

NOTCH3 is transcriptionally regulated via a MYC-bound enhancer. The *NOTCH3* 2 kb upstream proximal promoter contains a CpG island and no TATA sequence (Kent et al., 2002). This 2 kb region of the *NOTCH3* promoter was not sufficient to induce a luciferase reporter after 6 days of differentiation (Fig. 5A), at a time when endogenous *NOTCH3* was elevated over ~16-fold. We used two approaches to identify candidate enhancer regions. First, we labeled and identified short newly initiated transcripts at the *NOTCH3* transcriptional start site and enhancer elements using BruUV-seq (Magnuson et al., 2015). Dox induction in iPrEC-TetON-MKK6(CA) cells dramatically increased *NOTCH3* reads from the coding strand accumulating near the

transcription start site (Fig. 5B). Strikingly, there was also a peak of reads from the non-coding strand within the second intron, a locus previously reported to contain a *NOTCH3* enhancer (Gagan et al., 2012; Romano et al., 2012). The gene for MKK6 (*MAP2K6*) served as a positive control; induced only upon Dox treatment and with reads mapping only to the exons generated from the cDNA construct (supplementary Fig. S4A). Other controls included *CALB1* and *TRIM22*, which were increased and decreased, respectively, upon MKK6 induction (supplementary Fig.S5A).

Our second approach used a combination of DNase hypersensitivity, histone patterns (H3K27Ac + H3K4me1/2), and ChIP-seq data from ENCODE to identify potential enhancer elements (Consortium, 2012; Kent et al., 2002). Five different elements were cloned into a pNL1.1-miniTK luciferase reporter vector (supplementary Fig. S4B). En2.1, En2.2, and the *NOTCH3* promoter showed no induction by Dox in the MKK6(CA) model (Fig. 5C). However, two elements (En1 and En3) were upregulated 5- and 3-fold, respectively. En1 is ~10 kb upstream while En3 is in the second intron and corresponds to the site identified by BruUV-seq with bidirectional transcripts (Fig. 5B). Deletions within En1 (En1Δ) and En3 (En3Δ) that eliminated most (En1Δ) or all (En3Δ) of the predicted MYC binding sites completely ablated the ability of the En1 reporter to be induced but had no significant effect on En3 (Fig. 5C).

To determine if MYC can bind these enhancers, ChIP was carried out in iPrEC-TetON-MKK6(CA) cells. Two primer sets (set 1 being more 5') flanking predicted MYC binding sites were designed per element. MYC was inducibly bound to En1 (both primer sets) and En3 at the 3' end, and constitutively occupied at the 5' end (Fig. 5D). The inducible En3 Myc-binding region corresponds to that retained in En3Δ (Fig. 5D). In the presence of the MYC inhibitor 10058-F4, the induction of both En1 and En3Δ were sensitive to Myc inhibition (Fig. 5E). En1 was partially decreased (2.7- vs 4.5-fold, p<0.001) while En3Δ induction was more thoroughly blocked (0.7- vs 1.7-fold, p<0.001). In summary, the 5' 360bp of En1 and 3' end of En3 (En3Δ) are each sufficient for induction by MKK6(CA), the elements are bound by MYC, and sensitive to MYC inhibition.

***NOTCH3* expression is also controlled by mRNA stability**. *NOTCH3* contains an AU-rich element in its 3' UTR (supplementary Fig. S5A) and p38-MAPK is known to regulate RNA binding proteins (Cuadrado and Nebreda, 2010). Actinomycin D was used to halt transcription and nine time points were taken to measure mRNA decay (Harrold et al., 1991) at day 1 and day 4 of differentiation (Fig. 6A, Table 1). The *MYC* half-life, 0.8 hours, was similar to previous reports (Herrick and Ross, 1994). *MYC* and *NOTCH1* half-lives remained essentially the same at day 4 (p>0.2). However, *NOTCH3* mRNA half-life nearly doubled (11.5 vs 5.9 hours, p=0.1), along with an 8.5-fold increase in total mRNA levels. We similarly compared iPrEC-TetON-MKK6(CA) cells

stimulated with Dox for 16 h to non-Dox treated cells (Fig. 6B, Table 2). Both *NOTCH1* and *NOTCH3* mRNA half-lives more than doubled: 3.3 to 8.8 hours (p=0.02) for *NOTCH1* and 7.6 to 17.6 hours (p=0.14) for *NOTCH3*. However, the overall mRNA level of *NOTCH1* decreased ~4-fold while *NOTCH3* increased ~9-fold (Table 2). Thus, differentiation and acute p38-MAPK activation both lead to increased *NOTCH3* mRNA half-life, indicating *NOTCH3* is regulated post-transcriptionally through mRNA stabilization.

DISCUSSION

Differential regulation of NOTCH1 and NOTCH3 in differentiation. NOTCH1 expression has been reported primarily in basal cells of mouse and human prostate, while NOTCH3 has been reported (with some disagreement) to be more luminal (Pedrosa et al., 2016; Shou et al., 2001; Valdez et al., 2012). We detected abundant NOTCH1 and NOTCH2 and very low NOTCH3 in undifferentiated human basal cells. NOTCH4 protein was detectable but at a very low level and did not increase during differentiation (not shown). Due to their dynamic regulation during differentiation, we focused on NOTCH1 and NOTCH3. We observed a dramatic induction of *NOTCH3* mRNA and protein during differentiation which coincided with the appearance of luminal cells. Therefore, NOTCH3 is likely a primary driver of luminal cell differentiation, while NOTCH1 serves its previously described role in maintaining the basal population (Pedrosa et al., 2016; Shou et al., 2001; Valdez et al., 2012). The function of NOTCH3 has been controversial, but recent reports show that it drives luminal differentiation of airway basal cells and mammary epithelium (Baeten and Lilly, 2015; Bhat et al., 2016; Gomi et al., 2015; Mori et al., 2015; Ohashi et al., 2010). Moreover, of the four NOTCH receptors only NOTCH3 is sufficient to drive hepatocyte differentiation in embryonic mouse liver cells (Ortica et al., 2014). Our data supports the idea that NOTCH3 defines a more luminal phenotype in prostate epithelium.

Transcriptional regulation of *NOTCH3* by p38-MAPK. Part of the mechanistic insight from this work demonstrates that p38-MAPK can regulate *NOTCH3* transcription in a MYC-dependent manner. Although a relationship between p38-MAPK and NOTCH has previously been suggested, mechanistic details were not clearly established (Brown et al., 2009; Gonsalves and Weisblat, 2007; Kiec-Wilk et al., 2010; Park et al., 2009). We found that p38-MAPK induction, whether by MKK6(CA) or KGF/androgen-induced differentiation, induces NOTCH3. MYC has been reported as a potential downstream target of p38-MAPK and was previously shown to be required for PrEC differentiation (Berger et al., 2014; Marderosian et al., 2006). Consequently, we found that suppressing MYC expression by siRNA or blocking its ability to bind MAX with a

pharmacological inhibitor, 10058-F4, suppressed the induction of NOTCH3 by MKK6(CA). However, in both cases suppression was not complete and MYC overexpression was not sufficient to induce *NOTCH3* mRNA. Thus, although MYC is required for full induction of NOTCH3 by p38-MAPK, additional unidentified factors are likely involved.

      Identification and validation of a novel *NOTCH3* enhancer. We investigated potential regulatory regions of the *NOTCH3* gene and found two elements capable of inducing a luciferase reporter upon MKK6(CA) induction, both bind Myc, and both are sensitive to Myc inhibition. One element lies ~10 kb upstream (En1) and has not previously been identified. A 5' deletion that eliminates all of the predicted Myc binding sites (Mathelier et al., 2016) in En1 severely compromises is induction; however, it is only partially sensitive to Myc inhibition. Thus, there are likely to be other factors that cooperate with Myc to fully activate this enhancer and may explain why Myc alone is not sufficient to induce NOTCH3 and its inhibition only partially reduces NOTCH3 induction. A second element (En3) lies in a previously implicated locus within the second intron (Gagan et al., 2012; Romano et al., 2012). Our report is the first to show functional validation of En3 in human cells. Furthermore, we identified bi-directional eRNA from En3 upon p38-MAPK stimulation, as measured by BruUV-seq (Kim et al., 2010; Lam et al., 2014; Magnuson et al., 2015). Interestingly, En3 was still induced even when all predicted MYC sites (Mathelier et al., 2016) were removed (En3Δ). However, En3Δ was still sensitive to MYC inhibition and MYC was inducibly bound. Thus, there is likely to be another element within the remaining En3Δ region controlled by MYC, either directly or indirectly. Both elements contain numerous potential transcription factor binding sites (Consortium, 2012; Mathelier et al., 2016) and furhter detailed analysis will be required to completely define all possible mechanisms of *NOTCH3* transcriptional regulation.

      ***NOTCH3* regulation via mRNA stability.** We also demonstrate that *NOTCH3* is post-transcriptionally regulated through mRNA stability during differentiation by p38-MAPK. *NOTCH1* expression is reported to be regulated by RNA stability through AU-rich elements in its 3' UTR and is modulated by p38-MAPK (Cisneros et al., 2008; Gonsalves and Weisblat, 2007). p38-MAPK is known to regulate mRNA stability through phosphorylation of mRNA binding proteins (Cuadrado and Nebreda, 2010). *NOTCH3* also has predicted AU-rich elements in its 3' UTR (Gruber et al., 2011). Interestingly, p38-MAPK activation via MKK6(CA) for 16 h increased both *NOTCH1* and *NOTCH3* mRNA half-life, but only *NOTCH3* stability was increased after 6 days of differentiation. This may reflect differences in the extent of p38-MAPK in the two models or may suggest other modes of stabilization are involved. There are reports of post-transcriptional NOTCH regulation by miRNAs which may also contribute to long term stability (Furukawa et al.,

2013; Gagan et al., 2012; Liu et al., 2015). Further research will be needed to fully comprehend the mechanisms of *NOTCH1* and *NOTCH3* post-transcriptional regulation.

Day 8 is a critical transition point in differentiation. Temporal regulation of NOTCH3 throughout differentiation is dynamic. We observed two phases of *NOTCH3* mRNA induction: an early steady increase up to day 8 followed by a more dramatic increase. Considering that *NOTCH3* mRNA is stabilized by day 6, it could be that early upregulation is less dependent on transcriptional mechanisms and more so on message stability. Formation of the luminal layer becomes noticeable around day 8, coinciding with induction of downstream targets *HES/HEY*. Additionally, it is at this transition point that p38-MAPK and MYC are activated. Thus, robust transcriptional induction of *NOTCH3* appears to peak around this time and may drive the secondary phase of *NOTCH3* induction. Though there are still unsolved mechanisms, it appears that the window around day 8 is a key point for NOTCH3 activation and cell commitment to luminal transition.

Potential downstream effects of NOTCH activity. The direct effectors of NOTCH signaling include the canonical *HES/HEY* transcriptional repressor family. Though all these genes increase during differentiation, *HEY2* is unique in that it is much higher in the luminal layer upon terminal differentiation. Whether *HEY2* is preferentially increased by NOTCH3 is unknown but may define a unique target for NOTCH3 signaling. MYC is known to be a direct target of NOTCH1 in some cancers (Weng et al., 2006). However, we did not see an induction of MYC after day 8 (when *HES/HEY* expression increases). Thus, in a normal differentiation context MYC does not appear to be a downstream NOTCH target. Additional reported downstream pathways of NOTCH signaling include PTEN and CDH1/E-Cadherin, both of which are critical for luminal cell survival (Bertrand et al., 2014; Lamb et al., 2010). Furthermore, NOTCH can downregulate adhesion genes, including integrins, which is required for basal cell detachment from the extracellular matrix (Cress et al., 1995; Mazzone et al., 2010; Nguyen et al., 2006). There are also reports that NOTCH can upregulate MKP1, a phosphatase that targets p38-MAPK, thus providing a potential feedback mechanism in terminally differentiated cells to balance p38-MAPK activity (Gagan et al., 2012; Yoshida et al., 2014). Further research will be needed to validate which downstream NOTCH targets are most relevant to prostate differentiation.

Conclusion. Our goal is to define the mechanisms that drive basal to luminal differentiation in the normal prostate epithelium. In this study, we report on a novel mechanism for crosstalk between p38-MAPK, MYC, and NOTCH. Moreover, we identify two distinct regulatory mechanisms for *NOTCH3* in the prostate: a coordination of elevated mRNA stability and increased transcription from multiple enhancers. These findings provide a better

14

understanding for how these differentiation pathways are connected in normal prostate epithelium and opens the door to investigating how their dysregulation may impact prostate cancer development and progression.

COMPETING INTERESTS

The authors have no competing interests to declare.

AUTHOR CONTRIBUTIONS

S.B.F. was responsible for experimental design, execution, analysis, and writing. P.L.B. was responsible for ChIP, immunofluorescence staining, and consultation. M.L. was responsible for BruUV-seq, RNA isolation, library prep, sequencing and expression analysis, and reviewing the manuscript. C.K.M. was responsible for experimental design, analysis, writing, editing, communication, and supervising the project.

Table 1: Day 4 vs Day 1 mRNA half-life calculations.

		Line Equation Y= mx+b	*r^2	Half Life (1/m)	p-value (m1 vs m2)	Overall Expression
MYC	*Day1*	Y= -1.30x + 0.05	0.98	0.8 h	0.25	+ 1.2 fold
	Day4	Y= -1.08x + 0.27	0.99	0.9 h		
NOTCH1	*Day1*	Y= -0.267x + 0.03	0.82	3.8 h	0.23	+ 1.2 fold
	Day4	Y= -0.197x + 0.29	0.85	5.1 h		
NOTCH3	*Day1*	Y= -0.170x - 0.10	0.74	5.9 h	0.11	+ 8.5 fold
	Day4	Y= -0.0867x + 2.99	0.55	11.5 h		

*r^2 values indicate how well the 9 data points fit each linear regression line. p-values compare slopes between lines using ANCOVA analysis.

Table 2: MKK6(CA) mRNA half-life calculations.

		Line Equation Y= mx+b	*r^2	Half Life (1/m)	p-value (m1 vs m2)	Overall Expression
MYC	*-Dox*	Y= -1.55x - 0.05	1.00	0.6 h	0.50	+ 1.7 fold
	+Dox	Y= -1.17x - 0.82	0.90	0.9 h		
NOTCH1	*-Dox*	Y= -0.302x - 0.26	0.85	3.3 h	0.02	- 4.1 fold
	+Dox	Y= -0.113x - 2.30	0.42	8.8 h		
NOTCH3	*-Dox*	Y= -0.132x - 0.27	0.73	7.6 h	0.14	+ 8.8 fold
	+Dox	Y= -0.057x + 2.86	0.25	17.6 h		

*r^2 values indicate how well the 9 data points fit each linear regression line. p-values compare slopes between lines using ANCOVA analysis.

FIGURE LEGENDS

Figure 1: p38α- and p38δ-MAPK are required for differentiation. **(A)** Plot of counts per million (CPM) reads for the four p38-MAPK isoforms taken from RNA-seq data of basal iPrECs. Line indicates mean of biological triplicates. **(B)** Lysates from stable pools of iPrECs expressing Tet-inducible p38α or p38δ shRNAs treated with Dox for 72 h and probed by immunoblot. **(C,D)** Primary (PrEC) and immortalized (iPrEC) cells differentiated with KGF and R1881 and lysates collected at indicated time points for immunoblotting. Luminal cells (L) were separated from the basal cells (B) at the final time point before lysis. **(E)** iPrECs were differentiated 16 days with DMSO+Dox (Control), 1 µM SB202190, or 0.1 µM BIRB796 while shRNA lines were induced with Dox. Top row: phase-contrast. Bottom row: merged epifluorescence of Hoescht-stained nuclei in blue, luminal (L) immunofluorescence of Androgen Receptor (AR) in red and basal (B) Integrin α6 (ITGα6) in green. Luminal layer is outlined (dashed line) in control cells. Scale bar = 200 µm.

Figure 2: NOTCH1 and NOTCH3 are required for differentiation. **(A)** iPrECs were differentiated and analyzed by immunoblot as in Fig. 1D. Antibody notes: p-MYC recognizes T58/S62. NOTCH2 is ICD-specific. NOTCH1/3 recognize full length (FL), transmembrane (TM), and intracellular domain (ICD). **(B)** RNA was collected over differentiation for qRT-PCR examination of ligands and downstream targets of the NOTCH signaling. Luminal (L, solid line) cells were separated from basal (B, dashed line) cells at days 10 and 14. Data were normalized to day 1. Graph shows mean±s.d. of biological triplicates. **(C)** iPrEC pools expressing TetON-shRNA were treated with Dox and differentiated for 4 days; NOTCH receptor expression was measured by immunoblot. **(D)** iPrECs were differentiated 16 days with DMSO+Dox (Control) or 1 µM RO4929097 while shRNA lines were induced with Dox. Cells were stained by immunofluorescence. Top row: phase-contrast. Bottom row: merged epifluorescence of Hoescht-stained nuclei in blue, AR in red as a luminal (L) marker, and Integrin α6 in green as a basal (B) marker. Luminal layer is outlined (dashed line) in control cells. Scale bar = 200 µm.

Figure 3: p38-MAPK induces NOTCH3. **(A)** Diagram explaining the MKK6(CA) model. iPrECs were engineered to stably express a Dox-inducible constitutively active MKK6 mutant, MKK6(CA), which phosphorylates all p38 isoforms. Differentiation involves a low/moderate elevation of p38-MAPK over days whereas this model utilizes acute p38-MAPK activation. **(B)** iPrEC-TetON-MKK6(CA) cells were treated with Dox for 16 h plus DMSO or 5 µM SB202190 and analyzed by qRT-PCR. Data were normalized to DMSO-only cells. Graph shows mean±s.d. of

biological triplicates. Text within bars is rounded fold change. **(C)** iPrEC-TetOn-MKK6(CA) cells were treated with Dox for up to 16 h and harvested at indicated times for immunoblot. Myc-tagged MKK6(CA) was recognized with a MYC antibody (LE = long exposure). **(D)** iPrEC-TetON-MKK6(CA) cells were treated as in (C) and analyzed by qRT-PCR. Data were normalized to 0 h samples. Graph shows mean±s.d. of biological triplicates. **(E)** iPrEC-TetON-MKK6(CA) cells were differentiated 1-4 days ±Dox pulse (4 h) after day 1 and analyzed by immunoblot. **(F)** iPrECs were differentiated 4 days with DMSO or 5 µM SB202190 and analyzed by qRT-PCR. Data were normalized to day 1. Graph shows mean±s.d. of biological triplicates. Text within bars is rounded fold change.

Figure 4: MYC is an intermediate for p38-MAPK induction of NOTCH3. **(A)** iPrEC-TetON-MKK6(CA) cells were induced with Dox for a total of 12 h with Cyclohexamide (CHX) added at 6 (blue), 8 (orange), or 10 (green) hours. *NOTCH3* mRNA was measured by qRT-PCR. Data were normalized to 0 h. **(B)** iPrEC-TetON-MKK6(CA) cells were transfected with siMyc or siScram for 24 h, then induced with Dox for 12 h and analyzed by qRT-PCR. Data were normalized to non-transfected, untreated controls. Graph shows mean±s.d. of biological triplicates. Text within bars is rounded fold change. **(C)** iPrEC-TetON-MKK6(CA) cells were treated 16 h with Dox plus DMSO or increasing doses of MYC inhibitor 10058-F4. Protein was analyzed by immunoblot. FL=full length, TM=trans-membrane. **(D)** iPrECs expressing Dox-inducible MYC (iPrEC-TetON-Myc) were treated with Dox for 0-24 h and analyzed by immunoblot.

Figure 5: *NOTCH3* **transcription requires a MYC-driven enhancer element**. **(A)** iPrECs were transfected with a selectable pGL4.15 vector containing 2kb of *NOTCH3* upstream sequence. A stable pool was differentiated 1 or 6 days and analyzed by qRT-PCR. Data were standardized to *18S* and *ACTB* and normalized to day 1. Graph shows mean±s.d. of biological triplicates. **(B)** iPrEC-TetON-MKK6(CA) cells were treated with Dox for 10 h and processed for BruUV-seq. Y-axis is RPKM (reads per kilobase of transcript per million mapped reads). Plus strand reads are (+), minus strand reads are (-). Blue = -Dox; Orange = +Dox. *NOTCH3* gene diagram shows orientation (arrow) and exons (black lines). **(C)** iPrEC-TetON-MKK6(CA) cells were transfected with pNL1.1 reporter constructs, split, and then treated ±Dox for 16 h. Luciferase assay was performed with pNL1.1-miniTK as a negative control. Graph shows mean±c.i. (n=8). p-value details are in methods. **(D)** iPrEC-TetON-MKK6(CA) cells were treated ±Dox for 8 h. MYC binding to enhancer regions was assessed by ChIP and qRT-PCR. Positive and negative control MYC loci were *ODC1* and *HIST3*, respectively. IgG served as IP control (-Dox). Primer set (1)

is 5' of set (2). **(E)** Same as in (D) except that transfected pools were split and treated 16 h with DMSO, Dox, 10058-F4 (20 µM), or a combination. Graph shows mean±c.i. (n=8), normalized to DMSO. p-value details are in methods.

Figure 6: **p38-MAPK upregulates *NOTCH3* mRNA stability. (A)** iPrECs were differentiated 1 day (closed circle, solid line) or 4 days (open circle, dashed line) and at each time treated with ActD for 0-8 h. RNA was harvested for qRT-PCR analysis. Samples were standardized to *18S* rRNA and normalized to the Day1, 0 h sample. For *MYC*, only 1-4 h time points were used to maintain a linear range. **(B)** Same experiment as in (A) but using the iPrEC-TetON-MKK6(CA) model. Cells were treated ±Dox for 16 h prior to ActD treatment. Samples were normalized to the -Dox, 0 h sample. Open circle/dashed line = -Dox. Closed circle/solid line = +Dox.

REFERENCES

Alonso, G., Ambrosino, C., Jones, M. and Nebreda, A. R. (2000). Differential activation of p38 mitogen-activated protein kinase isoforms depending on signal strength. *The Journal of biological chemistry* **275**, 40641-40648.

Andrade-Lima, L. C., Veloso, A., Paulsen, M. T., Menck, C. F. and Ljungman, M. (2015). DNA repair and recovery of RNA synthesis following exposure to ultraviolet light are delayed in long genes. *Nucleic acids research* **43**, 2744-2756.

Baeten, J. T. and Lilly, B. (2015). Differential Regulation of NOTCH2 and NOTCH3 Contribute to Their Unique Functions in Vascular Smooth Muscle Cells. *The Journal of biological chemistry* **290**, 16226-16237.

Belleudi, F., Purpura, V. and Torrisi, M. R. (2011). The receptor tyrosine kinase FGFR2b/KGFR controls early differentiation of human keratinocytes. *PloS one* **6**, e24194.

Berger, P. L., Frank, S. B., Schulz, V. V., Nollet, E. A., Edick, M. J., Holly, B., Chang, T. T., Hostetter, G., Kim, S. and Miranti, C. K. (2014). Transient induction of ING4 by Myc drives prostate epithelial cell differentiation and its disruption drives prostate tumorigenesis. *Cancer research* **74**, 3357-3368.

Bertrand, F. E., McCubrey, J. A., Angus, C. W., Nutter, J. M. and Sigounas, G. (2014). NOTCH and PTEN in prostate cancer. *Advances in biological regulation* **56**, 51-65.

Bhat, V., Sun, Y., Weger, S. and Raouf, A. (2016). Notch-induced expression of FZD7 requires noncanonical NOTCH3 signalling in human breast epithelial cells. *Stem cells and development*.

Brown, D., Hikim, A. P., Kovacheva, E. L. and Sinha-Hikim, I. (2009). Mouse model of testosterone-induced muscle fiber hypertrophy: involvement of p38 mitogen-activated protein kinase-mediated Notch signaling. *The Journal of endocrinology* **201**, 129-139.

Campeau, E., Ruhl, V. E., Rodier, F., Smith, C. L., Rahmberg, B. L., Fuss, J. O., Campisi, J., Yaswen, P., Cooper, P. K. and Kaufman, P. D. (2009). A versatile viral system for expression and depletion of proteins in mammalian cells. *PloS one* **4**, e6529.

Carvalho, F. L., Simons, B. W., Eberhart, C. G. and Berman, D. M. (2014). Notch signaling in prostate cancer: a moving target. *The Prostate* **74**, 933-945.

Cisneros, E., Latasa, M. J., Garcia-Flores, M. and Frade, J. M. (2008). Instability of Notch1 and Delta1 mRNAs and reduced Notch activity in vertebrate neuroepithelial cells undergoing S-phase. *Molecular and cellular neurosciences* **37**, 820-831.

Conacci-Sorrell, M., McFerrin, L. and Eisenman, R. N. (2014). An overview of MYC and its interactome. *Cold Spring Harbor perspectives in medicine* **4**, a014357.

Consortium, E. P. (2012). An integrated encyclopedia of DNA elements in the human genome. *Nature* **489**, 57-74.

Cress, A. E., Rabinovitz, I., Zhu, W. and Nagle, R. B. (1995). The alpha 6 beta 1 and alpha 6 beta 4 integrins in human prostate cancer progression. *Cancer metastasis reviews* **14**, 219-228.

Cuadrado, A. and Nebreda, A. R. (2010). Mechanisms and functions of p38 MAPK signalling. *The Biochemical journal* **429**, 403-417.

Defoiche, J., Zhang, Y., Lagneaux, L., Pettengell, R., Hegedus, A., Willems, L. and Macallan, D. C. (2009). Measurement of ribosomal RNA turnover in vivo by use of deuterium-labeled glucose. *Clinical chemistry* **55**, 1824-1833.

Deng, G., Ma, L., Meng, Q., Ju, X., Jiang, K., Jiang, P. and Yu, Z. (2015). Notch signaling in the prostate: critical roles during development and in the hallmarks of prostate cancer biology. *Journal of cancer research and clinical oncology*.

Edick, M. J., Tesfay, L., Lamb, L. E., Knudsen, B. S. and Miranti, C. K. (2007). Inhibition of integrin-mediated crosstalk with epidermal growth factor receptor/Erk or Src signaling
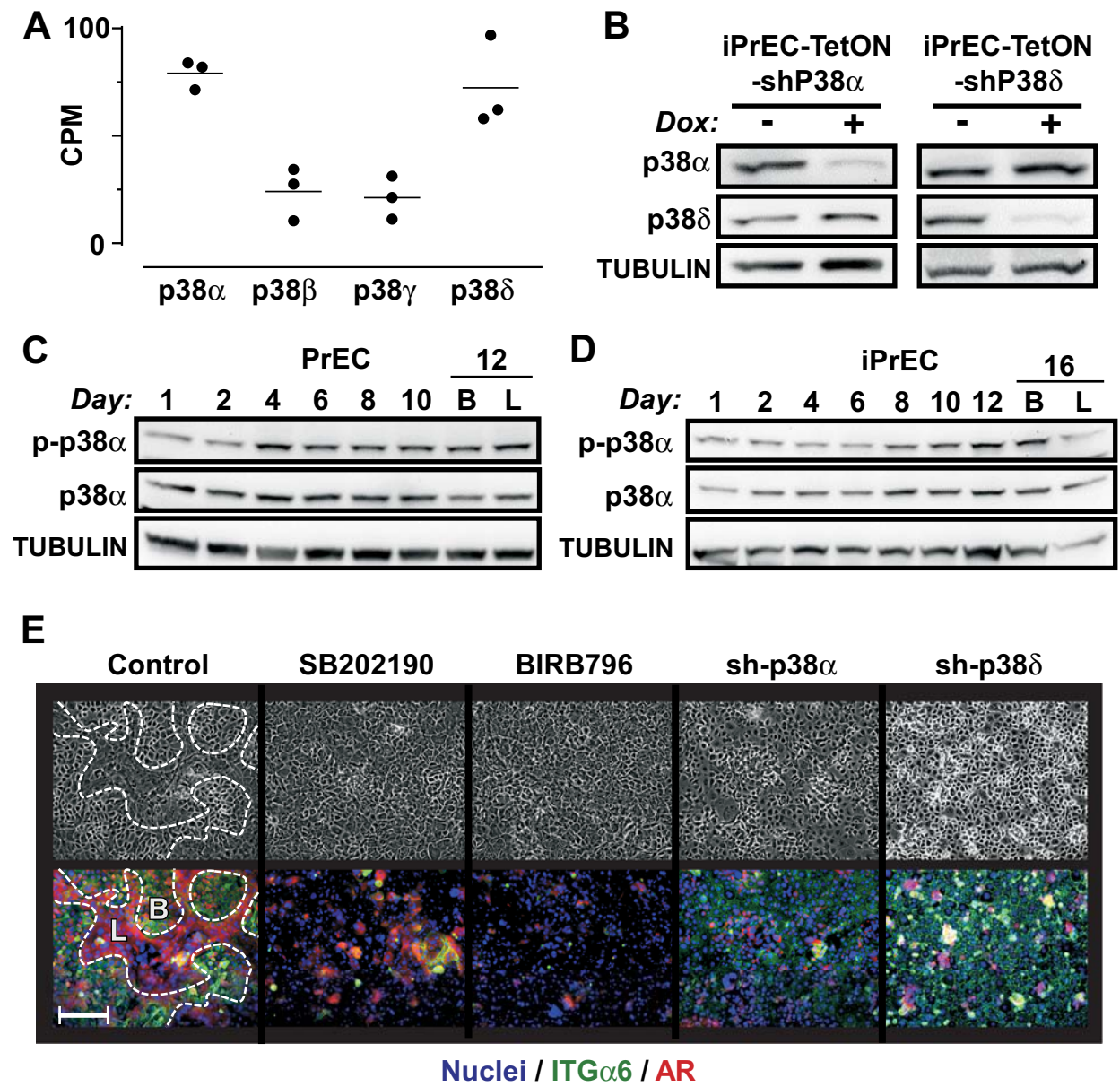
pathways in autophagic prostate epithelial cells induces caspase-independent death. *Molecular biology of the cell* **18**, 2481-2490.

Frank, S. B. and Miranti, C. K. (2013). Disruption of prostate epithelial differentiation pathways and prostate cancer development. *Frontiers in oncology* **3**, 273.

Furukawa, S., Kawasaki, Y., Miyamoto, M., Hiyoshi, M., Kitayama, J. and Akiyama, T. (2013). The miR-1-NOTCH3-Asef pathway is important for colorectal tumor cell migration. *PloS one* **8**, e80609.

Gagan, J., Dey, B. K., Layer, R., Yan, Z. and Dutta, A. (2012). Notch3 and Mef2c proteins are mutually antagonistic via Mkp1 protein and miR-1/206 microRNAs in differentiating myoblasts. *The Journal of biological chemistry* **287**, 40360-40370.

Gebhardt, A., Frye, M., Herold, S., Benitah, S. A., Braun, K., Samans, B., Watt, F. M., Elsasser, H. P. and Eilers, M. (2006). Myc regulates keratinocyte adhesion and differentiation via complex formation with Miz1. *The Journal of cell biology* **172**, 139-149.

Gomi, K., Arbelaez, V., Crystal, R. G. and Walters, M. S. (2015). Activation of NOTCH1 or NOTCH3 signaling skews human airway basal cell differentiation toward a secretory pathway. *PloS one* **10**, e0116507.

Gonsalves, F. C. and Weisblat, D. A. (2007). MAPK regulation of maternal and zygotic Notch transcript stability in early development. *Proceedings of the National Academy of Sciences of the United States of America* **104**, 531-536.

Gruber, A. R., Fallmann, J., Kratochvill, F., Kovarik, P. and Hofacker, I. L. (2011). AREsite: a database for the comprehensive investigation of AU-rich elements. *Nucleic acids research* **39**, D66-69.

Guo, J., Parise, R. A., Joseph, E., Egorin, M. J., Lazo, J. S., Prochownik, E. V. and Eiseman, J. L. (2009). Efficacy, pharmacokinetics, tisssue distribution, and metabolism of the Myc-Max disruptor, 10058-F4 [Z,E]-5-[4-ethylbenzylidine]-2-thioxothiazolidin-4-one, in mice. *Cancer chemotherapy and pharmacology* **63**, 615-625.

Harrold, S., Genovese, C., Kobrin, B., Morrison, S. L. and Milcarek, C. (1991). A comparison of apparent mRNA half-life using kinetic labeling techniques vs decay following administration of transcriptional inhibitors. *Analytical biochemistry* **198**, 19-29.

Heer, R., Collins, A. T., Robson, C. N., Shenton, B. K. and Leung, H. Y. (2006). KGF suppresses alpha2beta1 integrin function and promotes differentiation of the transient amplifying population in human prostatic epithelium. *Journal of cell science* **119**, 1416-1424.

Herrick, D. J. and Ross, J. (1994). The half-life of c-myc mRNA in growing and serum-stimulated cells: influence of the coding and 3' untranslated regions and role of ribosome translocation. *Molecular and cellular biology* **14**, 2119-2128.

Hodkinson, P. S., Elliott, P. A., Lad, Y., McHugh, B. J., MacKinnon, A. C., Haslett, C. and Sethi, T. (2007). Mammalian NOTCH-1 activates beta1 integrins via the small GTPase R-Ras. *The Journal of biological chemistry* **282**, 28991-29001.

Hogarty, M. D., Norris, M. D., Davis, K., Liu, X., Evageliou, N. F., Hayes, C. S., Pawel, B., Guo, R., Zhao, H., Sekyere, E., et al. (2008). ODC1 is a critical determinant of MYCN oncogenesis and a therapeutic target in neuroblastoma. *Cancer research* **68**, 9735-9745.

Huang, M. J., Cheng, Y. C., Liu, C. R., Lin, S. and Liu, H. E. (2006). A small-molecule c-Myc inhibitor, 10058-F4, induces cell-cycle arrest, apoptosis, and myeloid differentiation of human acute myeloid leukemia. *Experimental hematology* **34**, 1480-1489.

Kent, W. J., Sugnet, C. W., Furey, T. S., Roskin, K. M., Pringle, T. H., Zahler, A. M. and Haussler, D. (2002). The human genome browser at UCSC. *Genome research* **12**, 996-1006.

Kiec-Wilk, B., Grzybowska-Galuszka, J., Polus, A., Pryjma, J., Knapp, A. and Kristiansen, K. (2010). The MAPK-dependent regulation of the Jagged/Notch gene expression by

VEGF, bFGF or PPAR gamma mediated angiogenesis in HUVEC. *Journal of physiology and pharmacology : an official journal of the Polish Physiological Society* **61**, 217-225.

Kim, T. K., Hemberg, M., Gray, J. M., Costa, A. M., Bear, D. M., Wu, J., Harmin, D. A., Laptewicz, M., Barbara-Haley, K., Kuersten, S., et al. (2010). Widespread transcription at neuronal activity-regulated enhancers. *Nature* **465**, 182-187.

Koh, C. M., Bieberich, C. J., Dang, C. V., Nelson, W. G., Yegnasubramanian, S. and De Marzo, A. M. (2010). MYC and Prostate Cancer. *Genes & cancer* **1**, 617-628.

Kopan, R. and Ilagan, M. X. (2009). The canonical Notch signaling pathway: unfolding the activation mechanism. *Cell* **137**, 216-233.

Kwon, O. J., Valdez, J. M., Zhang, L., Zhang, B., Wei, X., Su, Q., Ittmann, M. M., Creighton, C. J. and Xin, L. (2014). Increased Notch signalling inhibits anoikis and stimulates proliferation of prostate luminal epithelial cells. *Nature communications* **5**, 4416.

Kwon, O. J., Zhang, L. and Xin, L. (2016). Stem Cell Antigen-1 Identifies a Distinct Androgen-Independent Murine Prostatic Luminal Cell Lineage with Bipotent Potential. *Stem cells* **34**, 191-202.

Lam, M. T., Li, W., Rosenfeld, M. G. and Glass, C. K. (2014). Enhancer RNAs and regulated transcriptional programs. *Trends in biochemical sciences* **39**, 170-182.

Lamb, L. E., Knudsen, B. S. and Miranti, C. K. (2010). E-cadherin-mediated survival of androgen-receptor-expressing secretory prostate epithelial cells derived from a stratified in vitro differentiation model. *Journal of cell science* **123**, 266-276.

Liu, X. D., Zhang, L. Y., Zhu, T. C., Zhang, R. F., Wang, S. L. and Bao, Y. (2015). Overexpression of miR-34c inhibits high glucose-induced apoptosis in podocytes by targeting Notch signaling pathways. *International journal of clinical and experimental pathology* **8**, 4525-4534.

Luscher, B. and Vervoorts, J. (2012). Regulation of gene transcription by the oncoprotein MYC. *Gene* **494**, 145-160.

Magnuson, B., Veloso, A., Kirkconnell, K. S., de Andrade Lima, L. C., Paulsen, M. T., Ljungman, E. A., Bedi, K., Prasad, J., Wilson, T. E. and Ljungman, M. (2015). Identifying transcription start sites and active enhancer elements using BruUV-seq. *Scientific reports* **5**, 17978.

Marderosian, M., Sharma, A., Funk, A. P., Vartanian, R., Masri, J., Jo, O. D. and Gera, J. F. (2006). Tristetraprolin regulates Cyclin D1 and c-Myc mRNA stability in response to rapamycin in an Akt-dependent manner via p38 MAPK signaling. *Oncogene* **25**, 6277-6290.

Mathelier, A., Fornes, O., Arenillas, D. J., Chen, C. Y., Denay, G., Lee, J., Shi, W., Shyr, C., Tan, G., Worsley-Hunt, R., et al. (2016). JASPAR 2016: a major expansion and update of the open-access database of transcription factor binding profiles. *Nucleic acids research* **44**, D110-115.

Mazzone, M., Selfors, L. M., Albeck, J., Overholtzer, M., Sale, S., Carroll, D. L., Pandya, D., Lu, Y., Mills, G. B., Aster, J. C., et al. (2010). Dose-dependent induction of distinct phenotypic responses to Notch pathway activation in mammary epithelial cells. *Proceedings of the National Academy of Sciences of the United States of America* **107**, 5012-5017.

McKeown, M. R. and Bradner, J. E. (2014). Therapeutic strategies to inhibit MYC. *Cold Spring Harbor perspectives in medicine* **4**.

Mori, M., Mahoney, J. E., Stupnikov, M. R., Paez-Cortez, J. R., Szymaniak, A. D., Varelas, X., Herrick, D. B., Schwob, J., Zhang, H. and Cardoso, W. V. (2015). Notch3-Jagged signaling controls the pool of undifferentiated airway progenitors. *Development* **142**, 258-267.

Nguyen, B. C., Lefort, K., Mandinova, A., Antonini, D., Devgan, V., Della Gatta, G., Koster, M. I., Zhang, Z., Wang, J., Tommasi di Vignano, A., et al. (2006). Cross-regulation
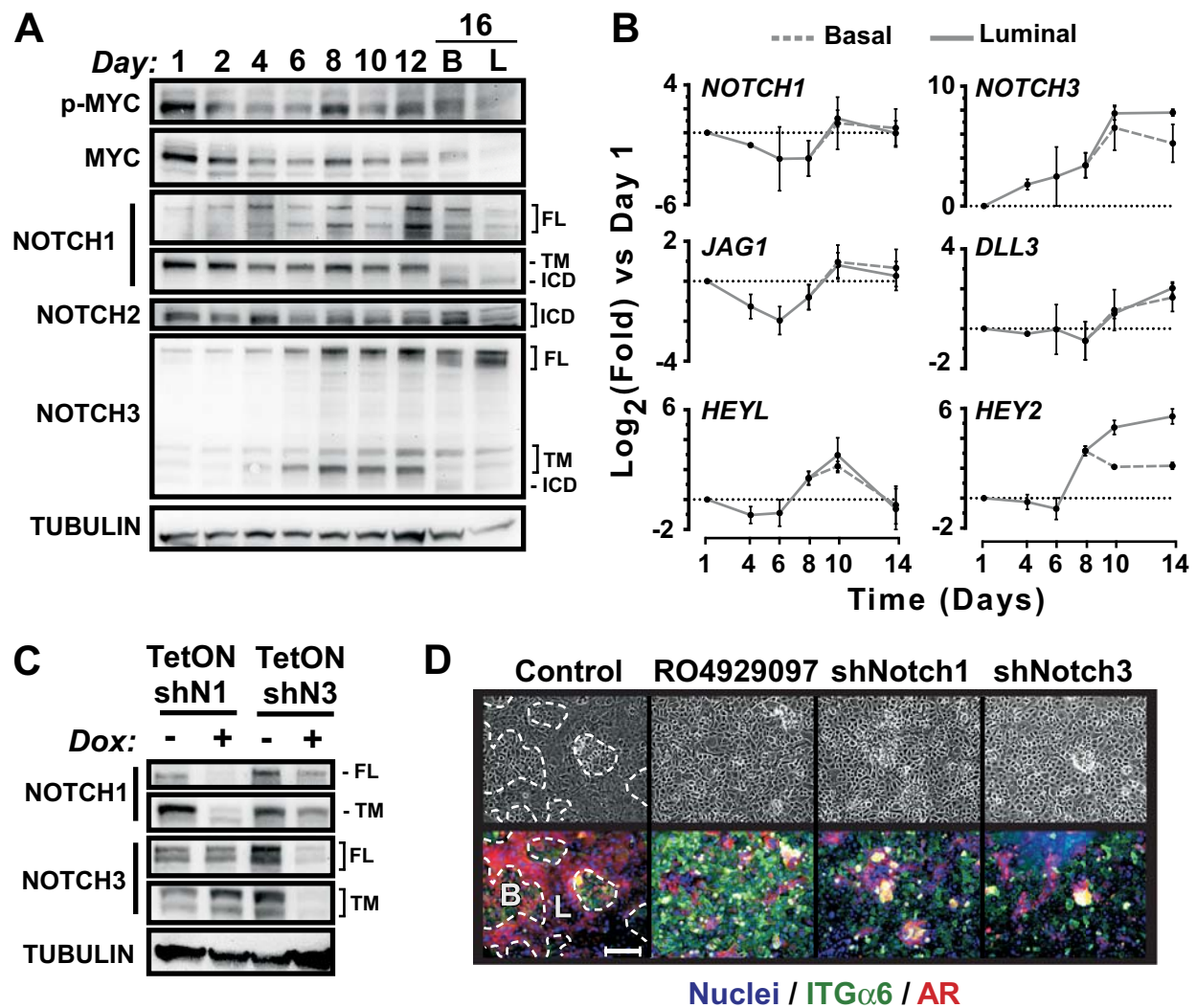
between Notch and p63 in keratinocyte commitment to differentiation. *Genes & development* **20**, 1028-1042.

Ohashi, S., Natsuizaka, M., Yashiro-Ohtani, Y., Kalman, R. A., Nakagawa, M., Wu, L., Klein-Szanto, A. J., Herlyn, M., Diehl, J. A., Katz, J. P., et al. (2010). NOTCH1 and NOTCH3 coordinate esophageal squamous differentiation through a CSL-dependent transcriptional network. *Gastroenterology* **139**, 2113-2123.

Ortica, S., Tarantino, N., Aulner, N., Israel, A. and Gupta-Rossi, N. (2014). The 4 Notch receptors play distinct and antagonistic roles in the proliferation and hepatocytic differentiation of liver progenitors. *FASEB journal : official publication of the Federation of American Societies for Experimental Biology* **28**, 603-614.

Ousset, M., Van Keymeulen, A., Bouvencourt, G., Sharma, N., Achouri, Y., Simons, B. D. and Blanpain, C. (2012). Multipotent and unipotent progenitors contribute to prostate postnatal development. *Nature cell biology* **14**, 1131-1138.

Park, J. S., Kim, Y. S. and Yoo, M. A. (2009). The role of p38b MAPK in age-related modulation of intestinal stem cell proliferation and differentiation in Drosophila. *Aging* **1**, 637-651.

Paulsen, M. T., Veloso, A., Prasad, J., Bedi, K., Ljungman, E. A., Magnuson, B., Wilson, T. E. and Ljungman, M. (2014). Use of Bru-Seq and BruChase-Seq for genome-wide assessment of the synthesis and stability of RNA. *Methods* **67**, 45-54.

Pedrosa, A. R., Graca, J. L., Carvalho, S., Peleteiro, M. C., Duarte, A. and Trindade, A. (2016). Notch signaling dynamics in the adult healthy prostate and in prostatic tumor development. *The Prostate* **76**, 80-96.

Rangarajan, A., Talora, C., Okuyama, R., Nicolas, M., Mammucari, C., Oh, H., Aster, J. C., Krishna, S., Metzger, D., Chambon, P., et al. (2001). Notch signaling is a direct determinant of keratinocyte growth arrest and entry into differentiation. *The EMBO journal* **20**, 3427-3436.

Romano, R. A., Smalley, K., Magraw, C., Serna, V. A., Kurita, T., Raghavan, S. and Sinha, S. (2012). DeltaNp63 knockout mice reveal its indispensable role as a master regulator of epithelial development and differentiation. *Development* **139**, 772-782.

Shou, J., Ross, S., Koeppen, H., de Sauvage, F. J. and Gao, W. Q. (2001). Dynamics of notch expression during murine prostate development and tumorigenesis. *Cancer research* **61**, 7291-7297.

Tokar, E. J., Ancrile, B. B., Cunha, G. R. and Webber, M. M. (2005). Stem/progenitor and intermediate cell types and the origin of human prostate cancer. *Differentiation; research in biological diversity* **73**, 463-473.

Uzgare, A. R., Xu, Y. and Isaacs, J. T. (2004). In vitro culturing and characteristics of transit amplifying epithelial cells from human prostate tissue. *Journal of cellular biochemistry* **91**, 196-205.

Valdez, J. M., Zhang, L., Su, Q., Dakhova, O., Zhang, Y., Shahi, P., Spencer, D. M., Creighton, C. J., Ittmann, M. M. and Xin, L. (2012). Notch and TGFbeta form a reciprocal positive regulatory loop that suppresses murine prostate basal stem/progenitor cell activity. *Cell stem cell* **11**, 676-688.

Wang, J., Ma, X., Jones, H. M., Chan, L. L., Song, F., Zhang, W., Bae-Jump, V. L. and Zhou, C. (2014). Evaluation of the antitumor effects of c-Myc-Max heterodimerization inhibitor 100258-F4 in ovarian cancer cells. *Journal of translational medicine* **12**, 226.

Weng, A. P., Millholland, J. M., Yashiro-Ohtani, Y., Arcangeli, M. L., Lau, A., Wai, C., Del Bianco, C., Rodriguez, C. G., Sai, H., Tobias, J., et al. (2006). c-Myc is an important direct target of Notch1 in T-cell acute lymphoblastic leukemia/lymphoma. *Genes & development* **20**, 2096-2109.

Wiederschain, D., Wee, S., Chen, L., Loo, A., Yang, G., Huang, A., Chen, Y., Caponigro, G., Yao, Y. M., Lengauer, C., et al. (2009). Single-vector inducible lentiviral RNAi system for oncology target validation. *Cell cycle* **8**, 498-504.

Yoshida, Y., Hayashi, Y., Suda, M., Tateno, K., Okada, S., Moriya, J., Yokoyama, M., Nojima, A., Yamashita, M., Kobayashi, Y., et al. (2014). Notch signaling regulates the lifespan of vascular endothelial cells via a p16-dependent pathway. *PloS one* **9**, e100359.

FIGURE 1

Nuclei / **ITGα6** / **AR**
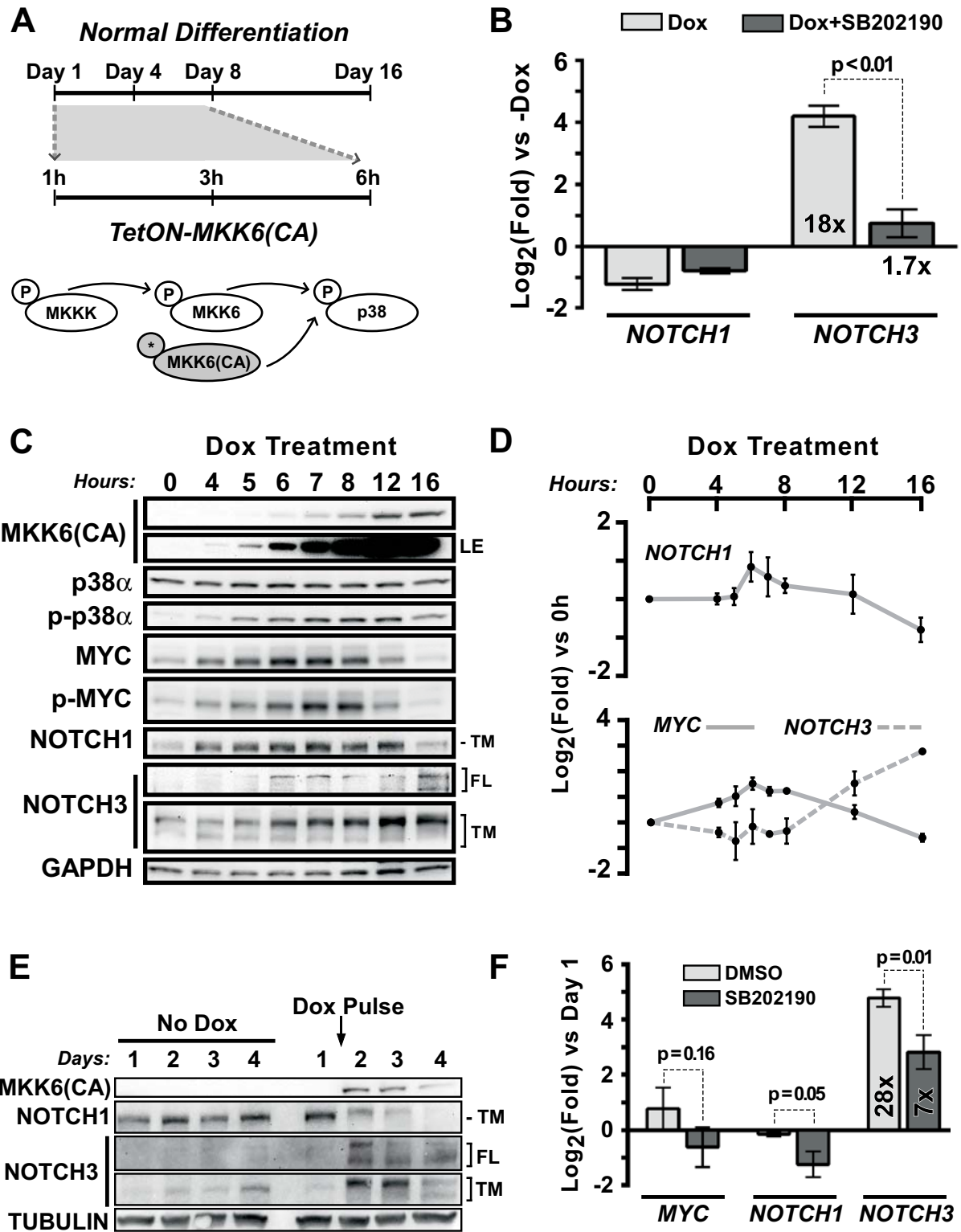
FIGURE 2

FIGURE 3

FIGURE 4
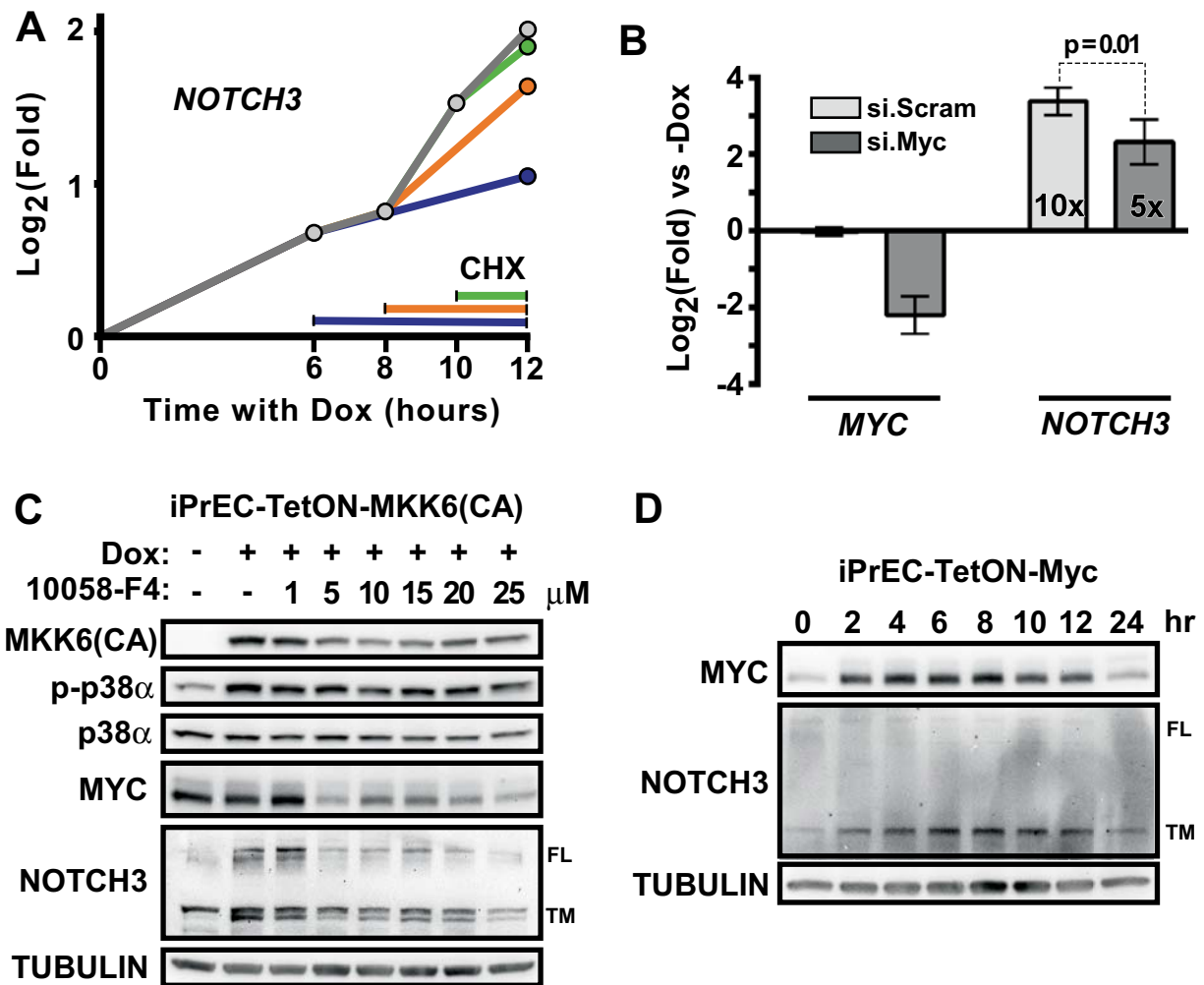
FIGURE 5

FIGURE 6

FIGURE S1

A

BIRB796 (μM):	-	-	-	-	-	0.1	1
SB202190 (μM):	-	-	0.1	1	5	-	-
Dox:	-	+	+	+	+	+	+

MKK6(CA)

p-CREB1

CREB1

TUBULIN

B

| Control | SB202190 | BIRB796 | sh-p38α | sh-p38δ |

Nuclei / **Propidium Iodide**

FIGURE 2

A

Day: 1 2 4 6 8 10 12 | 16 B L

p-MYC
MYC
NOTCH1 — FL
— TM
— ICD
NOTCH2 — ICD
NOTCH3 — FL
— TM
— ICD
TUBULIN

B

- - - - Basal ——— Luminal

Log₂(Fold) vs Day 1

NOTCH1   NOTCH3
JAG1   DLL3
HEYL   HEY2

Time (Days)

C

TetON shN1   TetON shN3

Dox: − + − +

NOTCH1 — FL
— TM
NOTCH3 — FL
— TM
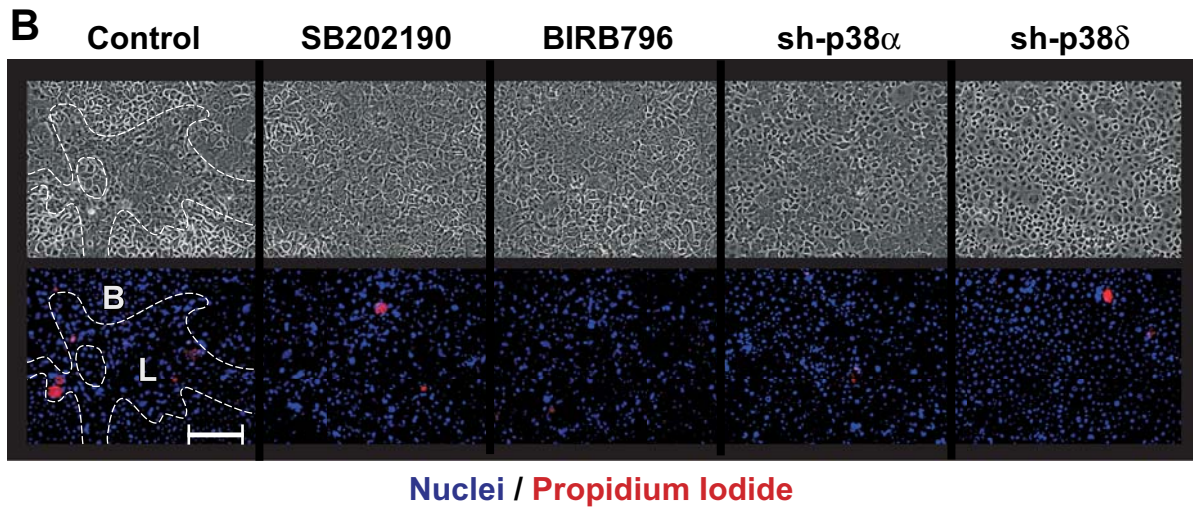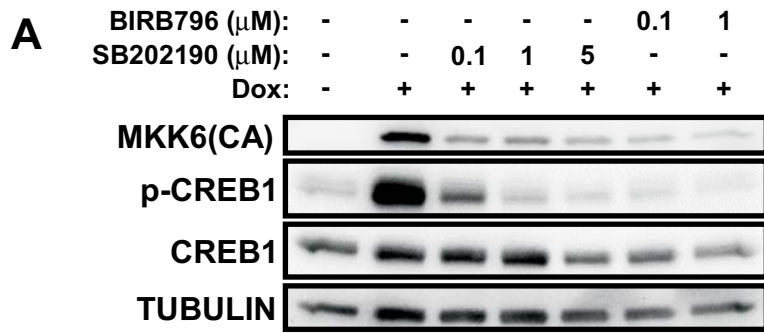TUBULIN

D

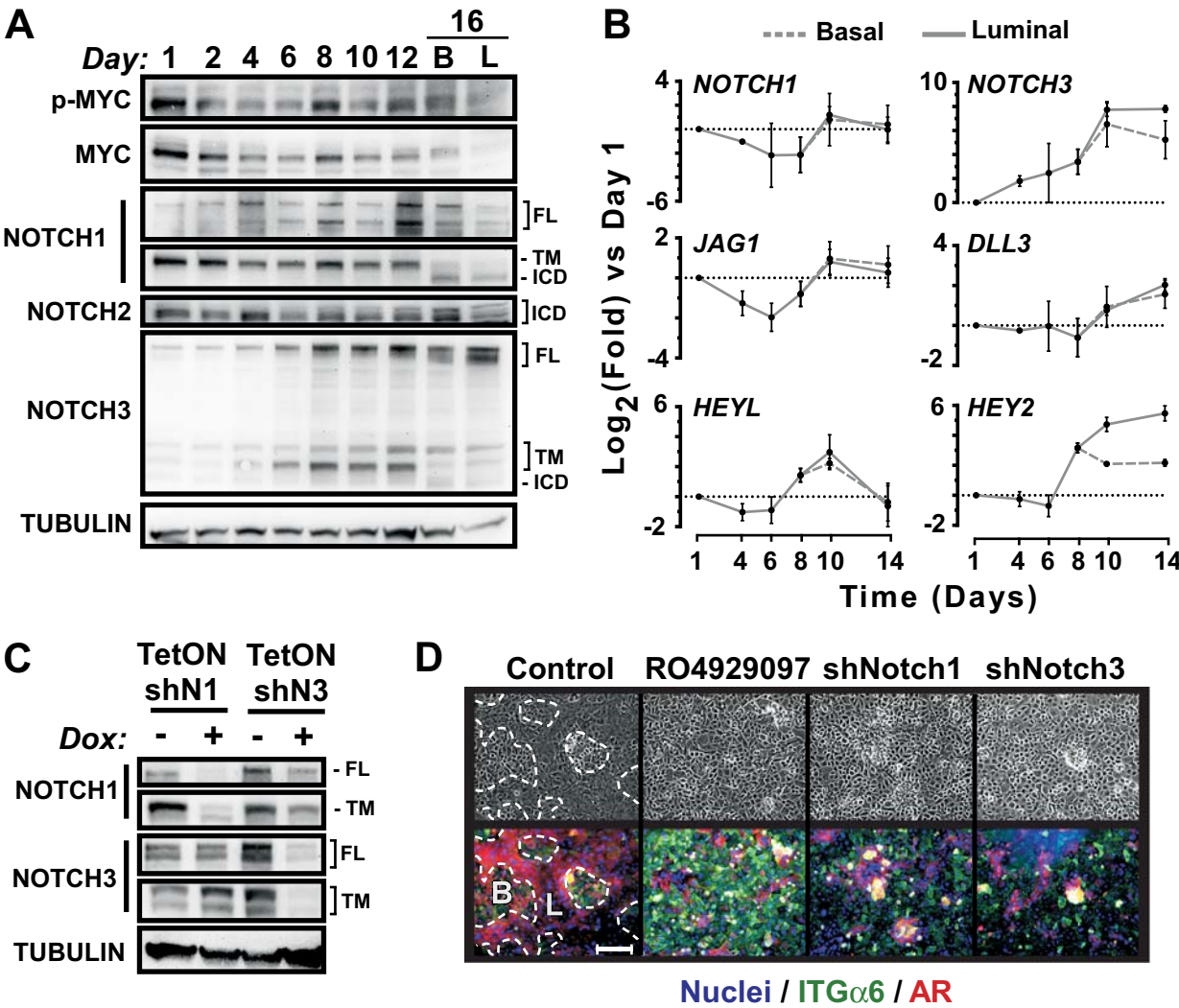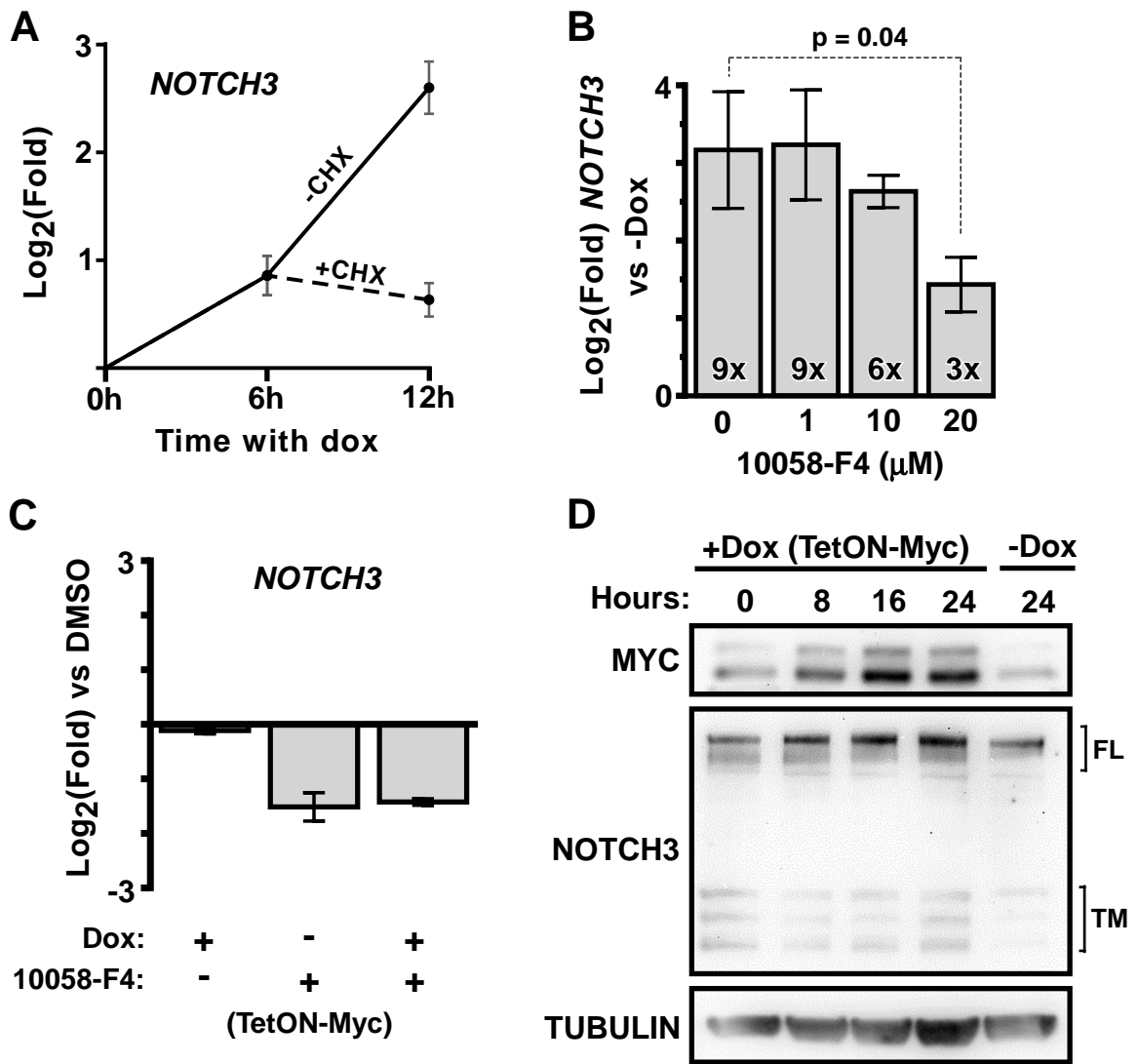Control   RO4929097   shNotch1   shNotch3
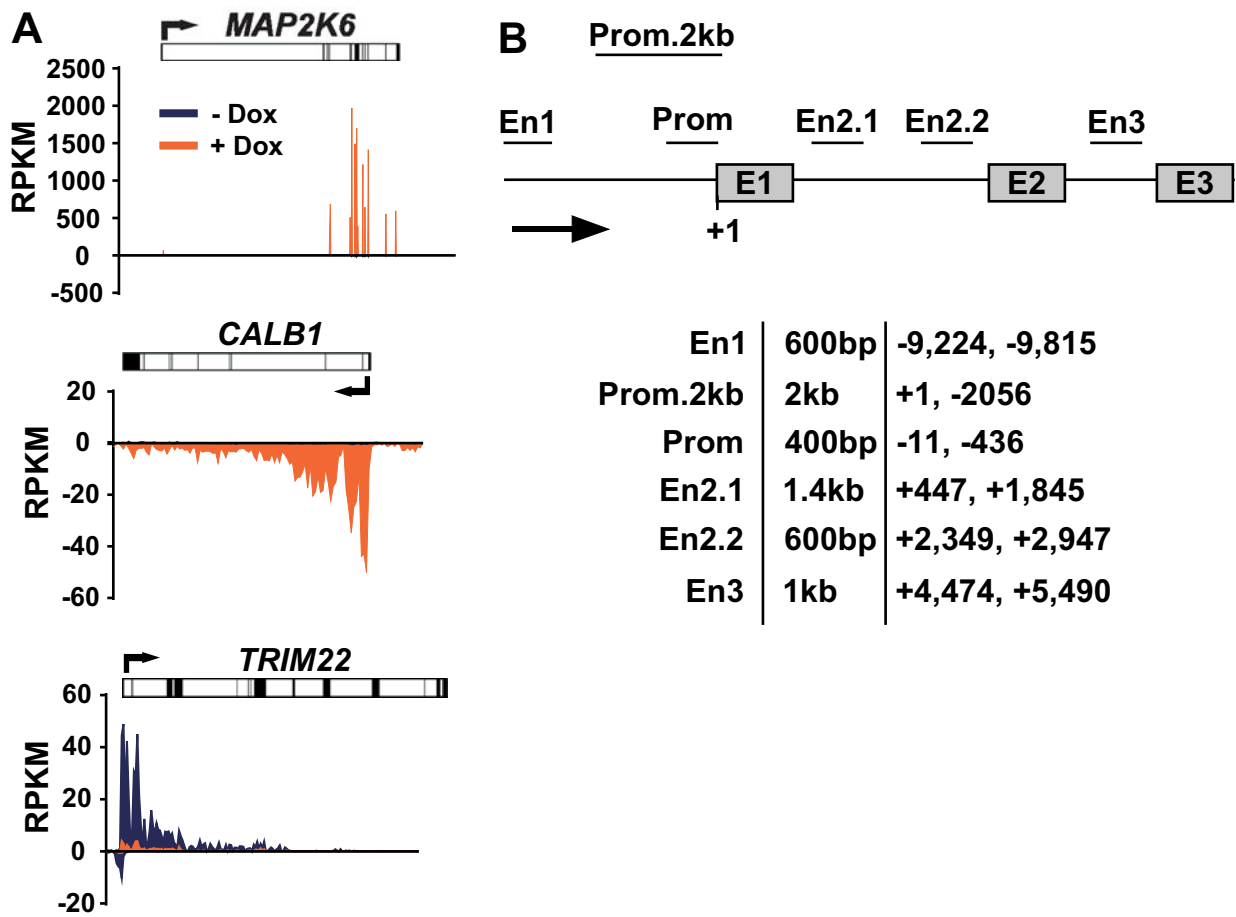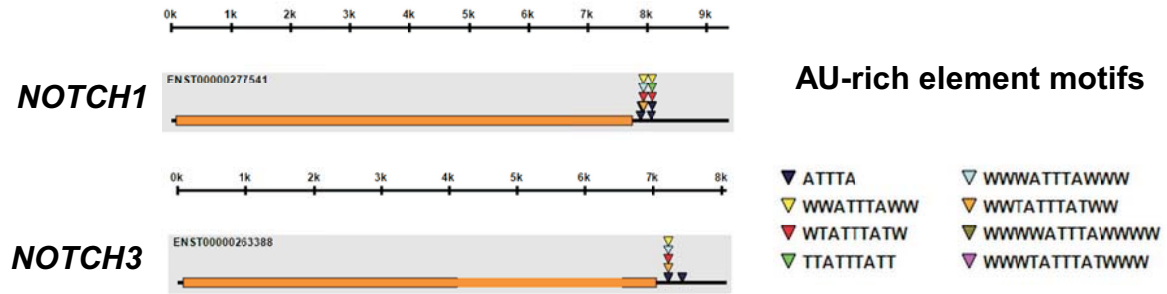
Nuclei / ITGα6 / AR

FIGURE S3

FIGURE S4

FIGURE S5

A

Figure S1: p38 inhibitor titration and cell death assay (A) iPrEC-TetON-MKK6(CA) cells were treated with Dox for 6 h in the presence of increasing concentrations of p38-MAPK inhibitors SB202190 or BIRB796. Protein was analyzed by immunoblot. MKK6(CA) was detected via a Myc-tag. **(B)** iPrECs were treated with DMSO+Dox (Control), 1 µM SB202190, or 0.1 µM BIRB796 while shRNA lines were induced with Dox over 16 days of differentiation. Top row: phase contrast microscopy. Bottom row: merged epifluorescence images of Hoescht-stained nuclei (blue) and propidium iodide (red), to which only dead cells are permeable. Luminal layer (L) is outlined (dashed line) in control cells and sits on top of basal (B) cells. Scale bar = 200 µm.

Figure S2: NOTCH signaling increases during differentiation and is required for survival (A) Primary PrECs were differentiated for indicated days and cell lysates collected for immunoblotting. Antibody notes: p-MYC recognizes T58/S62. NOTCH2 is ICD-specific. NOTCH1/3 recognize full length (FL), transmembrane (TM), and intracellular domain (ICD). **(B)** RNA was collected from iPrECs differentiated for the indicated days and analyzed by qRT-PCR. Luminal (L, solid line) cells were separated from basal (B, dashed line) cells at days 10 and 14. Graph shows mean±s.d. of biological triplicates. Data were normalized to day 1. **(C)** iPrEC pools with Tet-inducible shNOTCH1 (shN1) or shNOTCH3 (shN3) were treated 48 h ±Dox and analyzed by qRT-PCR for expression of NOTCH1, NOTCH2, and NOTCH3. Data were standardized to *18S* and *RPL19* and normalized to -Dox. Graph shows mean±s.d. of biological triplicates. **(D)** iPrECs were treated with DMSO+Dox (Control) or 1 µM RO4929097 and shRNA lines were induced with Dox over a 16 day differentiation. Top row: phase contrast microscopy. Bottom row: merged epifluorescence images of Hoescht-stained nuclei (blue) and propidium iodide (red), to which only dead cells are permeable. Luminal layer (L) is outlined (dashed line) in control cells and sits on top of basal (B) cells. Scale bar = 200 µm.

Figure S3: MYC is required but not sufficient for full *NOTCH3* upregulation (A) iPrEC-TetON-MKK6(CA) cells were treated with Dox ±Cyclohexamide (CHX) at 6 h. *NOTCH3* mRNA was measured by qRT-PCR. Samples were normalized to 0 h.   Graph shows mean±s.d. of biological triplicates. **(B)** iPrEC-TetON-MKK6(CA) cells were treated with Dox for 16 h plus DMSO or varying amounts of the MYC inhibitor 10058-F4. *NOTCH3* mRNA was measured by qRT-PCR. Data were standardized to *18S* and *RPL19* and normalized to untreated controls (-Dox). Graph shows mean±s.d. of biological triplicates. Text within bars is rounded fold change. p-value details are in methods. **(C)** Basal, undifferentiated iPrEC-TetON-Myc cells were treated

with Dox, DMSO, or 10058-F4 (10 µM) for 8 h and *NOTCH3* mRNA was measured by qRT-PCR.   Data were standardized to *18S* and *RPL19* and normalized to untreated controls (DMSO).   Graph shows mean±s.d. of biological triplicates.   **(D)** iPrEC-TetON-Myc cells were differentiated five days then treated with Dox for up to 24 h.   Lysates collected for immunoblot. FL=full length, TM=trans-membrane.

Figure S4: UV-BrU-Seq controls and map of reporter elements (A) Additional controls for the UV-BrU-seq data from Fig. 5B.   iPrEC-TetON-MKK6(CA) cells were treated with Dox for 10 h and processed for UV-BrU-Seq.   Y-axis is RPKM (reads per kilobase of transcript per million mapped reads).   Plus strand reads are (+), minus strand reads are (-).   Blue = -Dox; Orange = +Dox.   Gene diagram shows orientation (arrow) and exons (black lines).   **(B)** Diagram (not to scale) of the first three exons of *NOTCH3* and regions cloned for reporter assays.   Note: *NOTCH3* is on the minus strand but is depicted here on plus.   The table shows the size of the cloned regions and their location in relation to the *NOTCH3* start codon (ATG = +1).

Figure S5: *NOTCH3* 3'UTR contains an AU-rich element (A) The online tool ARE Site (v1) was used to search the *NOTCH1 and NOTCH3* transcripts for common AU-rich motifs that are binding sites for RNA binding proteins.   Link to site is in methods.

Chromatin Immunoprecipitation. Cells (3 million) were fixed with 1% formaldehyde (Thermo Scientific) for 1-5 min. Cells were washed 3X with ice cold Calcium-Magnesium Free PBS (CMF-PBS) plus protease inhibitors. Pelleted cells were treated with swelling buffer (5 mM PIPES pH 8.0, 85 mM KCl, 0.5 % IGEPAL) on ice for 30 min. Nuclei were dounce homogenized and pelleted at 4000 rpm for 10 min, 4°C (Eppendorf 5415d). Sonication buffer (0.1% SDS, 10 mM EDTA, 50 mM Tris-HCl pH 8.1) was added to nuclei and incubated on ice for 10 min prior to sonication. Chromatin was sheared at 4°C using the Covaris E220 Ultra Sonicator following manufacturer's suggested settings of 2% Duty Cycle, 105 Watt Peak Intensity, 200 Cycles/Burst. In order to achieve 300-500 bp fragments, samples were sonicated for 7 min.

Chromatin immunoprecipitations were performed with 1.5-2 million cells per IP. The following antibodies were used: c-Myc (sc-764, Santa Cruz) and Rabbit IgG (CST). 6 µg of primary antibody was incubated with chromatin overnight at 4°C with rotation. Next, and 25 µL of Protein A magnetic beads (NEB) was added to samples and incubated 6 h at 4°C with rotation. Beads were then washed in the following buffers at 4°C for 10 min with rotation: Triton Wash Buffer (50 mM Tris-HCl pH 7.4, 150 mM NaCl, 1% Triton X-100), followed by Lysis Buffer 500 (0.1% NaDOC, 1 mM EDTA, 50 mM HEPES pH 7.5, 500 mM NaCl, 1% Triton X-100), LiCl Detergent buffer (0.5% NaDOC, 1 mM EDTA, 250 mM LiCl, 0.5% IGEPAL, 10 mM Tris HCl pH 8.1), and Tris-EDTA pH 8.1. Protein was eluted from beads in Elution Buffer (10 mM EDTA, 1% SDS, Tris-HCl pH 8.0) for 30 min at 65°C. Samples were then treated with 20 µg proteinase K and10 µg RNase A, then NaCl (200 mM) was added and incubated at 65°C over night to reverse cross-links.   DNA was purified using phenol/chloroform extraction and ethanol precipitation.

Table S1. shRNA information. Source includes RNAi Consortium ID used for target sequences (http://www.broadinstitute.org/rnai/public/). Target bp is the first base targeted by the shRNA based on cDNA sequence. All shRNAs were cloned into the Tet-pLKO-Puro vector and included a terminator sequence (TTTTT).

Target Gene	Target bp	Source		Sequence (sense_loop_antisense)
p38α	1971	TRCN0000196472	5'	GTACTTCCTGTGTACTCTTTA_AACTAGTGA _TAAAGAGTACACAGGAAGTAC
p38δ	993	TRCN0000197043	5'	GAAACTCACAGTGGATGAATG_TACTAGT _CATTCATCCACTGTGAGTTTC
NOTCH1	6258	TRCN0000350330	5'	CCGGGACATCACGGATCATAT_ACTAGT _ATATGATCCGTGATGTCCCGG
NOTCH3	1958	TRCN0000363316	5'	TTTGTAACGTGGAGATCAATG_TACTAGT _CATTGATCTCCACGTTACAAA

Table S2. Antibody information.

Target	Species	Mono/Poly-clonal	Company	Product no.	Lot no.	Dilution for WB	Dilution for IF	Additional Info
AR	Rabbit	Poly	Santa Cruz	sc-815	B1513		200	
CREB1	Rabbit	Mono	CST	4820	3	1,000		
p-CREB1	Rabbit	Mono	CST	9198	10	1,000		pSer133
GAPDH	Mouse	Mono	Millipore	CB1001	NG1780785	10,000		
ITGA6	Rat	Mono	BD	555734	4353644		200	
MYC	Rabbit	Poly	Millipore	06-340	DAM1770290	1,000		
MYC	Mouse	Mono	Santa Cruz	sc-40	G310	1,000		Used for myc-tag
p-MYC	Rabbit	Mono	Millipore	04-217	2433275	5,000		pThr58/pSer62
NOTCH1	Rabbit	Mono	CST	3608	3	1,000		
NOTCH2	Rabbit	Poly	Millipore	07-1234	NG1853763	500		ICD-specific
NOTCH3	Rabbit	Mono	CST	5276	2	1,000		
p38α	Rabbit	Poly	CST	9218	5	2,000		
p-p38α	Rabbit	Mono	Epitomics	1229-1	YH080601C	2,000		pThr180/pTyr182
p38δ	Mouse	Mono	Santa Cruz	sc-136063	G0209	1,000		
TUBULIN	Mouse	Mono	Sigma	T9026	093K4880	10,000		

Table S3. qRT-PCR Primer information. Primer sequences and source if not self designed.

Gene			Sequence	Source
18S	Fwd	5'	CCGCAGCTAGGAATAATGGA	
	Rev	5'	CGGTCCAAGAATTTCACCTC	
ACTB	Fwd	5'	CCCTCCATCGTGGGGC	
	Rev	5'	GACGATGCCGTGCTCGATG	
DLL3	Fwd	5'	GGCGGCTTGTGTGTCGGG	
	Rev	5'	GCAGTCGTCCAGGTCGTGC	
DLL4	Fwd	5'	AGGCCTGTTTTGTGACCAAG	PMID:
	Rev	5'	CTCCAGCTCACAGTCCACAC	22002304
GAPDH	Fwd	5'	GATCATCAGCAATGCCTCCTGC	
	Rev	5'	CTTCTGGGTGGCAGTGATGGC	
HES1	Fwd	5'	AATGACAGTGAAGCACCTCCG	
	Rev	5'	ATGCACTCGCTGAAGCCG	
HES6	Fwd	5'	GAGGACGGCTGGGAGACG	
	Rev	5'	TCGCTCGCTTCCGCCTGC	
HEY1	Fwd	5'	AGAGTGCGGACGAGAATGGAAACT	PMID:
	Rev	5'	CGTCGGCGCTTCTCAATTATTCCT	18663143
HEY2	Fwd	5'	AAGATGCTTCAGGCAACAGGG	
	Rev	5'	GGATCCGAGGAGTCCAGGC	
HEYL	Fwd	5'	CAGGATTCTTTGATGCCCGAG	PMID:
	Rev	5'	GACAGGGCTGGGCACTCTTC	21834989
ITGA6	Fwd	5'	GCTGGTTATAATCCTTCAATATCAATTGT	PMID:
	Rev	5'	TTGGGCTCAGAACCTTGGTTT	20048343
ITGB1	Fwd	5'	CTGGCAAATTCTGCGAGTGTG	
	Rev	5'	CACTCACACACACGACACTTGC	
ITGB4	Fwd	5'	AACGGCGGTGAGCTGCATC	
	Rev	5'	GAGTGCTCAAAGTGAAGGCGG	
JAG1	Fwd	5'	ATAAGTGCATCCCACACCCG	
	Rev	5'	AGACACGGCTGATGAGTCCC	
LUC	Fwd	5'	GGCCTGACAGAAACAACCAGCG	
	Rev	5'	GGACGCACAGCTCGCCGC	
MYC	Fwd	5'	TTCGGGTAGTGGAAAACCAG	Integrated DNA
	Rev	5'	AGTAGAAATACGGCTGCACC	Technologies
NOTCH1	Fwd	5'	CGCAGATGCCAACATCCAGG	
	Rev	5'	CCCAGGTCATCTACGGCGTTG	
NOTCH3	Fwd	5'	CGTGGCTTCTTTCTACTGTGC	
	Rev	5'	CGTTCACCGGATTTGTGTCAC	
RPL19	Fwd	5'	CGGCTGCTCAGAAGATACCG	
	Rev	5'	TTGTCTGCCTTCAGCTTGTGG	

TableS4. Enhancer element PCR cloning and mutagenesis primers.

Element			Flank_Restriction Enzyme_Target
Prom.2kb	Fwd	5'	ATTAT_CTCGAG_CCGGCCCCATGGCGGCC
(2kb)	Rev	5'	ATAAT_GCTAGC_GATACAGGGCTGGAGCCTTAGCC
Prom	Fwd	5'	ATTAT_AAGCTT_TGGGTCCATGAGCCTCTCAGG
(400bp)	Rev	5'	ATTAT_AAGCTT_TCCCTCCTTCCCTGGGC
En1	Fwd	5'	ATTAT_GGTACC_CTGGGTGTCTCAGGCAGAGGG
(600bp)	Rev	5'	ATTAT_GGTACC_GCCTAGAGTTCGAGACCAGCC
En2.1	Fwd	5'	ATTAT_AGATCT_CGCCTGGAGTCCTGGG
(1.4kb)	Rev	5'	ATTAT_AGATCT_CCTGTGGGTGTTCGTGA
En2.2	Fwd	5'	ATTAT_GCTAGC_GCTGGTCTCGAACTCCTGACC
(600bp)	Rev	5'	ATTAT_GCTAGC_TTCAGGGGTAATAGAAGGG
En3	Fwd	5'	ATTAT_CTCGAG_TCTCCCACTCGGGCTCACC
(1kb)	Rev	5'	ATTAT_CTCGAG_CCAGAGAGTCCAAGCTCCGCC
En1Δ1-360		5'	CCTAACTGGCCGGTACCGTCACTGAGACCCAGG
En3Δ1-350		5'	GCTCGCTAGCCTCGAGACGGTCTCAAATACTC
miniTK		5'	TTCGCATATTAAGGTGACGCGTGTGGCCTCGAACACCGA GCGACCCTGCAGCGACCCGCTTAA

Table S5. ChIP primer information. Details for primers used in ChIP, including amplicon size.

Target			Sequence
HIstone3	Fwd	5'	CCGAACCAAGCAGACTGCG
(118bp)	Rev	5'	GCGGTGCGGCTTCTTCACG
ODC1	Fwd	5'	AACAGACGGGCTCTGATGACG
(119bp)	Rev	5'	GGGCTTTACATGTGCGTGGTC
En1 (1)	Fwd	5'	TCCTGGGTGGTAGGCATGACG
(94bp)	Rev	5'	GGGGCACACACTGACTCACGG
En1 (2)	Fwd	5'	TGGCCGGGAGTCACTGAGACC
(135bp)	Rev	5'	AGTTCCAGACTGCAGGGAGCC
En3 (1)	Fwd	5'	GGGCTCAGTCCTCCGAGTTGG
(109bp)	Rev	5'	GGGGGCATCCTTGAAAGGAC
En3 (2)	Fwd	5'	GGGACCAGCTATCCTCGGC
(99bp)	Rev	5'	TCCCGTCCCCTCCTCCAAGG